SATURATION OF CURRENT TRANSFORMERS AND ITS IMPACT ON DIGITAL OVERCURRENT RELAYS

by

NABIL H. AL-ABBAS

A Thesis Presented to the

DEANSHIP OF GRADUATE STUDIES

In Partial Fulfillment of the Requirements

for the degree of

MASTER OF SCIENCE

IN

ELECTRICAL ENGINEERING

KING FAHD UNIVERSITY

OF PETROLEUM & MINERALS
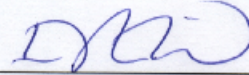
DHAHRAN, SAUDI ARABIA

August 2005

KING FAHD UNIVERSITY OF PETROLEUM AND MINERALS
DHAHRAN 31262, SAUDI ARABIA

DEANSHIP OF GRADUATE STUDIES

This thesis, written by **Nabil Habib M. Al-Abbas**, under the direction of his Thesis Advisor and approved by his Thesis Committee, has been presented to and accepted by the Dean of College of Graduate Studies, in partial fulfillment of the requirements of the degree of **MASTER OF SCIENCE IN ELECTRICAL ENGINEERING.**

Thesis Committee

_____
Dr. Ibrahim M. El-Amin (Chairman)
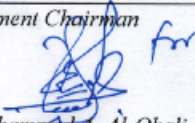
_____
Dr. Mohammad Ali Abido (Co-Chairman)

_____
Dr. Zakariya M. Al-Hamouz (Member)
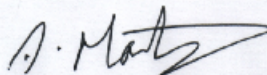
J. M. Bakhashwain

Dr. Jamil M. Bakhashwain

_____
Department Chairman

_____
Dr. Abdul-Aal H. Mantawy (Member)

Dr. Mohammed A. Al-Ohali

_____
Dean of Graduate Studies

_____
Dr. Ibrahim O. Habiballah (Member)

Date: August 21st, 2005

اهدي هذه الرسالة لوالدي العزيز

This thesis is dedicated to my dear father

ACKNOWLEDGMENTS

I would like to acknowledge all those who helped me to complete this thesis. Acknowledgment is due to the King Fahd University of Petroleum & Minerals for providing the support to carry out this research.

I am indebted to my thesis advisor Professor Ibrahim El-Amin who provided me with his constant encouragement and valuable instructions and suggestions that helped me in accomplishing this work successfully. I would like to express my deep appreciation to him. Many thanks are also due to the other members of my thesis committee Dr. Mohammad Ali Abido, Dr. Zakariya M. Al-Hamouz, Dr. Abdul-Aal H. Mantawy and Dr. Ibrahim O. Habiballah for their valuable advices throughout the research.

I would like also to thank Saudi Aramco management and specifically Power Distribution Department for providing the support and facilities to conduct the necessary tests in this research. Ahmed Al-Shaikh-Nassir, Jaffar Sheef and Samir Zainddin showed great interest in helping me technically. I am proud to have such fellows who deserve my high appreciation.

My sincere and profound gratitude are due to my father and mother. I cannot forgot their kind care and their interest in my success. Their prayers and moral support

will always boost my progress. Specially and most sincerely, I would like to pay my warmest tribute to my beloved wife whose patient love and strong emotional support made my life pleasant even in the hardest times.

TABLE OF CONTENT

LIST OF TABLES

LIST OF FIGURES

THESIS ABSTRACT

Name of Student Nabil H. Al-Abbas

Title of Study   Saturation of Current Transformers and its Impact on Digital Overcurrent Relays

Major Field   Electrical Engineering

Date   August 2005

A current transformer transient model was implemented, using Electromagnetic Transient Program (EMTP), nonlinear inductor (Type-96) in order to investigate the effects of CT's saturation on digital overcurrent relays. The model was validated by testing in laboratory and found to be effective, reliable and accurate for evaluations of digital overcurrent relays, during CT's saturation. Factors that lead to CT's saturations were comprehensively discussed and evaluated.

A typical digital overcurrent relay was tested in the laboratory to investigate the effects of secondary burden, short circuit level, asymmetrical fault with dc offset components and remenant flux on CT's saturations and digital overcurrent relays operations. Evaluations of test results against the rules, specified by IEEE Standard C37.110-1996 were evaluated. The research includes studying the impact of CT saturation on both the instantaneous and time-delayed element of digital overcurrent relays. The results were satisfactory and guidelines and recommendations for CT's selection were presented.

Master of Science Degree

King Fahd University of Petroleum and Minerals

August 2005

خلاصـــة الرســـالـــة

اسم الطالب   : نبيل حبيب مكي آل عباس

عنوان الرسالة : إشباع محولات التيارات الكهربائية وتأثيرها على مرحلات الحماية الرقمية

التخصص   : هندسة كهربائية.

تاريخ الشهادة : أغسطس 2005م

نموذج لمحولات التيار الكهربائي تم تطبيقه بواسطة برنامج دراسة تأثير الكهرومغناطيسية
من خلال استخدام موصل كهربائي غير خطي بهدف تحري تأثيرات إشباع محول التيار الكهربائي
على مرحلات الحماية الرقمية. النموذج تم تصديقه من خلال اختبارات معملية أثبتت فعاليته لتقييم
مرحلات الحماية الرقمية، أثناء إشباع محولات التيار الكهربائي. لقد تم مناقشة وتقييم العوامل التي
تؤدي إلى إشباع محولات التيار بشكل شامل.

لقد تم اختبار مرحلات حماية رقمية في المختبر عن طريق دراسة الحالات المختلفة لبحث
تأثير العبء الثانوي، مستوى التيار المتماثل ولا متماثل، الجريان المتبقي داخل محولات التيار على
إشباع محولات التيار الكهربائي وتأثيرها على مرحلات الحماية الرقمية. جميع الاختبارات تمت
لتقييم المعايير العالمية. تتضمن البحث توصيات لكيفية اختيار محولات التيار الكهربائي لتتناسب مع
مرحلات الحماية الرقمية.

درجة الماجستير في العلوم

جامعة الملك فهد للبترول والمعادن

الظهران . المملكة العربية السعودية

أغسطس 2005م

CHAPTER 1
INTRODUCTION

In electrical distribution systems, saturation of low ratio current transformers (CTs) at high fault current locations may cause misoperation of overcurrent relays. It has been reported that relays act differently during CT saturations and their time-current characteristics do not meet the published characteristics [1-7]. These problems may cause severe loss of production to various plants or damages to very critical electrical equipment. The IEEE guide for the application of current transformers (IEEE Standard C37.110) contains steps to avoid the effects of AC and DC CT saturation [8]. However, many of these steps result in impractically large CTs, which are economically not acceptable [9]. Relatively small loads connected to a bus, with inherently high available short-circuit currents, usually have CT's with low ratio [10].

The thesis will investigate the transient behavior of CT's and the impact on digital overcurrent relays during high fault level. The research will also analyze the effect of different classes and sizes of C-class CT's on typical microprocessor-based overcurrent relays. The operation principles of all microprocessor-based relays are almost identical, although they utilize different filtering techniques. The transient saturable transformer and nonlinear reactor models available in Electromagnetic Transient Program (EMTP) for current transformers (CT) will be validated in the laboratory to ensure proper selection of the CT's models for the research. Moreover, different fault scenarios, implemented

through EMTP, will be converted in common-trade files in order to conduct laboratory tests to analyze the transient behavior of microprocessor-based overcurrent relays.

Chapter two of the thesis presents a literature survey to document the transient behavior of CT's and digital overcurrent relays during high fault level. The chapter will also present the recent research, analyzing the effect of different classes and sizes of CT's on microprocessor-based overcurrent relays. Chapter 3 discusses the theory and model formulation of a CT to be used to evaluate the performance of protective equipment. Details of model validations are presented in this chapter. Chapter 4 will demonstrate and investigate the effects of secondary burden, accuracy class, short circuit level, X/R ratio (DC offset) and remanent flux in the core on CT's behavior. Chapter 5 describes the modeling of a typical digital overcurrent relay and investigates the effects of CT's saturation on the modeled relay. The effects of CT saturation on microprocessor-based overcurrent relays will be evaluated by conducting various laboratory tests on a typical microprocessor-based overcurrent relay and will be presented in Chapter 6. The evaluations, in this chapter, will consider the instantaneous and time-delayed operations of digital overcurrent relays. Chapter 7 will present area of applications of thesis findings, followed by a case study. Chapter 8 contains test results evaluations, conclusion and recommendations.

CHAPTER 2

LITERATURE SURVEY

A literature survey was conducted to review the methods of CT's modeling, effects of CT's saturation and to investigate the published criteria of CT, C-class selection in IEEE/ANSI standards. In addition, researches covering effects of CT's saturation on digital overcurrent relays will be presented.

2.1 Methods for CT's Modeling

Most of published papers have considered the use of the EMTP to model current transformers and coupling capacitor Voltage Transformers [11-17]. Models for CT's are especially important for studying transformer saturation and its effect on the performance of protective relaying. Many iron core models were studied and considered. However, the majority of researchers considered the EMTP and alternative transients program (ATP) Inductor Models since accurate and acceptable results were successfully obtained.

The EMTP and ATP support two classes of nonlinear elements, a true nonlinear model (Type-93) and two pseudo-nonlinear models (Type-96 and Type-98). In the true nonlinear model, the nonlinearity is explicitly defined as a nonlinear function. The EMTP and ATP then resolve the combinations of nonlinear equations and the appropriate system equivalent at each step using a Newton Raphason iterative procedure. The disadvantage of this method is that flux equations need to be available in order to model the CT. In the

pseudo-nonlinear model, the nonlinearity is defined as a number of piece-wise linear segments. In the particular case of nonlinear inductor, the flux is monitored at each time step in order to determine which linear segment should be used to compute the inductance at that time step. This method does not model the true nonlinearity since the program relies on previous time step results to decide on what segment to operate next. Non-linear reactor-Type 96 accounts for the hysteresis effects in the transformer core and allows for analyzing the effects of residual flux left in the CT following primary current interruption. Many research papers showed that the EMTP nonlinear inductor (Type-96) is very effective in analyzing the relay performance under transient conditions in order to assure a high degree of dependability and security in their design and applications [11, 12, 15, 16].

2.2 IEEE/ANSI Requirements for Selecting CT's Rating

CT behavior under steady state and symmetrical fault conditions is well covered under ANSI/IEEE standard C57.13-1993 [18]. This standard specifies conditions for CT design which include "current transformer secondary terminal voltage rating is the voltage that the CT will deliver to a standard burden at 20 times rated secondary current without exceeding 10% ratio correction. Furthermore, the ratio correction shall be limited to 10% at any current from 1 to 20 times rated secondary current at the standard burden for any lower standard burden used for secondary terminal voltage ratings". However, asymmetrical current can cause the CT's to saturate at much smaller currents than symmetrical currents without DC offset [19, 20]. Flux remanence in the CT core also

contributes to CT saturation [2, 6]. Both the ANSI/IEEE C57.13 and C37.110 documents do not indicate the intensity of saturation and its possible impact on overcurrent relay operation. To study the impact of CT saturation on protection devices, an additional analysis is required [21].

Although there is an abiding interest in the application of current transformers for relaying, few written rules exist for selecting the ratings [21]. One important document is C37.110. 1996, which contains selection rules for CT's in general to avoid AC and DC saturations as follows:

To avoid AC saturation, the CT shall be applicable of a secondary saturation voltage:

$$V_X \geq I_S \cdot Z_S \qquad \textbf{(2.1)}$$

Where: I_S is the primary current divided by the turns ratio

Z_S is the CT secondary burden

Vx is the CT saturation voltage

Current transformer secondary terminal voltage rating is the voltage that the CT will deliver to a standard burden at 20 times rated secondary current without exceeding 10% ratio correction. Therefore, equation (2.1) can be rewritten as follows:

$$20 \geq i_f \cdot z_b \qquad \textbf{(2.2)}$$

Where: i_f is the maximum fault current in per unit of CT rating

z_b is the CT burden in per unit of standard burden

In addition, C37.110.1996 highlights the criteria to avoid saturation with a DC component in the primary wave as follows:

$$V_X \geq I_S \cdot Z_S (1 + \frac{X}{R})$$ **(2.3)**

Where: X and R   is the primary system reactance and resistance up to the point of fault. Similar to the AC saturation, equation (2.3) can be rewritten as follows:

$$20 \geq \left| \frac{X}{R} + 1 \right| \cdot i_f \cdot z_b$$ **(2.4)**

Where: i_f is the maximum fault current in per unit of CT rating

z_b is the CT burden in per unit of standard burden

X/R   is the system X/R ratio

However, most of the time, these rules result in impractically large CTs, which are not economically acceptable. This is true where small CT's connected to a bus with high short circuit current that can exceed 200 times the CT primary current rating [16]. IEEE Standard C37.110-1996 offers no guidance for other applications where those rules do not apply. Small cores, long leads, high burdens, and offset lead to saturated CT's [21]. In addition, the aforementioned standard does not specify the intensity of CT's saturation and its effects on overcurrent relays.

2.3 Effects of CT Saturation on Overcurrent Relays

Many papers have explored waveform distortion due to CT saturation and its

effect on electromechanical overcurrent relays [1-7]. These relays are considered obsolete and are not manufactured any more. Alternatively, all new electrical installations involve microprocessor-based relays installation. Few papers have considered the effects of CT saturation on microprocessor-based relays [13, 22]. The operation of these relays is not yet understood against CT saturation during high fault current. This increases the necessity to investigate the transient behavior of these relays during CT saturation. Kojovic has considered the effect of waveform distortion, in general, on protective relays, including microprocessor-based relays. The paper has attempted to show, theoretically and through laboratory tests, the influences of harmonics on various types of protective relays [13]. It showed that these relays will be affected by the DC offset and CT saturation. In addition, no clear and practical guidance for selecting CT's, to ensure overcurrent relays have been provided so far in the literature.

In many cases, saturated CT's may fail to deliver a true reproduction of primary current during high fault level and therefore may cause undesirable operations. One of the most critical concerns involves low-ratio CT's in any of the lower voltage systems area, particularly in 2.4-13.8 kV metal-enclosed switchgear relaying applications [1, 3, 10]. The operation of instantaneous and time-delayed digital relays needs to be further studied to check the transient behavior of these relays during CT's saturations.

There is thus a clear and urgent need to model low-ratio CT's and investigate the effects of its saturation on digital overcurrent relays. Chapter 3 presents a model description and its implementation through the EMTP

CHAPTER 3

IMPLEMENTATION OF CURRENT TRANSFORMERS MODEL

This chapter discusses the theory and model formulation of a current transformer to evaluate the protective relay performance. Few papers and researches had covered the performance and response of microprocessor-based overcurrent relay to CT's saturation although these relays executes algorithms that are mathematical procedures and can produce analytic characteristics that is described easily by an equation. The key to the behavior of microprocessor-based relays is in calculating and measuring the response of the current transformers and digital filter and comparing the deviation of the response to the ideal sine-wave signal. Therefore, the current transformers and relay modeling are very essential to evaluate the protection equipment performance.

In this chapter, set of software tools will be used to examine the behavior and performance of current transformers. These tools are as follows:

- Alternative Transients Program (ATP) version of EMTP will be used for current transformers transient model implementations.

- ATPDraw is a windows interface graphical preprocessor of ATP. Current transformer circuit and model can be drawn by selecting the components available in the program. ATPDraw then will create the ATP input file and will run the ATP.

- The output processor (TOP) program is a graphical postprocessor for transient data

and will be used to convert ATPDraw output programs to text files in order to be
utilized easily in interfacing with MATHCAD software that will be utilized for
digital relays modeling.

- Omicron Test Universe software will be utilized to save and capture the signals of
  the tested current transformers in the laboratory in common-trade format to be
  utilized for analysis in ATP [34].

3.1 Current Transformer Transient Analysis

The equivalent circuit of a current transformer is shown in Figure 3.1 [23- 29]. For ideal
CT, it will operate with an ampere-turn balance:

$$I_P \cdot N_P = I_S \cdot N_S \tag{3.1}$$

Where:

I_p, I_s is CT Primary and secondary currents

N_p, N_p is number of primary and secondary turns

An actual CT does not behave as an ideal transformer. The CT secondary voltage
is generated by the rate of flux change in the core. To produce flux in the CT core,
magnetizing (Exciting) current is required. This introduces ratio and phase errors.
Therefore, the equation of an actual CT can be written as:

$$I_P' = I_S + I_m \tag{3.2}$$

Where, I_p' is the primary current referred to the secondary, and I_m is magnetizing current.

Rp, Lp is the primary winding resistance and leakage inductance.
Rs, Ls is the secondary winding resistance and leakage inductance.
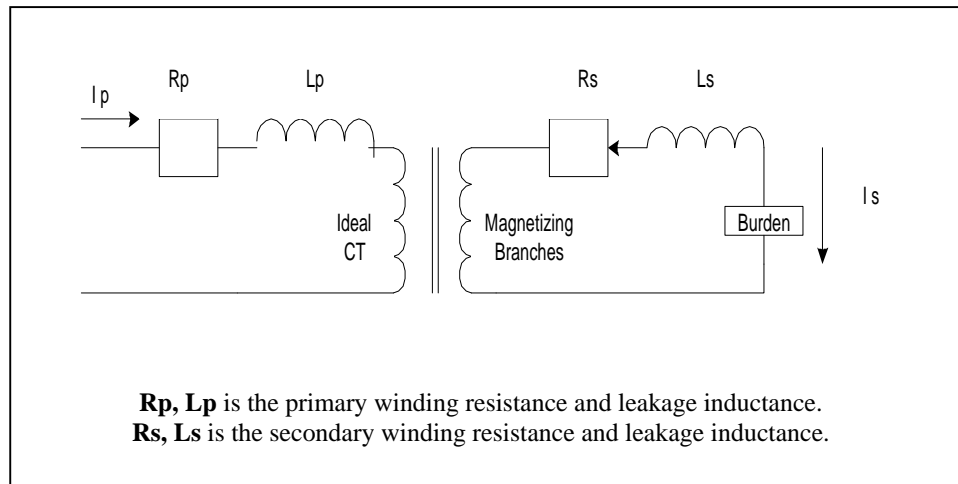
Fig. 3.1 Current Transformer Equivalent Circuit

Under steady state condition, all current transformer performance can be measured using the fundamental equation (3.3).

$$E = 4.44 B_S A N f \qquad\qquad (3.3)$$

Where, B_S is the maximum flux density in the core, A is the effective cross sectional area of the core, N is the transformer ratio and f is the system frequency. The use of the fundamental transformer equation is useful when the information on CT iron flux density characteristics and cross sectional area are available. Such information, most of the time, is not available.

For the purpose of transient analysis, the equivalent circuit of Figure 3.2 has been developed. To investigate the nonlinear behavior of the CT's, the magnetizing leg of the current transformer can be represented in Figure 3.3 to visualize the non-linear phenomenon of the magnetizing circuit. For each level of excitation, a different value of reactance is used. In figure 3.3, three B-H diagrams are shown, as flux versus magnetizing current I_m, representing low, medium and high level of excitations.

Lm-Magnetizing Inductance
Es- CT Secondary Voltage
Imx- Magnetizing current, Reactive component
Imr- Magnetizing current, Resistive component
Rm- Iron Loss equivalent resistance
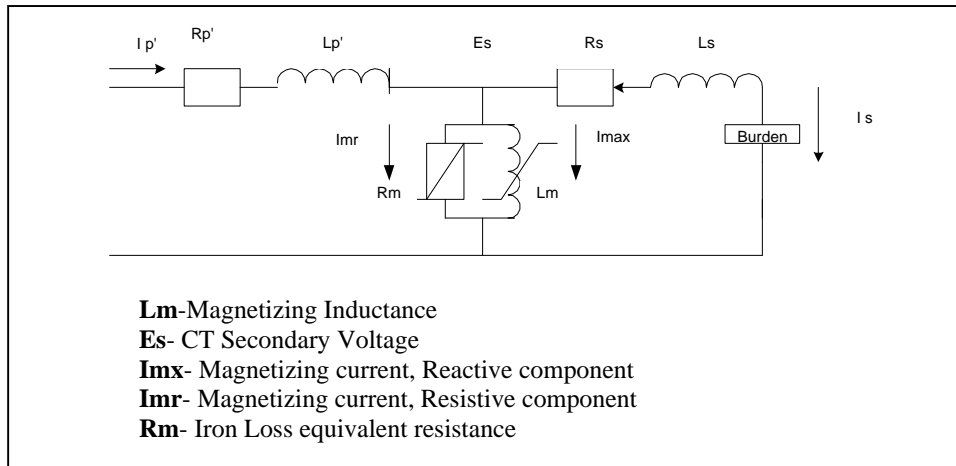
Fig. 3.2 Current Transformer Circuit Diagram
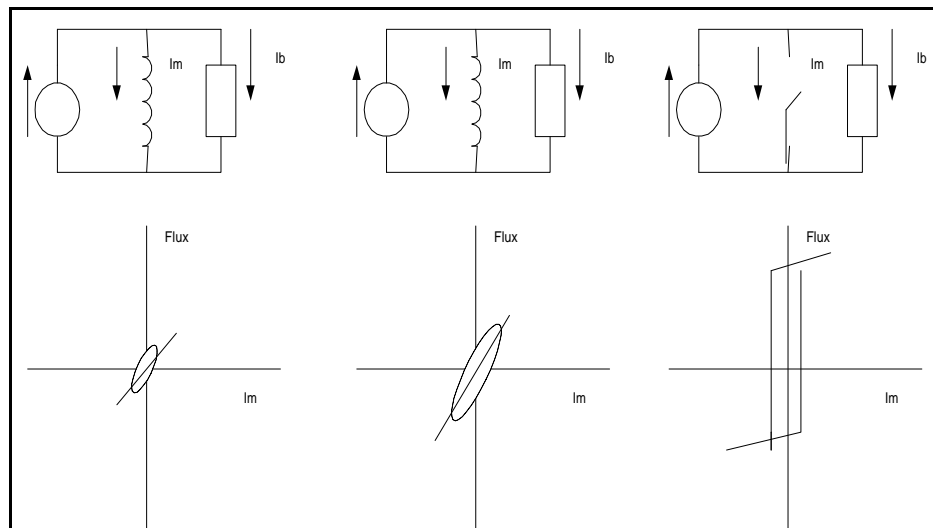
Fig. 3.3 CT Equivalent Circuits at Various Levels of Excitation

At low excitation, the slope *d?/dI* representing the inductance is low. This low slope represents a disproportionate amount of magnetizing current compared to the burden current at low excitation. At medium excitation, the *d?/dI* is relatively high and the magnetizing current is small compared to the current in the burden. At high excitation, the slope is infinite and the concept of impedance breaks down altogether. All that is apparent is the area of the hysteresis loop representing losses (and hence resistance). Otherwise, there is simply a change in flux from *–?* to *?* . The change takes place during a portion of the cycle of the current. The fact that magnetizing current is so small compared to the ratio current during the transition suggests that it can be ignored. Consequently, the saturation phenomenon is best represented by volt-time switch as shown in figure 3.3, which opens during a rate of flux change and closes during saturation [1, 23]. The volt-time area of the burden voltage wave represents flux from the expression:

$$V = N \cdot \frac{d\varphi}{dt} \qquad\qquad \textbf{(3.4)}$$

3.2 Mathematical Models of Magnetic Core Representations

The measure of a current transformer performance is its ability to reproduce accurately the primary current in secondary amperes both in wave shape and in magnitude. There are two parts: (1) the performance under the symmetrical ac component, and (2) the performance under the offset dc component [27]. Modern CTs do a remarkable job of reproducing wave shapes as long as they do not saturate. The major non-linear effects in iron cores are saturation, eddy currents, and hysteresis [16]. As a result, many investigations were conducted to study the nonlinearities in a current transformer and the effects of CT saturation on protective relays [30, 31, 32].

In order to accurately model the current transformers, the following shall be undertaken:

- Conversion of the rms *V-I* saturation curve data into peak *?-I* data with the hysteresis loop being ignored.
- Providing the hysteresis loop data required by the Type-96 Pseudo-nonlinear reactor model.

The algorithm for computing the saturation characteristics of transformer iron cores has been proven by different papers through laboratory measurements [11]. As shown in figure 3.3, the excitation branch is represented by a non-linear inductance in parallel with a non-linear resistance. The nonlinear characteristics are computed according to the following assumptions:

- The φ-I curve are symmetric with respect to the origin (L_k is the slope of segment k of the φ-I curve).

- The winding resistance and leakage inductances are ignored in the analysis.

The algorithm uses data points from the CT secondary excitation curve *Vrms-Irms* to calculate the peak φ-I curve. The results is a piece-wise linear model because a small finite number of data points are used, usually 10 or less.

The conversion of rms voltage values to flux is only a rescaling procedure. For each linear segment in the φ-I curve,

$$\varphi_k = \frac{\sqrt{2}V_K}{\omega} \tag{3.5}$$

Assuming that $\varphi_k(\theta) = \varphi_k \sin\theta$, then for the following segments ($k \geq 2$). The peak current is obtained by evaluating for I_{k-rms} for each segment k, using the following equation:

$$I^2{}_{k-rms} = \frac{2}{\pi} \left(\int_0^{\theta 1} \left(\frac{\varphi_k \sin\theta}{L1} \right)^2 d\theta + \int_{\theta 1}^{\theta 2} \left(I_1 + \frac{\varphi_k \sin\theta - \varphi_1}{L2} \right)^2 d\theta + \dots + \int_{\theta_{k-1}}^{\pi 2} \left(I_K + \frac{\varphi_k \sin\theta - \varphi_{K-1}}{L_K} \right)^2 d\theta \right) \tag{3.6}$$

In Figure 3.4 only the last segment L_k is unknown. Therefore, the equation can be rewritten in the form:

$$a_{lk}Y_K^2 + b_{lk}Y_K + c_{lk} = 0 \tag{3.7}$$

If constants a_{lk}, b_{lk}, and a_{lk} are known, and $Y_k = 1/L_k$ can be computed. Y_k can then be solved from 3.7 and it must be positive. The peak current i_{lk} is computed from the following equation:

$$i_k = i_{k-1} + Y_K \left(\varphi_K - \varphi_{K-1} \right) \tag{3.8}$$

Then, one point is entered in the subroutine HYSTERESIS in the ATP to provide the hysteresis loop data. The routine contains predefined trajectories in the *?-I* plane to decide which path to follow when the flux increases or decreases [33].
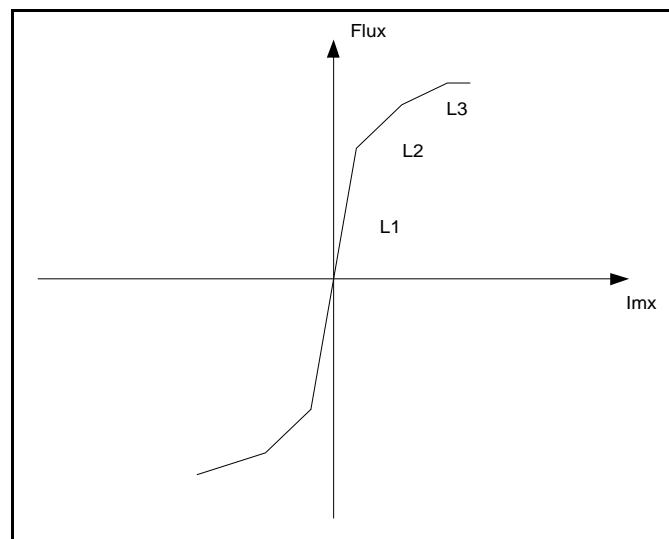
Fig. 3.4 Piece-wise Linear Segments of the ?-I curve

3.3 Validations of Current Transformer EMTP Model

In order to create the identical operating conditions as those during actual measurements, laboratory tests were conducted for model validation purposes. Primary advanced injection test equipment (Omicron-CPC100) has been utilized to carry out different kinds of testing for the current transformer. This device can inject up to 2000A primary [34]. In addition, it is a software-based devise that can provide the automatic capability to implement, for example, CT Ratio, CT Excitation and secondary winding resistance measurement tests. In the testing setup, a microprocessor-based relay (Basler Overcurrent Relay BE1-951) has been used in the tests to trace and capture the secondary signals for the current transformers with sampling rate with 12 samples/cycle. Figure 3.5 shows the testing set-up.

A current transformer, with 50/5 ratio and ANSI/IEEE class C20, has been tested at the Laboratory at Saudi Aramco to obtain the actual excitation curves to be implemented in the EMTP. The current transformer has been driven to saturation and secondary current has been captured by Digital Events Recording feature in the microprocessor-based relay (Basler Overcurrent Relay) for comparison with EMTP results. In addition, burden effects on the selected CT have been investigated by changing the secondary burden connected to the current transformer under test. All laboratory data was compared with EMTP results to validate the results and ensure having proper modeling for the current transformer.
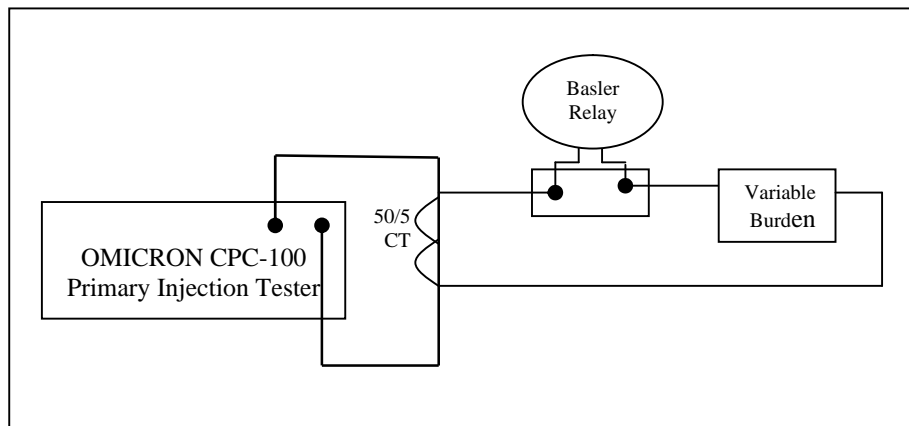
Fig. 3.5 Schematic Diagram for Test Circuit

An excitation test has been conducted on the selected current transformer in order to obtain the actual excitation curve of the CT by using the OMICRON CPC-100. The test was implemented by injecting current in the secondary side of the 50/5 CT. The measurement of the V-I curve was carried out according to the ANSI/IEEE standard C57.13. V-I curve is shown in figure 3.6.

The burden of a current transformer, as defined in IEEE C37-110, is the property of the circuit connected to the secondary winding, which determines the active and reactive power at the secondary terminals. The burden is expressed either as total ohms impedance, together with the effective resistance and reactance components, or as the total volt-amperes and power factor of the secondary devices and leads specified values of frequency and current. The accuracy of CT's is defined by IEEE C37-110-1996, as the extent to which the current in the secondary circuit reproduces the current in the primary circuit as stated by the marked ratio. The accuracy class can be obtained by calculations or by test, followed by the minimum secondary terminal voltage that transformer will produce at 20 times rated secondary current with one of the standard burdens without exceeding the accuracy class limit (10%).
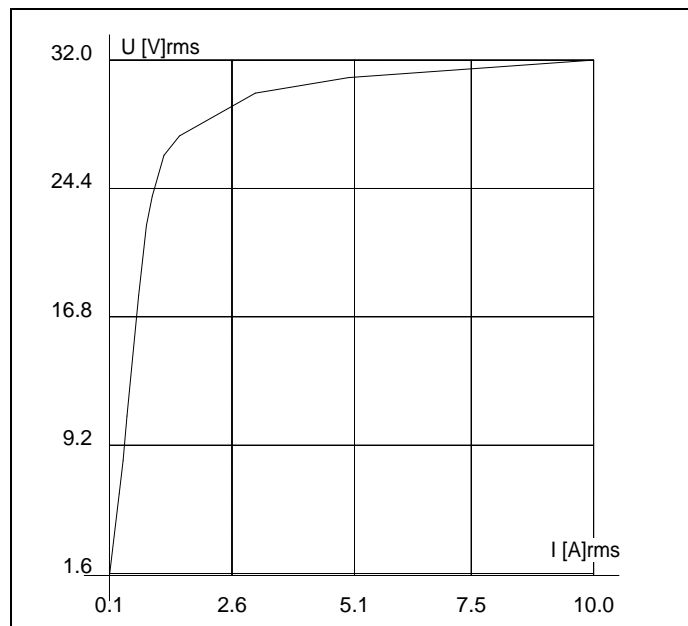
Figure 3.6 Laboratory Excitation Curve for 50/5 CT

The current transformer considered for testing, has a class of C20. Therefore, the maximum burden is 20/100 or 0.2 ohm. This burden does not include the secondary resistance of the current transformers. Table 3.1, shows the effects of the connected burden on the current transformer saturation and its capability to reproduce the primary signal on the secondary side. Although the standard burden involves power factor, a quick arithmetic (worst case) calculations of secondary terminal voltage Vb has been considered. The burden shown in Table 3.1 is the total burden, including the secondary resistance of the CT, wires resistance, and variable resistance.

For the purpose of Laboratory results validations, two saturation points were selected on the V-I curve for CT modeling in EMTP as shown in Figure 3.7. This has been done to ensure accurate representations of the non-linearity of the current transformer. The two Hysteresis loops obtained from the two different selected saturation points are shown in Figure 3.8.

Table 3.1. Cases applied in the Lab to examine the burden effect on CT's

Primary Injected Current	Total Burden (Ohm)			Effect on Secondary Current
	Case	R	X	
17.4 X CT Rating Current (870 RMS Current)	Case 1	0.3	0.302	Initial Saturation of CT. The output signal is slightly distorted.
As per IEEE/ANSI C37.110, Section 4.4.1, Saturation Voltage is , Vs = Is *(Rs + Zb) = 87.5*(0.0607) = 37.2V				
13 X CT Rating Current (652 RMS Current)	Case 2	1.0	1.508	Output signal is not sinusoidal anymore. More distortion in the signal.
As per IEEE/ANSI C37.110, Section 4.4.1, Saturation Voltage is , Vs = Is *(Rs + Zb) = 65*(1.809) = 117.6V				
13 X CT Rating Current (626 RMS Current)	Case 3	5.0	6.786	Severe Saturation of CT. Low secondary current is reflected.
As per IEEE/ANSI C37.110, Section 4.4.1, Saturation Voltage is , Vs = Is *(Rs + Zb) = 65*(8.429) = 547.9V				
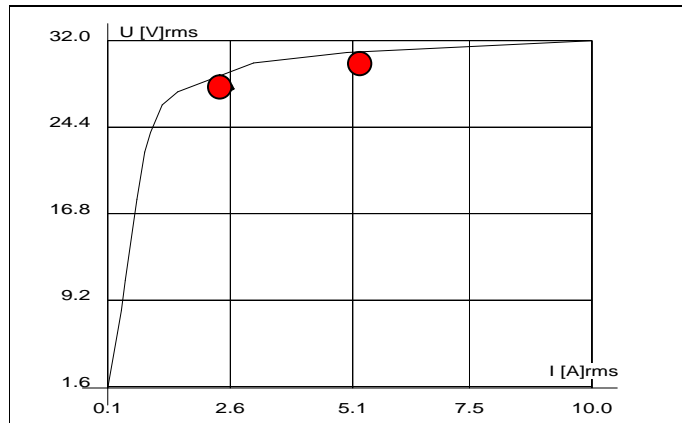
Figure 3.7 Selection of Saturation Point for Calculation of Hysteresis
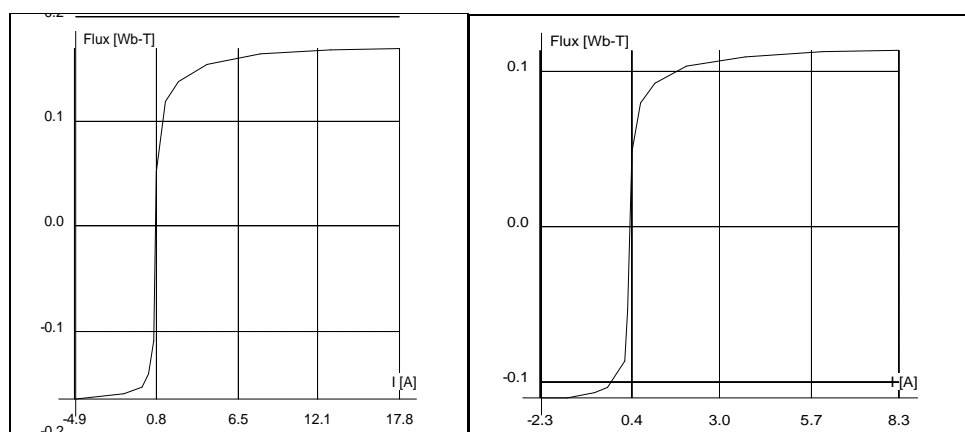
Figure 3.8 EMTP Generated Hysteresis Loop for Vs= 31V and 26V respectively

Figure 3.9 shows CT transient response obtained experimentally with different burden values connected. Effects of CT saturation are shown in case-3 where the primary current is clearly not re-produced in the secondary. Figures 3.10 and 3.11 give the CT transient response obtained by directly using the hysteresis generated, with 31V and 26V saturation voltage respectively. In the two EMTP models, with these two saturation voltages, the same experimental data and parameters were used, including the actual secondary burdens. Analysis of the two EMTP results show that CT transient response obtained by using CT's model with 31V gives satisfactory and close results to the actual values. Figure 3.12 compares between the laboratory results and EMTP model with 31V saturation voltage in the three cases, listed in Table 3.1.
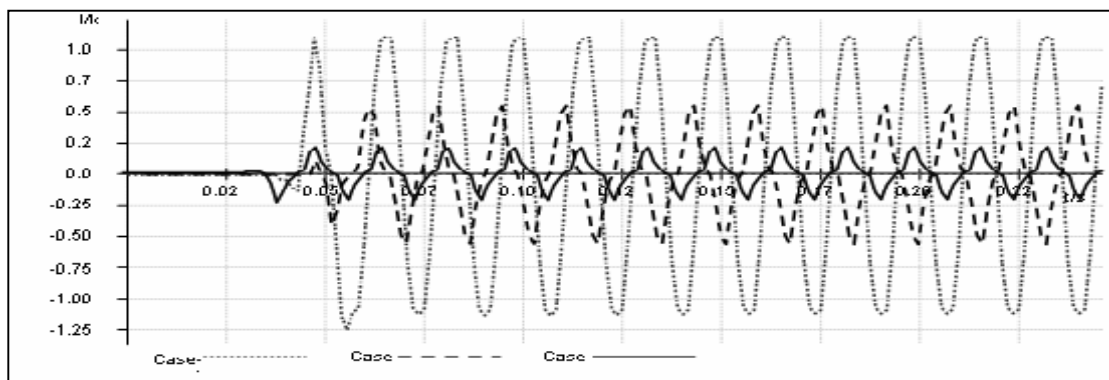
Figure 3.9 Laboratory Test Results Obtained for all Cases
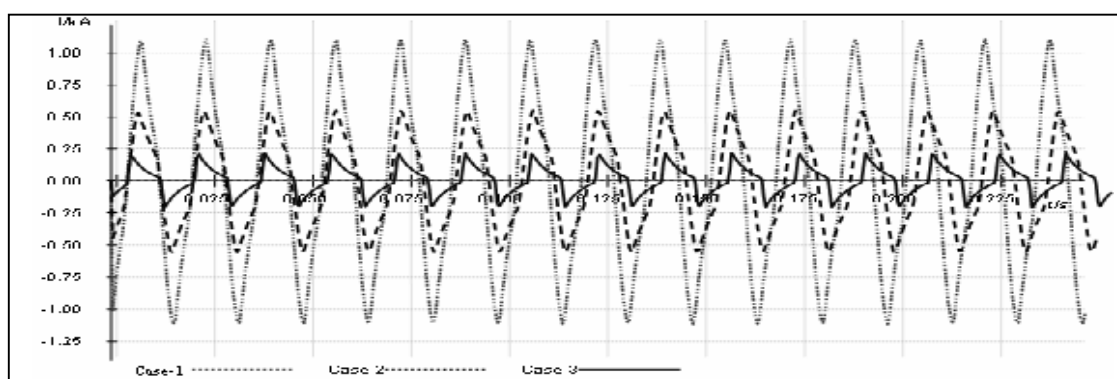
Figure 3.10 EMTP Results Obtained for all Cases, with 31V saturation Voltage Selection
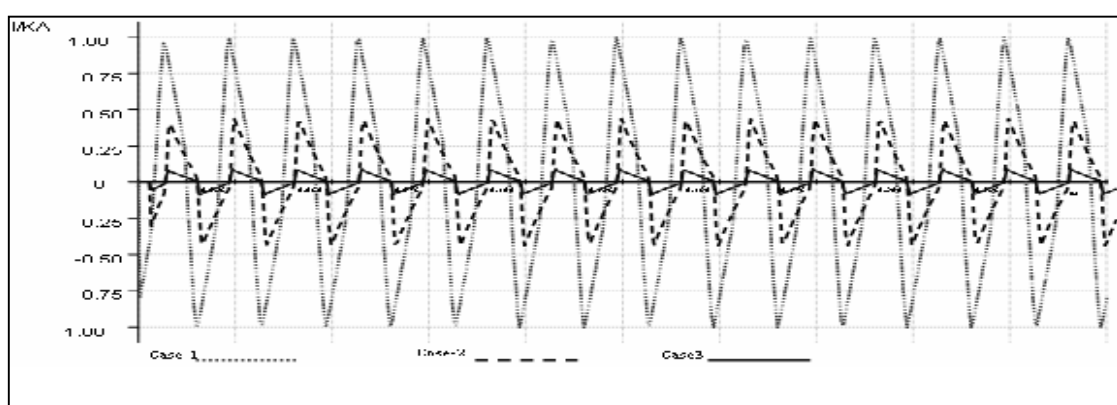
Figure 3.11 EMTP Results Obtained for all Cases, with 26V saturation Voltage Selection
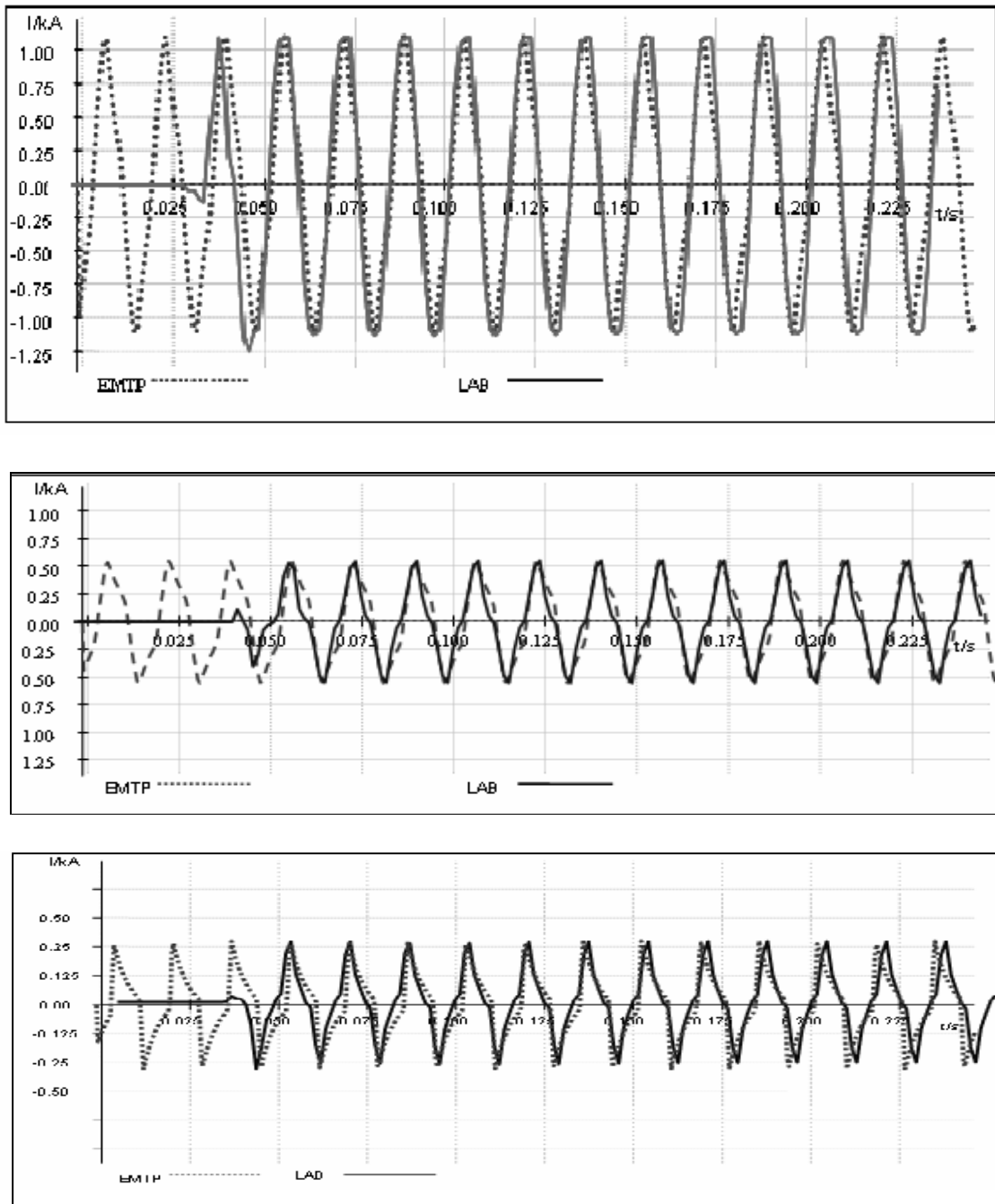
Figure 3.12 Comparison of EMTP and Lab results for cases 1, 2 and 3 respectively

Harmonic analysis, using EMTP has been carried out to compare the transient response of the CTs through testing and modeling. Figure 3.13 shows the harmonics analysis for case-1, where low secondary burden is used. The fundamental harmonic magnitude is almost the same for both test and model results. Although the harmonics above the fifth harmonics could not be traced by the relay due to the relatively low sampling rate of the relay (12 samples per cycle), acceptable results were obtained. Figure 3.14 compares the harmonic currents of the laboratory and model results for case-2 where higher secondary burden is used and more CT saturation is encountered. Similar to case-1, harmonics up to the fifth harmonics were captured by the relay. Harmonic analysis is also carried out for the third case and presented in figure 3.15. In this case, very severe CT saturation is experienced. Harmonics above the fifth harmonics have relatively higher magnitude due to the CT saturation. For comparison purposes, EMTP harmonics analysis was provided up to the fifth harmonics. However, harmonics above the fifth harmonics will be considered later in the error analysis.
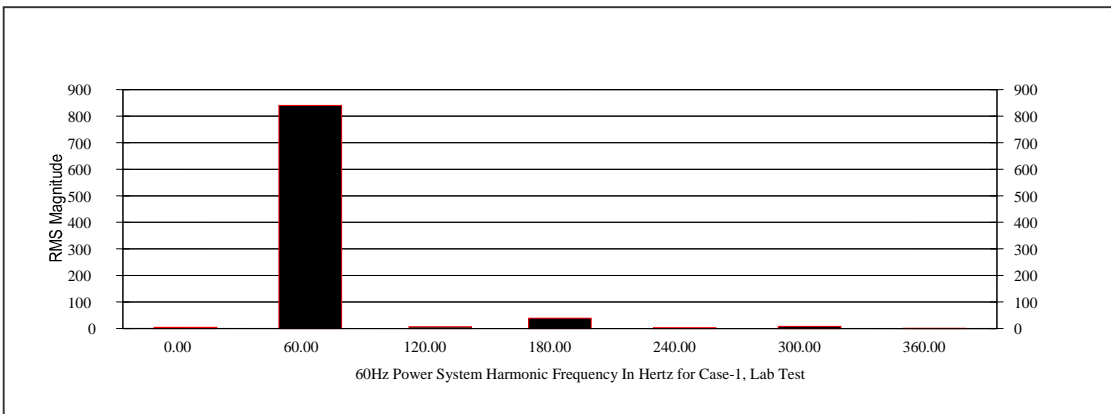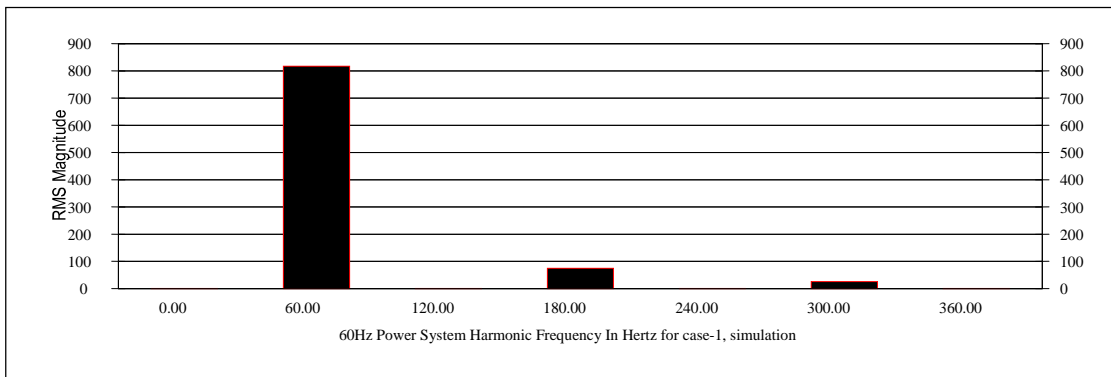
Figure 3.13 Harmonic analysis for Case-1 Lab and EMTP Output Signals
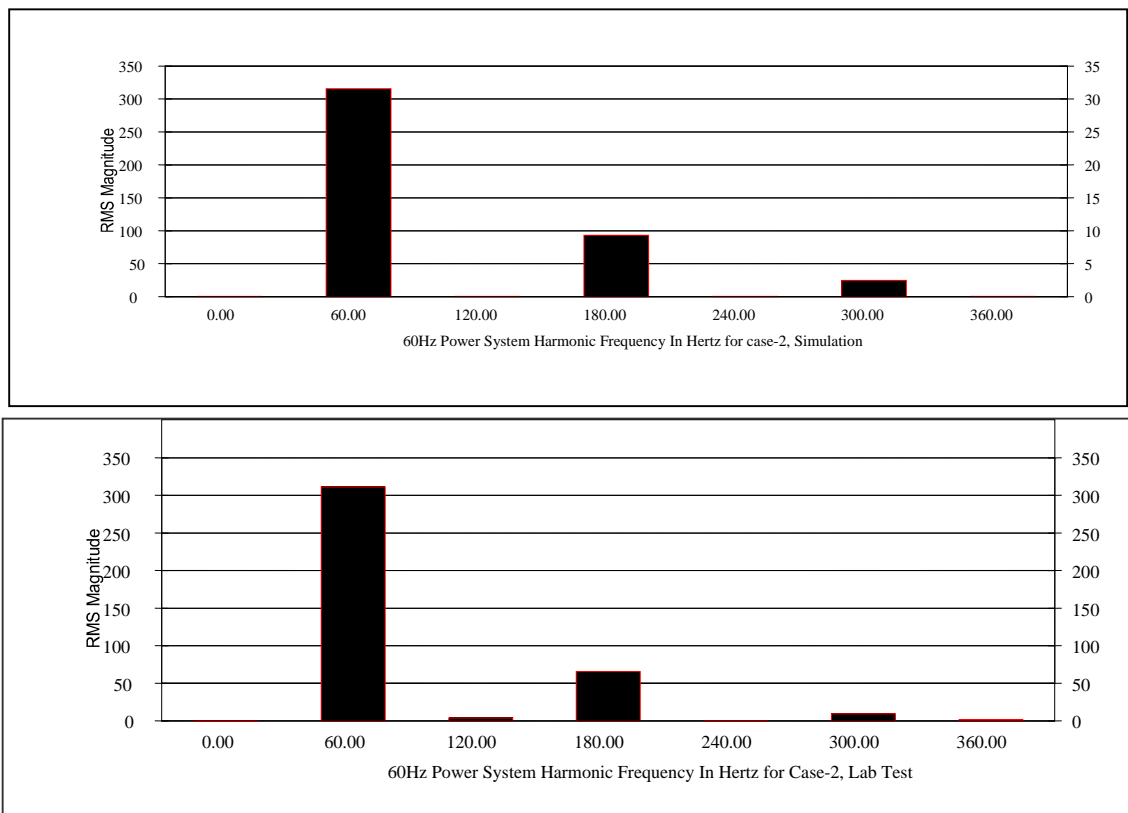
Figure 3.14 Harmonic analysis for Case-2 Lab and EMTP Output Signal
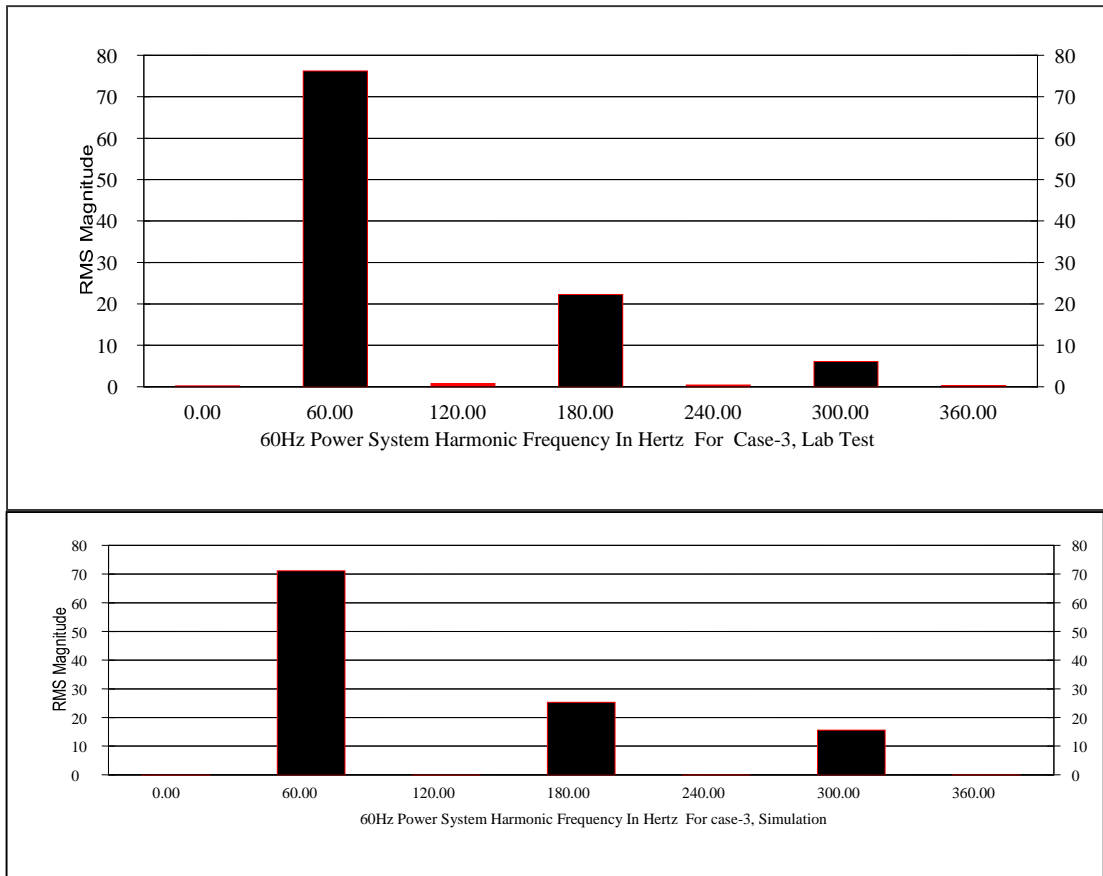
Figure 3.15 Harmonic analysis for Case-3 Lab and EMTP Output Signal

In order to analyze the harmonic analysis of EMTP and laboratory results, an error analysis of the harmonics presented in the current outputs of the current signals by measuring the total harmonic distortion (THD) factor as per IEEE Standard 519-1992 [35]. It is defined as the ratio of the root-mean-square of the harmonic content to the root-mean-square value of the fundamental quantity, expressed as a percent of the fundamental. It can be calculated by the following formula:

$$THD = \sqrt{\frac{\text{sum of all squares of amplitude of all harmonic currents}}{\text{square of the amplitude of the fundamental currents}}} \qquad (3.8)$$

The current output signals, obtained by both laboratory tests and EMTP simulations contain harmonics as shown in Figures 3.13-3.15 due to the effects of CT's saturations. Calculations of the THD in each case have been carried out. Table 3.2 highlights the THD level in each case. The results show that harmonic factor calculations for the simulated signals are always higher than the laboratory test results. This error is due mainly the quite low sampling rare (12 samples/cycle) of the relay used to capture the CT output current. Harmonics above the fifth harmonics could not be traced by the relay.

Table 3.2. Error analysis of harmonics Study for EMTP Model Validations

Case	Distortion Factor (THD) as per IEEE 519-1992		
	Lab Results	**EMTP Results**	**Difference**
Case-1	6.23%	9.67%	3.44%
Case-2	25.71%	30.47%	4.76%
Case-3	34.83%	41.68%	6.85%

3.4 Results and Conclusion

A comparison between transient response obtained by laboratory tests on the actual CT and those obtained by digital simulation using EMTP reveals the following:

- EMTP based CT models, using non-linear inductor model (Type-96) are a convenient way of simulating fault transient for relay study. They can easily be connected to an EMTP model of the power network.

- The harmonics contents of the output signals for both laboratory testes and simulations analysis proved that an acceptable modeling of the CT is achieved. Differences in the harmonics contents are mainly due to the quite low sampling rate (12 Samples/Cycle) of the relay used to capture the CT output current in laboratory. Harmonics above the fifth harmonics could not be traced by the relay.

- CT models, which use Type 96 element for the hysteresis representation, are sensitive to the selection of saturated point needed for hysteresis generation. That point is not precisely determined for the V-I curve. Points selected in deeper saturation, with excitation current of 2A or above give satisfactory and close results to the actual values.

- The EMTP developed CT model can be effectively utilized to test the digital relays as it provides very accurate representations of the actual CT performance.

After successfully validating the CT's developed EMTP Model, it will be used in the following chapter to demonstrate and investigate the effects of secondary burden, accuracy class, short circuit level, X/R ratio (DC offset) and remanent flux in the core on CT's behavior.

CHAPTER 4

EMTP TRANSIENTS ANALYSIS OF CURRENT TRANSFORMER PERFORMANCE

4.1 OBJECTIVE OF THE ANALYSIS

The EMTP model of the CT's, developed and validated in Chapter-3, will be utilized to demonstrate and investigate the effects of following factors:

- Secondary burden and accuracy class and their effects on CT's saturation.

- Short circuit level and its impact on the CT's operation.

- The effect of X/R ratio (DC offset) on CT's saturation.

- The effect of remanent flux in the core on CT's behavior.

The examination of these items will provide the necessary support to investigate the effects of CT's on protective relays and consequently on the protection system. The full understanding of the behavior of CT's will facilitate the study and evaluation of the digital overcurrent relay response to transient events. For the purpose of analysis, a multiple ratio CT (1200/5), Class C-200 with 900 tap will be used to examine the effects of the factors mentioned above. Figures 4.1 and 4.2 show the EMTP nonlinear model (Type-96) for the CT and the hysteresis loop developed respectively for the 1200/5 CT at tap 900. The EMTP nonlinear model consists of an ideal transformer and non-linear reactor to take into consideration the non-linearties of current transformers. The burden of the CT is represented by series resistor and reactor as shown in the model. The piece-wise linear

segment of the hysteresis loop, shown in figure 4.2, is obtained as an output of EMTP subroutines, explained in Chapter 3.

4.2 Effects of CT's Burden and Accuracy Class on its Saturation

The burden of a current transformer, as defined in IEEE C37-110, is the property of the circuit connected to the secondary of the circuit connected to the secondary winding that determines the active and reactive power at the secondary terminals. The burden is expressed either as total ohms impedance, together with the effective resistance and reactance components, or as the total volt-amperes and power factor of the secondary devices and leads at the specified values of frequency and current. The accuracy of CT's is defined by IEEE C37-110-1996, as the extent to which the current in the secondary circuit reproduces the current in the primary circuit in the proportion stated by the marked ratio, and represents the phase relationship of the primary current. The accuracy class can be obtained by calculations or by test. The test will determine the minimum secondary terminal voltage that transformer will produce at 20 times rated secondary current with one of the standard burdens without exceeding the accuracy class limit (10%).
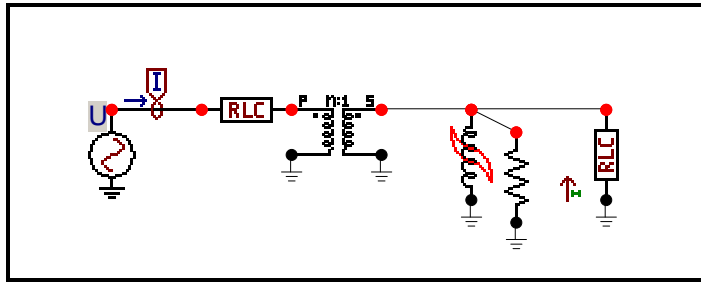
Figure 4.1 EMTP Nonlinear Model of Current Transformer
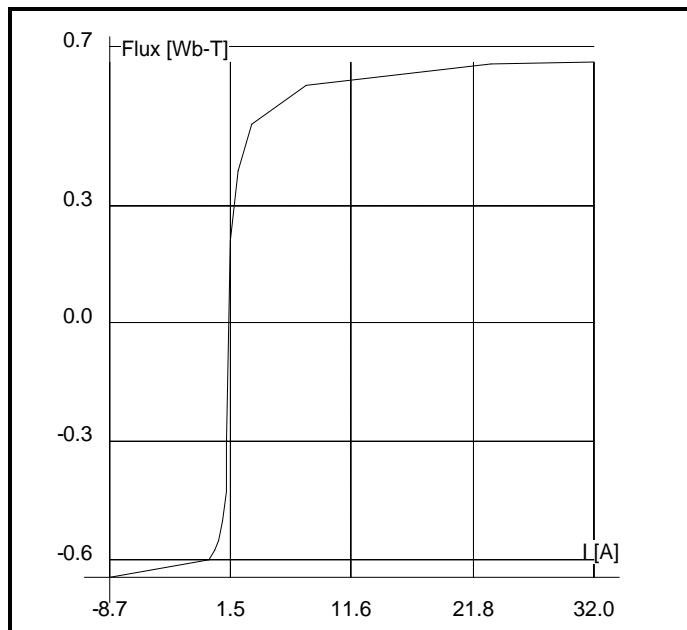
Figure 4.2 Hysteretic Loop for 1200/5 CT at Tap 900 (Output of EMTP Subroutines)

As highlighted previously and for the purpose of analysis, the transformer can deliver to a standard burden at 20 times the rated secondary current without exceeding the 10% ratio correction. The current transformer considered for analysis has been presented in a published paper [7]. The CT has a class of C200 at the maximum Tap (1200/5). Since the secondary voltage capability is directly proportional to the connected tap, the CT will support a voltage of (900/1200 x 200V) or 150V. Twenty times rated secondary current is 100 A. Therefore, the maximum burden is 150/100 or 1.5 ohm. This burden does not include the secondary resistance of the current transformers.

Table 4.1, shows the study cases to investigate effects of the connected burden on the CT saturation and its capability to reproduce the primary signal on the secondary side. The burden voltage V_b is considered resistive to reflect the worst-case condition. The burden values shown in Table 4.1 are the total burden, including the secondary resistance of the CT. The first case considers the standard burden for the CT, as found in the simulations. The burden value is then increased to show the effect of additional burden on the CT's performance. There is a practical concern where the CT's, are sometimes, located far away from the relay and thus will result in higher CT's burden.

Table 4.1. Cases applied to examine the burden effect on CT's

Primary Injected Current	Burden (Ohm)	
	Case 1	1.5
20 X CT Rating Current	Case 2	1.93
(18,000 RMS Current)	Case 3	5.0

Figure 4.3 shows the primary injected current with 20 times CT rating current. Figure 4.4 shows the secondary current output of the CT when a standard secondary burden is used. The primary current is reproduced accurately with no CT saturation. The magnitude and shape of the CT's output are accurately obtained, as expected, with no CT saturation.

In case-2, the secondary burden is increased to 1.93 ? and consequently initial saturation is observed as shown in figure 4.5. The magnitude of the CT's output is found to be 141A, matching with the anticipated magnitude. However, the shape of the secondary signals is slightly distorted. The secondary burden is then increased to 5 ? (3.3 times the standard burden). The secondary current magnitude is significantly reduced by 12% and the waveform shape is distorted as shown in Figure 4.6. The CT experienced severe saturation.

Figure 4.3 Injected Primary current (18,000 RMS Amp)
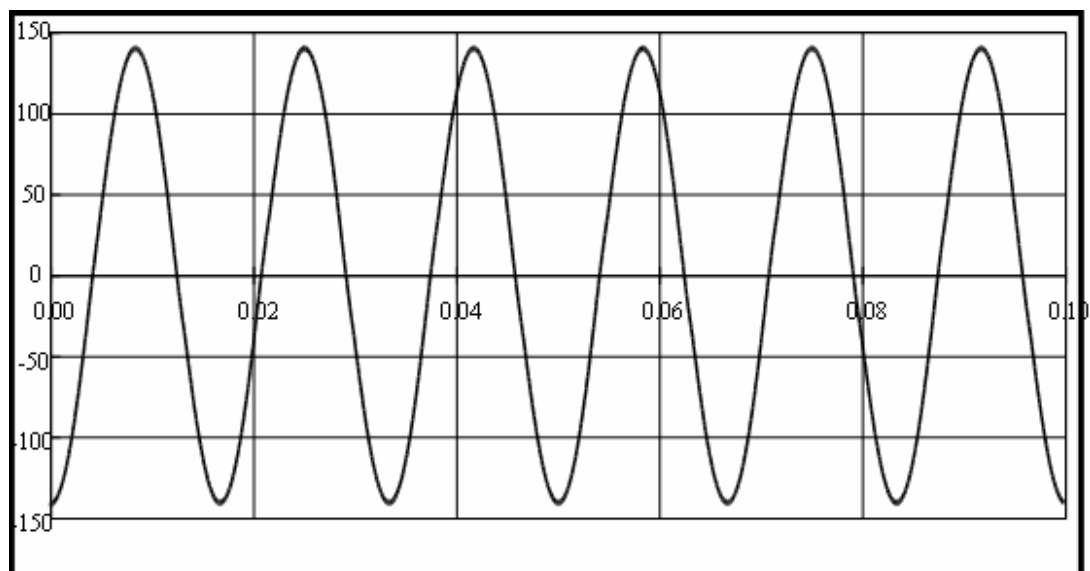
Figure 4.4. Full Reproduction of the Secondary Current with 1.5 Ohm
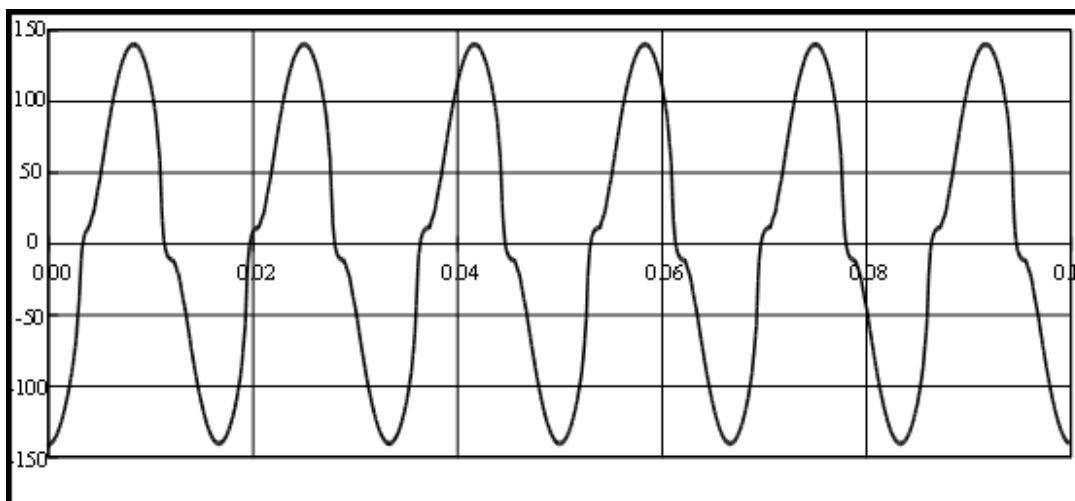
Figure 4.5 Initial CT Saturation- Secondary Current with 1.93 Ohm
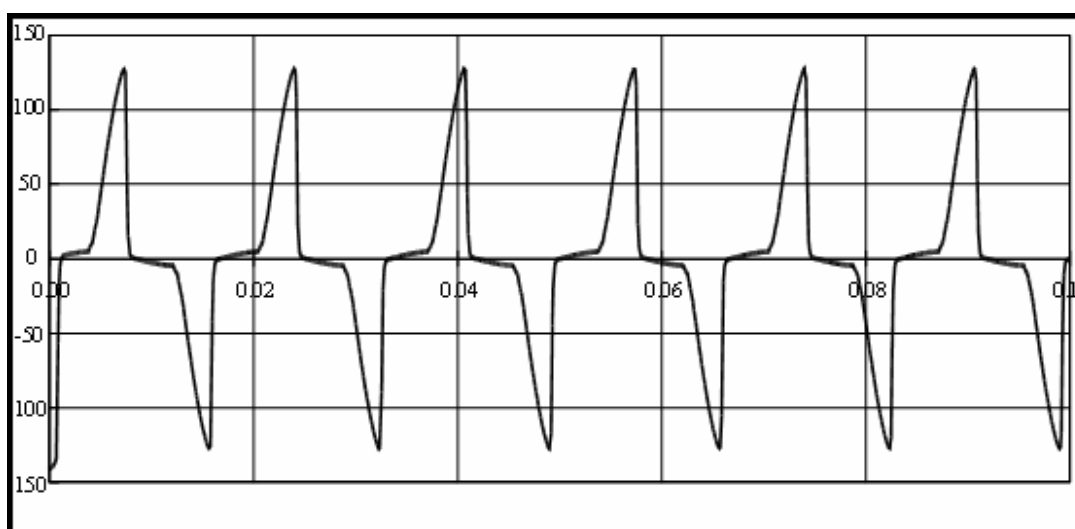
Figure 4.6 Severe CT Saturation - Secondary Current with 5.0 Ohm

4.3 Effects of the short circuit level on CT performance

In general, CT ratios are selected to match the maximum load current requirements, i.e., the maximum design load current should not exceed the CT rated primary current. The highest CT ratio permissible should usually be used to minimize wiring burden and to obtain the highest CT capability and performance. The CT should be large enough so that the CT secondary current does not exceed 20 times the rated current under symmetrical primary fault current.

The use of low ratio CT's on circuits of rated current where fault current levels are very high, presents problems of reduced CT capability. These problems can be minimized by using the highest CT ratio that is compatible with low current relays and instruments. In this analysis, the behavior of the CT's will be examined, considering the standard burden, to show its performance under various symmetrical short circuit levels. Summary of the analysis is provided in Table 4.2.

Table 4.2 Cases applied to examine the primary symmetrical faults effect on CT's

Primary Injected Current	Burden (Ohm)
Case 1 20 X CT Rating Current (18,000 RMS Current)	Standard Burden (1.5)
Case 2 23 X CT Rating Current (20,700 RMS Current)	
Case 3 40 X CT Rating Current (36,000 RMS Current)	

Case 1, considered injecting a primary current of 20 times the CT rating at the secondary standard burden. Figure 4.7 shows the simulated primary injected current. Full reproduction of the primary current at the CT secondary is achieved and is shown in figure 4.8. The primary current magnitude is accurately reproduced at the secondary of the CT with no error. Symmetrical fault current is then increased to 23 times the CT rating. As shown in figure 4.9, initial CT saturation is experienced where the shape of the secondary current wave is little distorted. The ideal CT should reflect sinusoidal current wave with peak magnitude of 163A. Due to CT saturation, only 152A peak current is obtained with a magnitude reduction of 7%. In case-3, very high symmetrical fault current is injected into the CT. The injected current is 40 times the CT rating. As a result, severe CT saturation is experienced at the secondary terminals of the CT. Both magnitude and shape of the secondary current are significantly affected as shown in figure 4.10. The ideal CT should reflect the primary current signal with a peak magnitude of 282A. However, the real model shows that the CT will be capable to deliver a distorted secondary current with a peak of 270A.
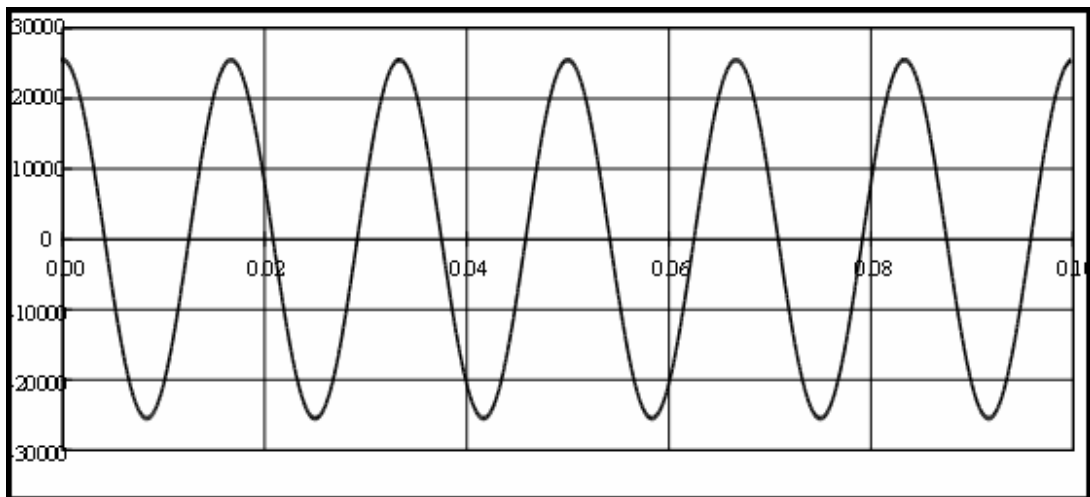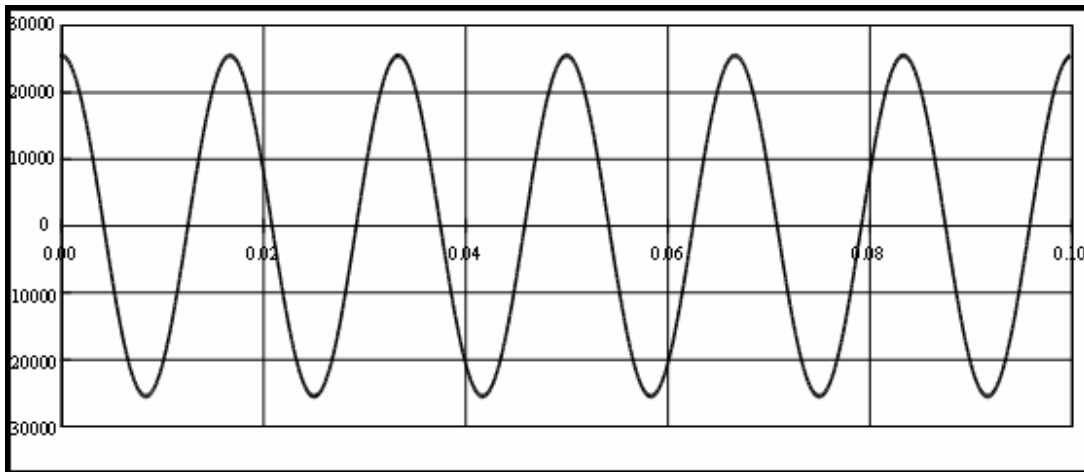
Figure 4.7 Injected Primary current (18,000 RMS Amp)
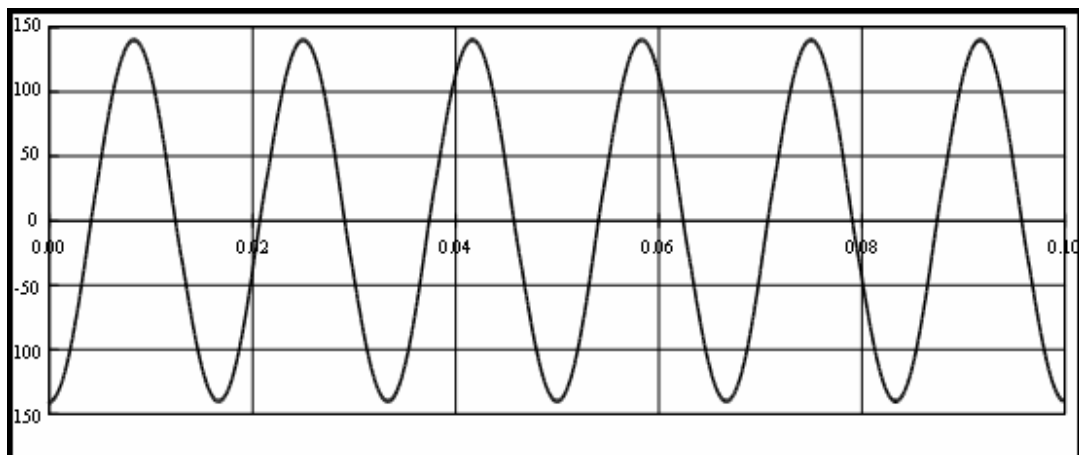
Figure 4.8 Full Reproduction of the Secondary Current (case-1)
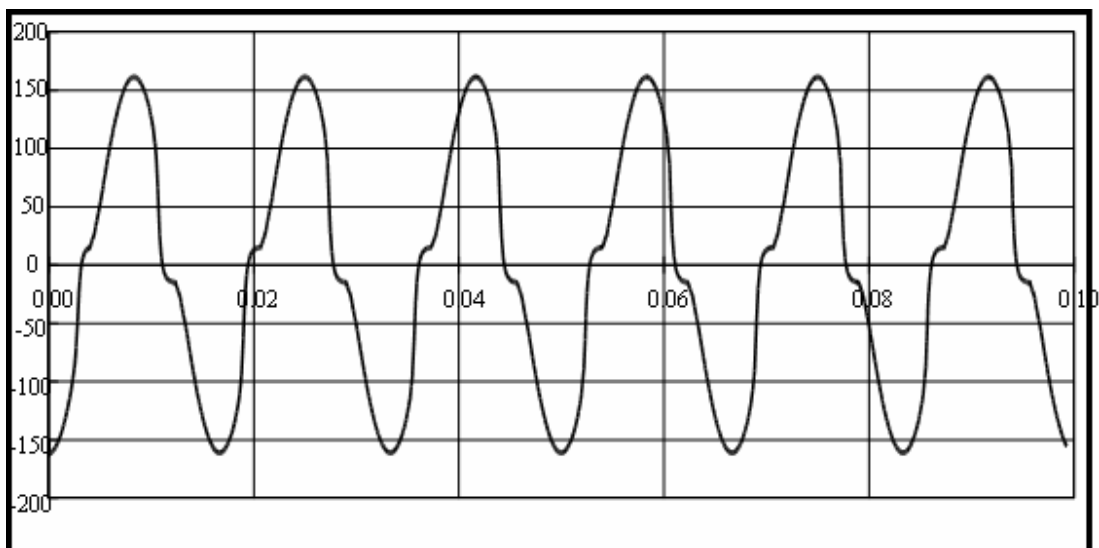
Figure 4.9 Initial CT Saturation- Secondary Current (case-2)
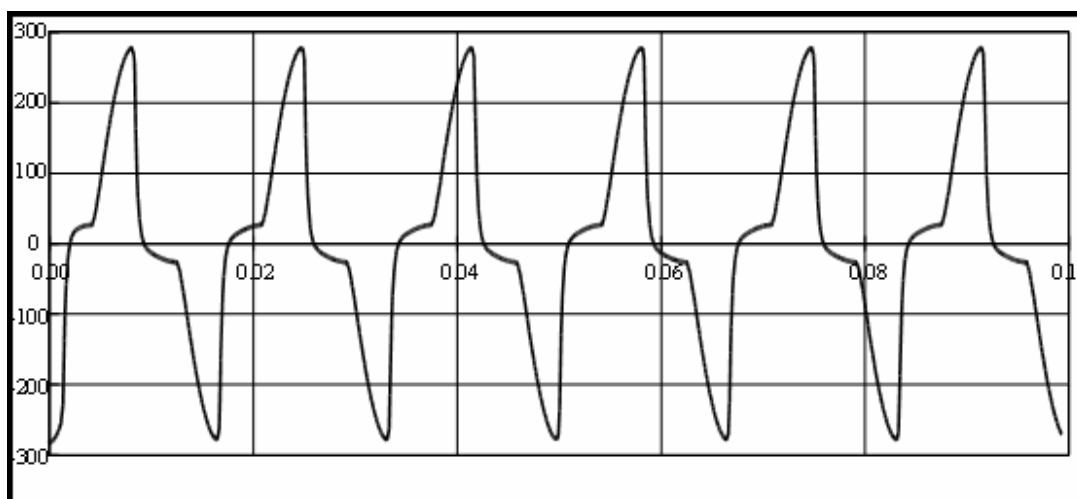
Figure 4.10 Severe CT Saturation-Secondary Current (case-3)

4.4 Effects of System X/R Ratio on CT's Saturation

CT performance is affected significantly by the dc component of the ac current. When a current change occurs in the primary ac system, one or more of the three-phase currents may contain some dc offset. This dc results from the necessity to satisfy two conflicting requirements that may occur: (1) in a highly inductive network, the current wave must be near maximum when the voltage is at or near zero, and (2) the actual current at the time of the change, which is determined by the prior networks conditions [17].

During asymmetrical faults, the fault current can be represented by two parts, namely the dc and ac components follows:

$$I_{Fault} = I_{dc} + I_{ac} \qquad (4.1)$$

The total fault current can be rewritten as:

$$I_{Fault} = I_F \cdot (e^{-\frac{R}{L}t} - \cos(\omega t)) \qquad (4.2)$$

Figure 4.11 shows the shaded volt-time area produced by asymmetrical fault current. Here I_F is the magnitude of the fault current in the secondary, Z_b is the burden impedance, and *L/R* is the time constant of the primary fault circuit. The sine wave and exponential components of the wave are shown dashed for comparison. The sine wave and the exponential represent the asymmetrical fault in equation 4.2. The plot shows the

change of burden voltage with the time. The volt-time area of the asymmetrical fault is increased compared to the normal sine wave and hence will affect the performance of the CT and the relay.

The burden voltage can be expressed as follows:

$$V = I_F \cdot Z_b \cdot (e^{-\frac{R}{L}t} - \cos(\omega t)) \tag{4.3}$$

The burden voltage V is related to the core turn N and the rate of change of the core flux by the induction as shown in equation [33]:

$$V = N \cdot \frac{d\varphi}{dt} \tag{4.4}$$

We can integrate Equation (4.4) to show that the flux density in the core is represented by the area under the voltage waveform. In other words, for a given secondary fault current, more burden voltage from the CT will be required and the core density is proportional to the time-integral of this voltage. Therefore, the flux linkages in the core are given by the integral of equation (4.5) where the flux is expressed as flux density B times the core cross sectional area A.

$$\varphi \cdot N = B \cdot A \cdot N = \int_0^t V \cdot dt \tag{4.5}$$
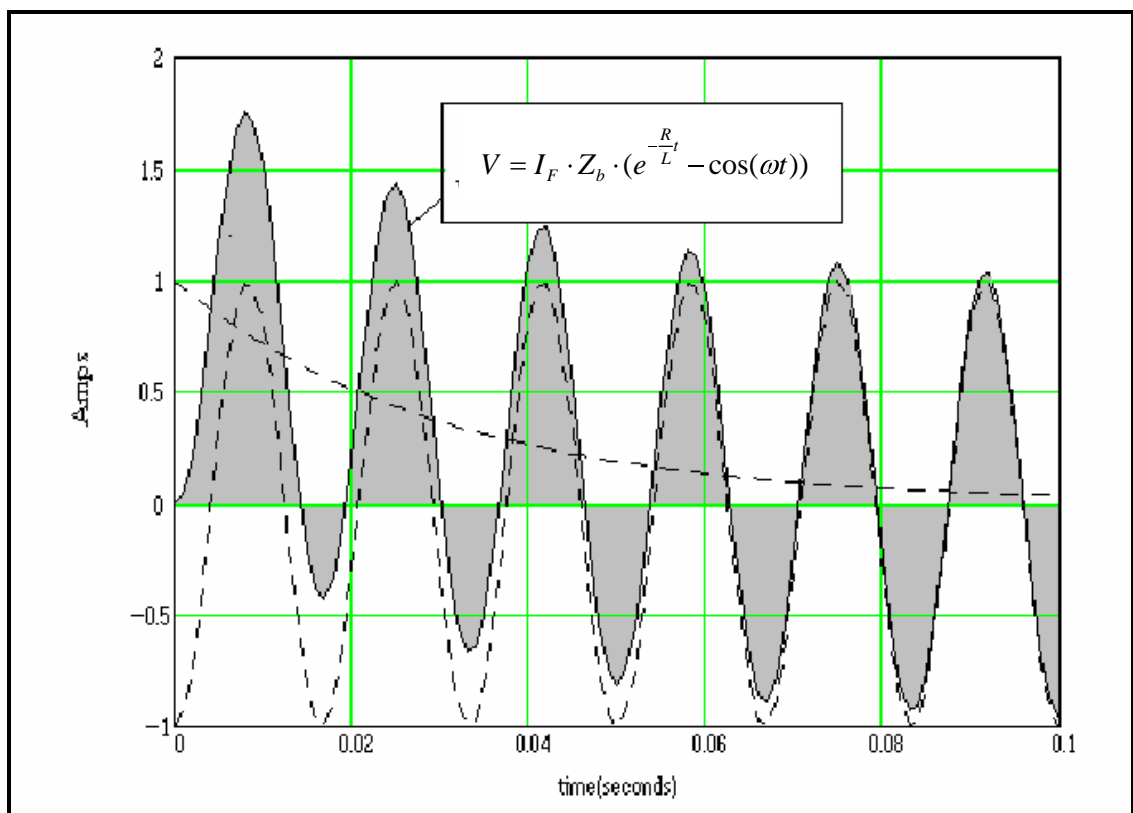
Figure 4.11 Fault Current with AC and DC components [21]

Using the asymmetrical burden voltage equation (4.3) and substituting in equation (4.5) will result in the following equation:

$$B_s \cdot N \cdot \omega \cdot A = I_F \cdot Z_b \left[-\frac{\omega L}{R} \int_0^t e^{-\frac{R}{L}t} \left| -\frac{R}{L} dt \right| - \int_0^t \cos(\omega t)(\omega dt) \right]$$

(4.6)

In Equation (4.6), the limit of the integral of the exponential term is the X/R ratio of the primary circuit. Since the limit integral of the cosine term is unity, we can write the equation as follows:

$$B_s \cdot N \cdot \omega \cdot A = \left| \frac{X}{R} + 1 \right| \cdot I_F \cdot Z_b$$

(4.7)

Equation (4.7) expresses the C-rating voltage in terms of the physical parameters of the CT, namely the saturated flux density B_S, the turns ratio N, the core cross-sectional area A, and the system frequency f.

A different form of Equation (4.7) can be derived by recognizing that the rating voltage is 20 times the voltage across the standard burden at rated current. If we then express the fault current I_F in per unit of the rated current and the burden Z_b in per unit of the standard burden, equation (4.7) becomes the simple IEEE Standard criterion to avoid saturation:

$$20 \geq \left| \frac{X}{R} + 1 \right| \cdot i_f \cdot z_b \tag{4.8}$$

Where: i_f is the maximum fault current in per unit of CT rating

        z_b is the CT burden in per unit of standard burden

        X/R   is the X/R ratio of the primary fault circuit

The EMTP CT model, in Figure 4.12 has been developed to analyze the effects of X/R ratio on the current transformer performance. Various cases were implemented, with different X/R ratios and injected primary current magnitude, assuming a standard burden with no remenance flux in the CT's core. Table 4.3, summarizes the studies that will be carried out using the developed EMTP CT model.
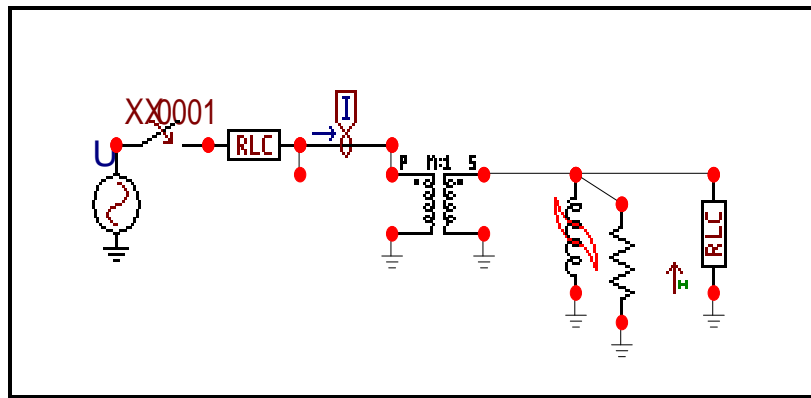
Figure 4.12 EMTP Model of Current Transformer for X/R Effects Analysis

Table 4.3. Cases applied to examine the X/R ratio effect on CT's

Case	Primary Symmetrical Current	Primary Asymmetrical Current	X/R Ratio	Saturation equation criteria
1 (a)	0.98 x CT rated Current	1.80 x CT Rating	16	(X/R+1)*If*Zb = 16.7
1(b)		2.34 x CT Rating	24	(X/R+1)*If*Zb = 24.5
2(a)	1.70 x CT rated Current	3.69 x CT Rating	16	(X/R+1)*If*Zb = 28.9
2(b)		4.08 x CT Rating	24	(X/R+1)*If*Zb = 42.5
3(a)	3.20 x CT rated Current	5.57 x CT Rating	16	(X/R+1)*If*Zb = 54.4
3(b)		6.46 x CT Rating	24	(X/R+1)*If*Zb = 80

Case-1 (a) represents the secondary current output of the developed CT model with DC offset (X/R =16) as can be seen from figure 4.13. The output is reproduced accurately and saturation could be avoided since IEEE Standard C37.110-1996 criteria in equation 4.8 is met. Case-1 (b) is similar to the previous cases, except that the system X/R is raised to 24. Figure 4.14 shows initial CT saturation. In case-2 (a) and case-2 (b), higher primary fault current is injected with system X/R ratios of 16 and 24 respectively. The CT is driven into saturation starting with the second cycle as shown in figures 4.15 and 4.16. More distortion in the secondary current waveform is experienced with higher X/R ratio. In cases 3 (a) and case-3 (b), secondary current of CT's experienced severe saturation and its peak remains low and distorted for the subsequent three cycles of the transient as shown in figure 4.17 and 4.18.
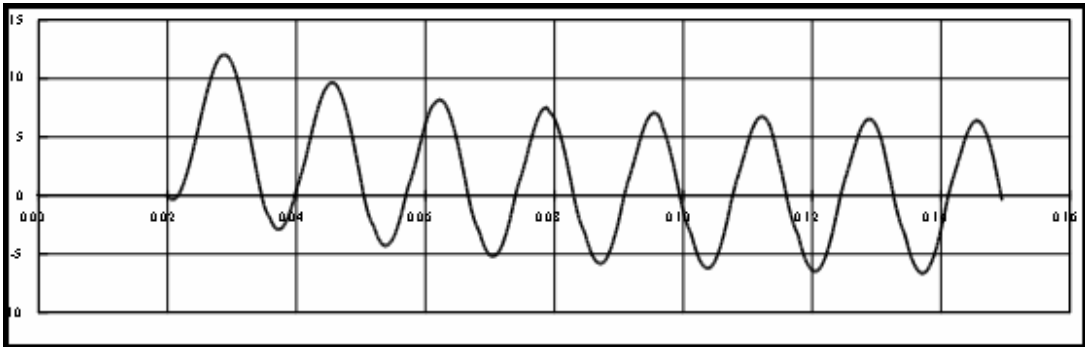
Figure 4.13 Case1 (a), Secondary current with X/R = 16
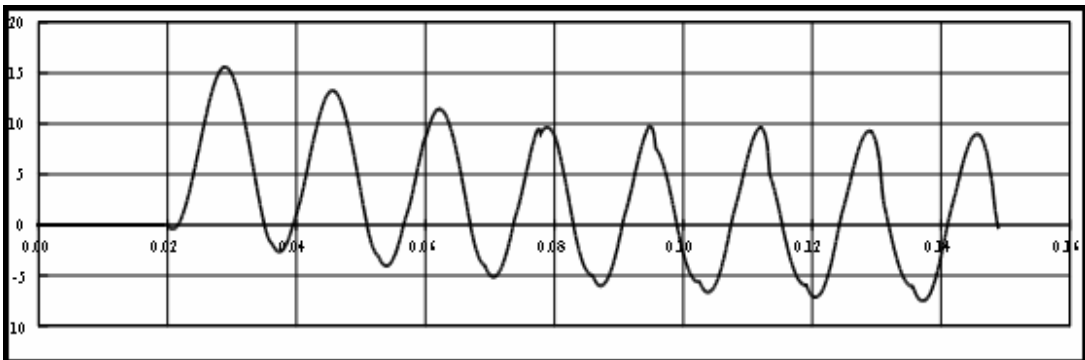
Figure 4.14 Case1 (b), Secondary current with X/R =24
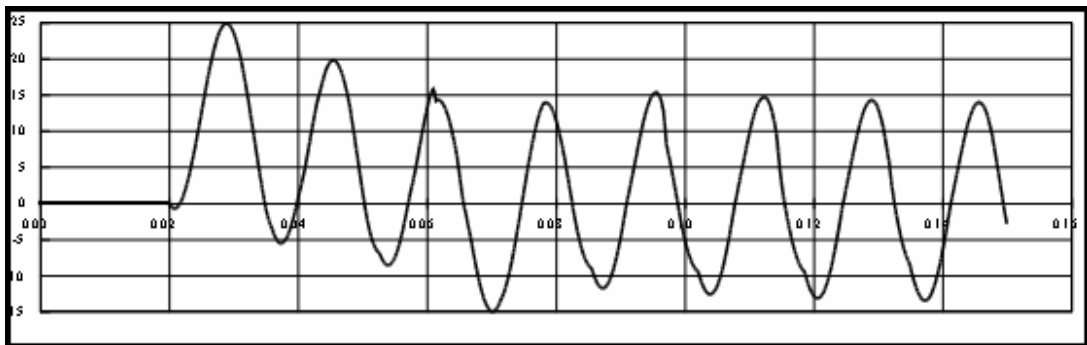
Figure 4.15 Case2 (a), Secondary current with X/R = 16
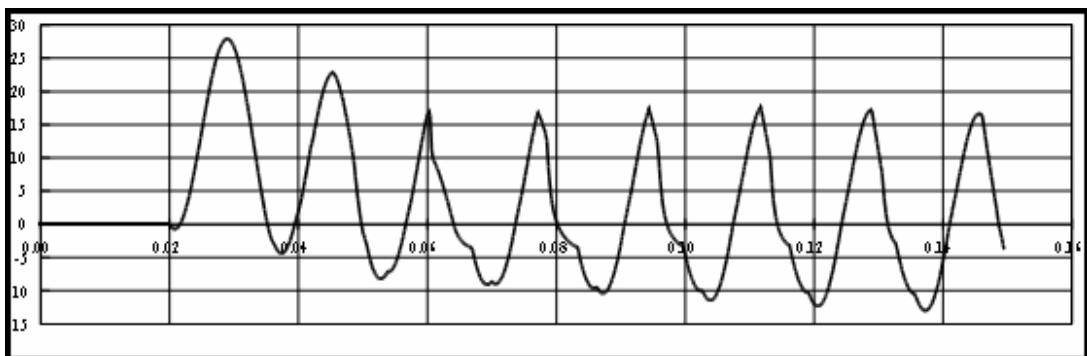
Figure 4.16 Case2 (b), Secondary current with X/R =24
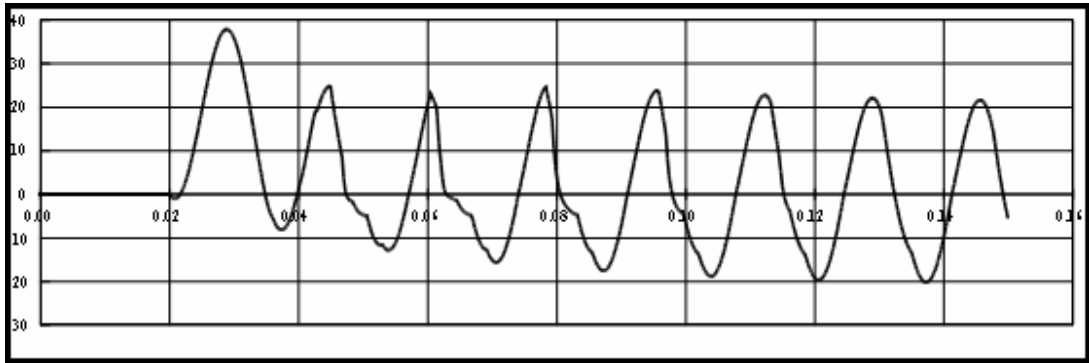
Figure 4.17 Case3 (a), Secondary current with X/R =16
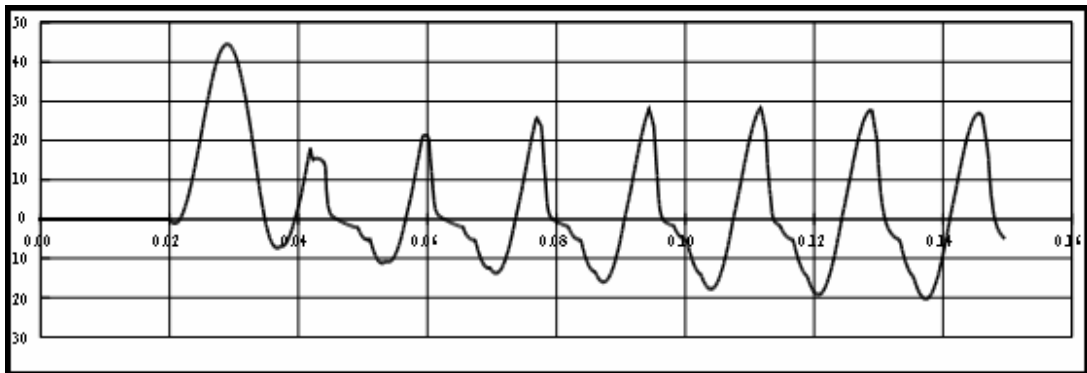
Figure 4.18 Case3 (b), Secondary current with X/R =24

4.5 Effects of Remanent Flux on CT Performance

As per IEEE standard C37.110-1996, the remanence is the magnetic flux density that remains in a magnetic circuit after the removal of an applied magnetomtoive force. The remanent flux in a CT core depends on the flux in the core immediately before primary current interruption. The magnitude of the flux is determined by the value of symmetrical   primary current, the dc offset, and the impedance of the secondary circuit. Maximum remanent flux is obtained when the primary current is interrupted while the transformer is in a saturated state. When the remanent flux, is of the opposite polarity to the flux due to the fault current and regardless of its percentage, the CT tends to produce an undistorted secondary current. However, if the remanent flux is of the same polarity as the flux due to the fault current, then a distorted secondary waveform is likely [8].

Figures 4.19, 4.20 and 4.21 show three waveforms representing the output current of a CT with and without remanence. The three waveforms show the CT behavior with remanence flux of 0%, 50%, and 100%. These waveforms relate to the 1200/5 C-200 multi-tap CT considered in the previous analysis. The fault current in each case is 24000 A and the dc offset has a time constant of 0.042 s (X/R = 24). The total burdens for all three cases are 1.8 ohm. In Figure 4.20, the same CT with same parameters is used, except that a 50 % remanent (residual) flux is imposed on the CT prior to subjecting it to transients. In this case, the CT is driven into saturation early in the first half cycle and the output current remains distorted throughout part of the test cycles. In Figure 4.21, a 100% remanent flux is imposed on the CT prior to subjecting it to the transient. Severe CT saturation and waveform distortions are experienced in the first half cycle.
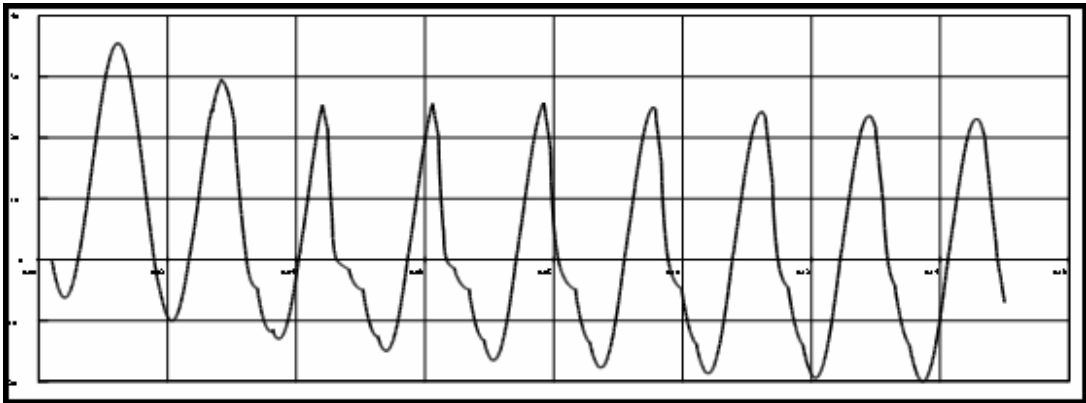
Figure 4.19 Secondary current with 0% remanent flux
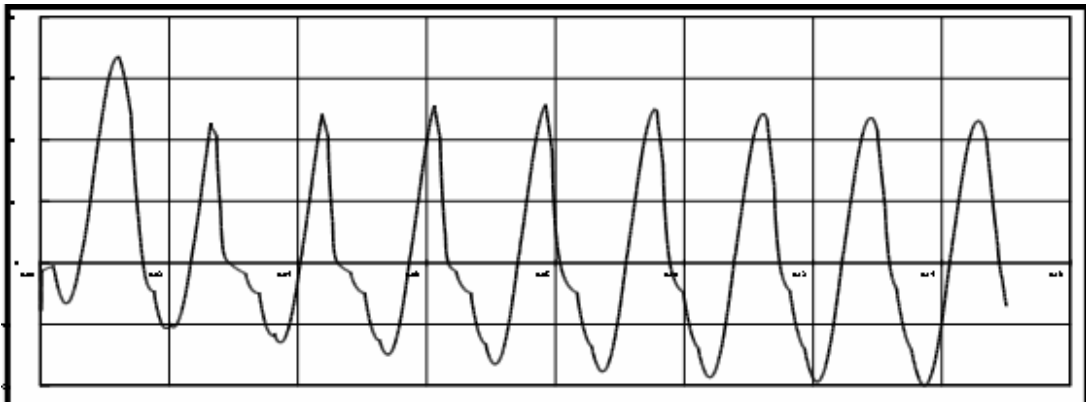
Figure 4.20 Secondary current with 50% remanent flux
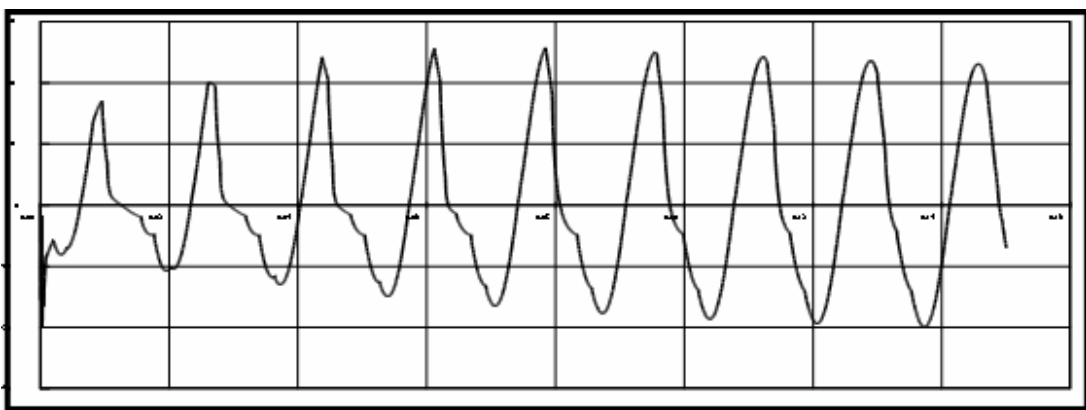
Figure 4.21 Secondary current with 100% remanent flux

The successful model of the CT will be utilized to test the performance of digital relays. In Chapter 5, a typical digital relay will be modeled and EMTP outputs will be utilized to examine its behavior.

CHAPTER 5

DIGITAL OVERCURRENT RELAY MODELING

5.1 Digital Relay Components

The operation principles of microprocessor-based relays are almost identical, although they utilize different filtering techniques. Figure 5.1 presents the schematic diagram of a typical microprocessor-based relay. The relay auxiliary transformer converts the secondary current of the CT to a scaled voltage signal. The anti-aliasing low pass filter (LPF) removes any high frequency signal present in the waveform. The A/D converter converts the signal into digital form at a typical sampling rate of 16 samples per cycle. The function of the filter is to reject all harmonics and to extract the magnitude of the fundamental content of the signal.
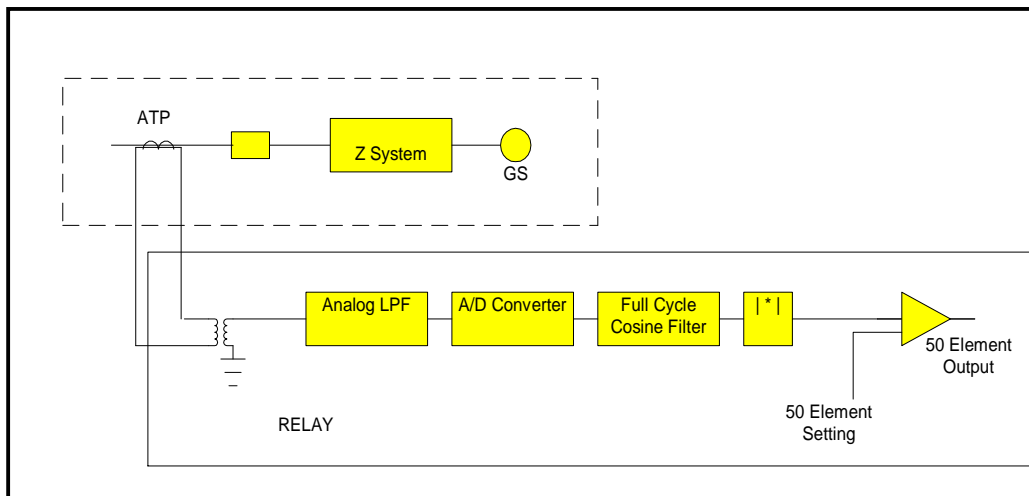
Figure 5.1 Digital Relay Schematic Diagram [22]

The aliasing phenomenon resulted from the appearance of high frequency signals, distorting the desired signal. This effect can be eliminated by filtering the high-frequency components from the input. The element that accomplishes this function is called an anti-aliasing filter. The "Nyquist criterion" states that in order to avoid the aliasing error, frequencies above one-half the sampling rate must be removed [29].

The key to the behavior of microprocessor relays is in calculating the response of the digital filter and comparing the deviation to the ideal sine-wave signal. This is obtained by sampling sine-wave currents and/or voltages at discrete time intervals. A fixed number of instantaneous samples per cycle are converted to digital quantities by an A/D converter and stored for processing. Digital filtering is the simple process of multiplying the successive samples by pre-determined coefficients and then combining them to obtain digital quantities representing the phasor components of the input.

The term "filtering" is used because the magnitude of the components change when the sampling interval remains fixed and the input frequency is varied. The filter output is then varied in magnitude and phase as a function of the input frequency. Consequently, more than two samples per cycle are used, and filter coefficients are scaled to obtain a favorable frequency response. A 16samples/cycle full cycle cosine filter is practically suited for protective relaying. While extracting the fundamental, the filter rejects all harmonics, including the decaying exponential.

The filter coefficents $\qquad CFC_n = \cos\left[\dfrac{2\pi}{16} \bullet n\right]$ $\qquad$ **(5.1)**

The Cosine filter $\qquad IX_{smpl+spc} = \dfrac{2}{N+1}\sum_{n=0}^{N} I_{smpl+spc-n} CFC_n$ $\qquad$ **(5.2)**

The phasor magnitude $\qquad \left|Io\right|_{smpl+spc} = \sqrt{(IX_{smpl+spc})^2 + (IX_{smpl+spc-\frac{spc}{4}})^2}$ $\qquad$ **(5.3)**

The Phasor Output $\qquad Io_{smpl+spc} = IX_{smpl+spc} + j \bullet IX_{smpl+spc-\frac{spc}{4}}$ $\qquad$ **(5.4)**

Where: $\quad$ N $\qquad$ = 15

$\qquad$ n $\qquad$ = 0, 1, 2,…….N

$\qquad$ smpl $\quad$ = sequence of samples 0, 1, 2, 3, ……

$\qquad$ spc $\qquad$ = number of samples per cycle (16)

$\qquad$ $I_{smpl+spc-n}$ = Current samples

$\qquad$ $IX_{smpl+spc}$ = Filter output

$\qquad$ Io $\qquad$ = Filter derived current phasor

In the cosine equation (5.2), any value of sequence of samples (smpl) indicates that 16 samples of the current have been stored. The index n, in the equation, ranges from 0 to 15 to apply the coefficient and sum the samples to produce the output. With 16 samples per cycle, 4 samples represent 90 electrical degrees. Therefore, the present output together with the output recorded four samples before constitute the real and imaginary component of the phasor [22].

5.2 Modeling Digital Overcurrent Relays

5.2.1   Why to Model the Digital Overcurrent Relays

In comparison to electromechanical relays, microprocessor relays execute algorithms that are mathematical procedures. They produce analytic characteristics that can be described accurately by an equation. Therefore, it is easy to calculate the response to specified waveforms and ensure relay operations, during abnormal conditions. The key to the behavior of microprocessor relays is in calculating the response of the digital filter and comparing the deviation to the ideal sine-wave signal.

5.2.2   Digital Relay Modeling

As explained in the previous section, the digital relay consists of the following main components:

- Analog low pass filter (LPF)

- Analog to digital converter

- Digital filter

A typical digital instantaneous overcurrent relay, with cosine filtering techniques will be modeled to examine its behavior with highly saturated current waveforms. Figure 5.2, shows the MATHCAD program developed to model the digital overcurrent relays [22].

Fisrt, secondary signal of the CT's obtained from EMTP will be used as an input the the relay model

Data =

R :=rows(Data) -1

$i := 0 .. 29999$

Data will be conveted to two colomns(Time and current) in the EXCEL sheet by using TOP program

$t := Data^{<0>}$

$IR := Data^{<1>}$

Enter the delta time used in the simulation

$De := 0.00001$

Enter the sampling rate

$RS := 16$

Calculate number of samples to crate an averaging Low Pass Filter

$lpw := floor \left(\dfrac{2}{60 \cdot De \cdot RS} \right)$

The LP averaging filter equation:

$LP(a) := \left(1 + \dfrac{1}{RS}\right) \cdot \left(\displaystyle\sum_{K=0}^{lpw-1} \dfrac{IR_{a-lpw+K}}{lpw} \right)$

$ii := lpw .. 29999$

$I_{ii} := LP(ii)$

$S := floor\left(t_{29999} \cdot RS \cdot 60\right)$

$s := 0 .. S$

$Ia_s := linterp\left(t, I, \dfrac{s}{RS \cdot 60}\right)$

Create a filter index and apply a full cycle cosine filter

$if := (RS-1) .. S$

$IF_{if} := \dfrac{2}{RS} \cdot \displaystyle\sum_{K=0}^{RS-1} cos\left(\left(K \cdot \dfrac{2 \cdot 3.14}{RS}\right)\right) \cdot Ia_{(if-(RS-1))+K}$

$iv := (RS+1) .. S$

$icpx_{iv} := IF_{iv} + IF_{iv-\frac{RS}{4}}$

$m_{iv} := \sqrt{\left(IF_{iv}\right)^2 + \left(IF_{iv-\frac{RS}{4}}\right)^2}$

Calculations of digital filter output magnitude and waveforms

$Magnitude_{iv} := m_{iv}$

$Filteroutput_{iv} := Ia_{iv}$

Figure 5.2 MATHCAD Program to model digital relay

5.3 Simulation to Test the Effects of CT's on Digital Relays, using Cosine Filtering Technique

In this section, various study cases will be presented to test the behavior of the instantaneous digital relays. Case description and results are summarized in table 5.1 for the 1200/5 CT, set at 900/5 tap that has been modeled in the Chapter 4.

In case 1, symmetrical fault with 20 X CT at the standard burden is simulated by using EMTP. No saturation is expected in the secondary current. The secondary current was injected to the MATHCAD software and output of relay is shown in figure 5.3. The relay has seen the peak current after half a cycle delay. In case 2, asymmetrical fault current with initial saturations has been injected to the relay. The injected simulated EMTP secondary current is shown in Figure 5.4. The response of the relay is shown in figure 5.5. A lower magnitude of secondary current, with 8.4A, has been seen by the relay after one cycle. In case 3, more severe saturated current signal is considered as shown in figure 5.6. The response of the relay took longer (around 10 cycles) to see the peak current as shown in figure 5.7.

Table 5.1 Cases injected to the Modeled Instantaneous Digital Relay

Case	Case Description	Primary Symmetrical Current	Result Analysis
Case 1	Symmetrical fault will be applied with no saturation	20 X CT at standard burden	Expected secondary peak value is 141.4A was seen by the relay after 0.5 cycle
Case 2	Asymmetrical fault will be applied with initial saturation	1.4 x CT at standard burden, with X/R = 24	Expected secondary peak value is 10A. 8.4A was seen by the relay after one cycle
Case 3	Asymmetrical fault will be applied with severe saturation	3.37 x CT at standard burden, with X/R = 24	Expected secondary peak value is 26.4A. 24A was seen by the relay after 10 cycles
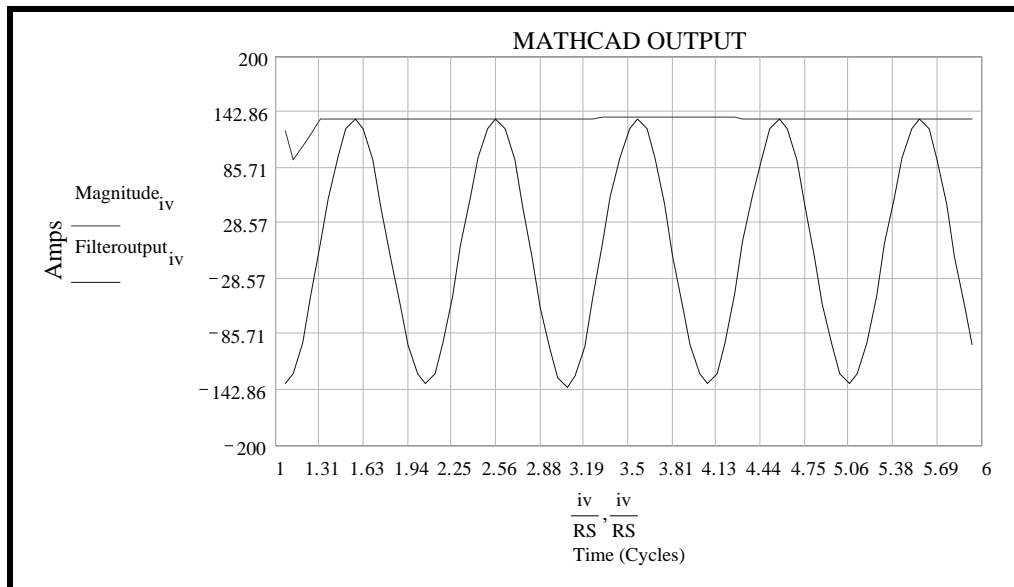
Figure 5.3 Output of the Digital Filter in the Digital Relay (Case-1)
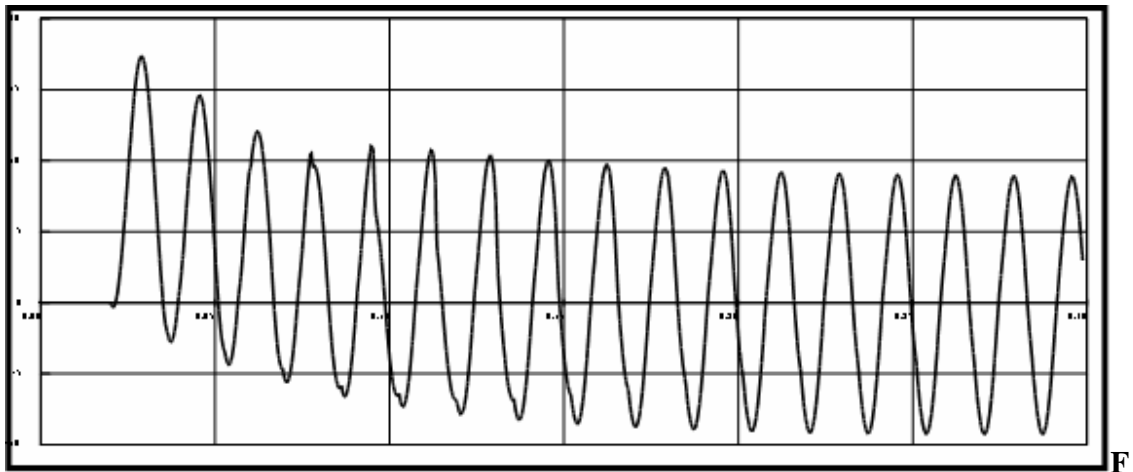
Figure 5.4 EMTP secondary current (Case-2)
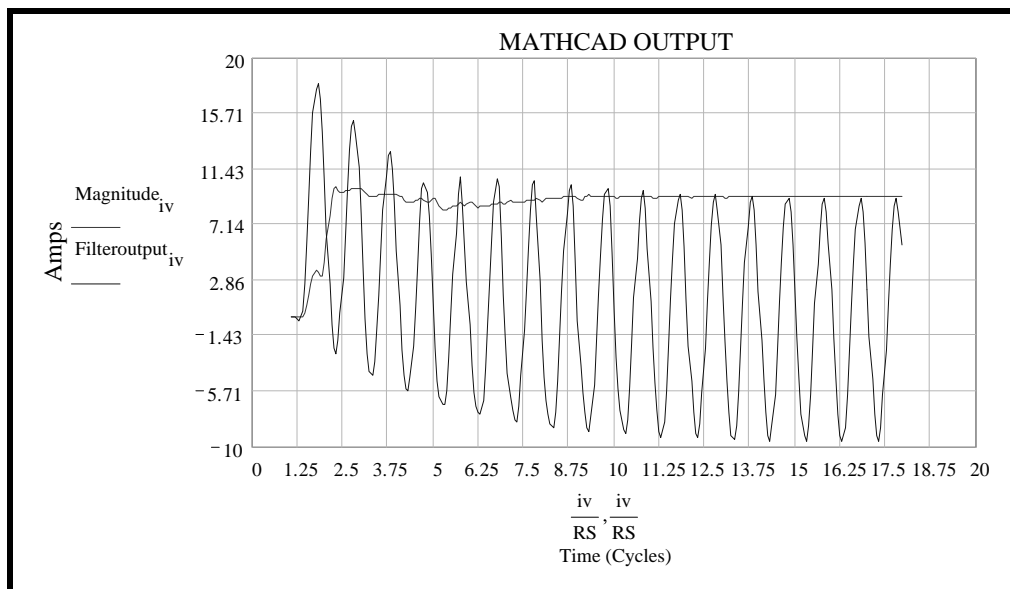
Figure 5.5 Output of the Digital Filter in the Digital Relay (Case-2)
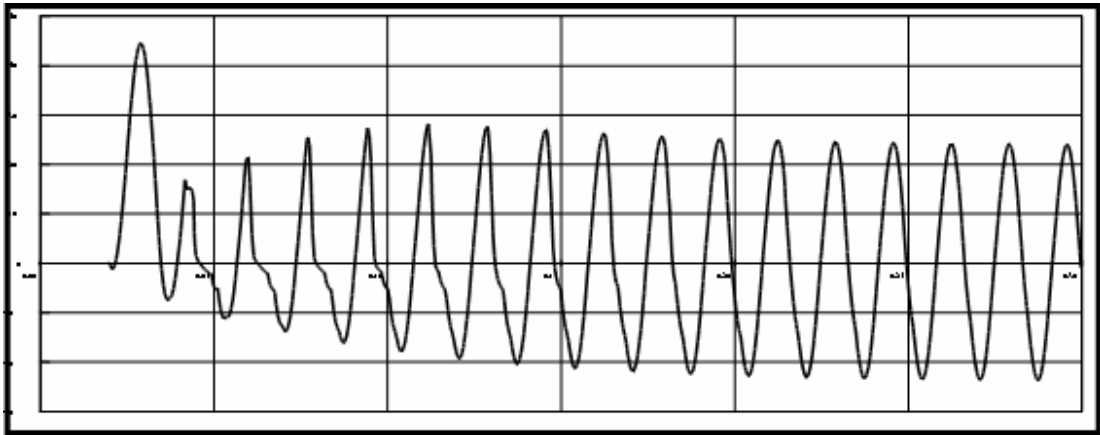
Figure 5.6 EMTP secondary current (Case-3)
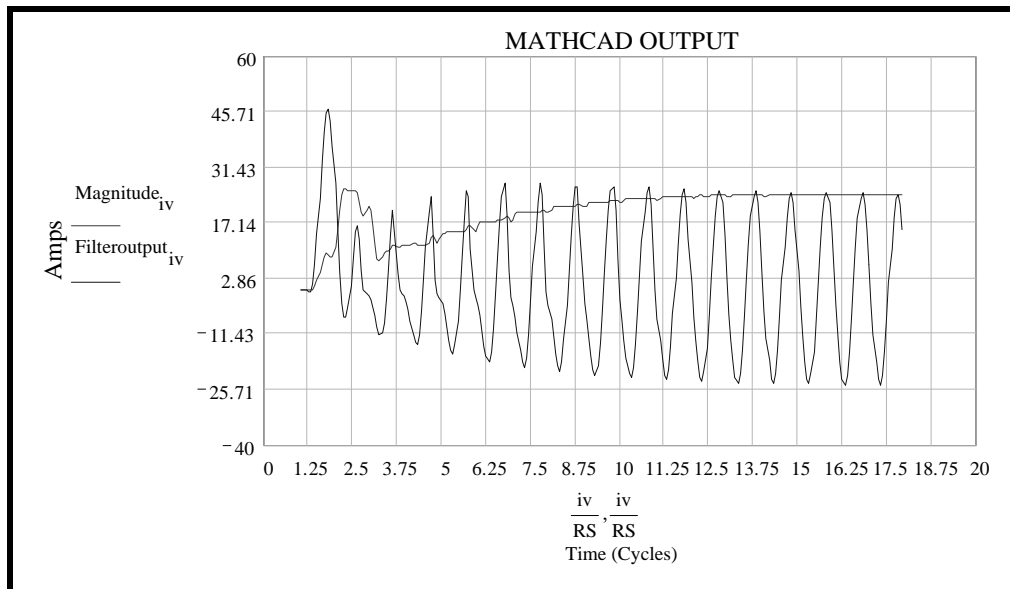
Figure 5.7 Output of the Digital Filter in the Digital Relay (Case-3)

It can be concluded from the above analysis that the relay response time is affected by CT's saturation, depending on how severe the saturation is. Chapter 6 will provide more evaluations of the digital overcurrent relays response by conducting comprehensive testing.

CHAPTER 6

TESTING THE EFFECTS OF CT SATURATIONS ON DIGITAL OVERCURRENT RELAYS

The measure of a current transformer performance is its ability to reproduce accurately the primary current in secondary amperes in both wave shape and magnitude. There are two parts: (1) the performance on the symmetrical ac component, and (2) the performance on the offset dc component. The impact of these two parts is the CT saturation, affecting protection device operations. The impact varies and depends on protective device types, their operating principles and overall protection scheme. In this chapter, the effects of CT saturation on microprocessor-based overcurrent relays will be evaluated by conducting various laboratory testing on a typical microprocessor-based overcurrent relay (Basler BE-1-951) [36]. The evaluations will consider the instantaneous and time-delayed operations of digital overcurrent relays.

6.1 Description of Digital Overcurrent Relay Testing

A set of devices and software tools are used to examine the transient behavior and performance of digital overcurrent relays during CT's saturation. These tools are as follows:

- EMTP transient model for the current transformer will be used to explore the

waveform distortion due to CT saturations and its effects on microprocessor-based overcurrent relays. The model has been selected and validated in the laboratory as explained in chapter-4.

- OMICRON CMC 256 is part of a test system that consists not only of the test device itself, but also of a PC and the testing software "OMICRON Test Universe.". External current amplifier (CMA 56) will be used as extension components to the test system in order to boost the single phase secondary injected current up to 150 A. The test equipment has the capability to inject common-trade format signals to relays. The configuration and control of the CMC 256 is performed through the test software of the OMICRON Test Universe in order to inject the developed transient case current by EMTP transient CT model to the digital overcurrent relay [37].

- Microprocessor-based overcurrent protection system (Basler BE1-951). The relay will be considered for testing. The behavior of the relay will be captured with sampling rate of 12 samples/cycle. The events will be downloaded for further analysis [36].

Figure 6.1 shows the circuit used to test the transient behavior of digital overcurrent relays. The test will be carried out through Omicron Test Universe software by controlling the secondary current injection equipment to simulate the transient cases developed by the EMTP CT model. The EMTP cases will provide an acceptable modeling of CT with high primary current. This eliminated the need for a primary current injection device and CT's along with the cables.
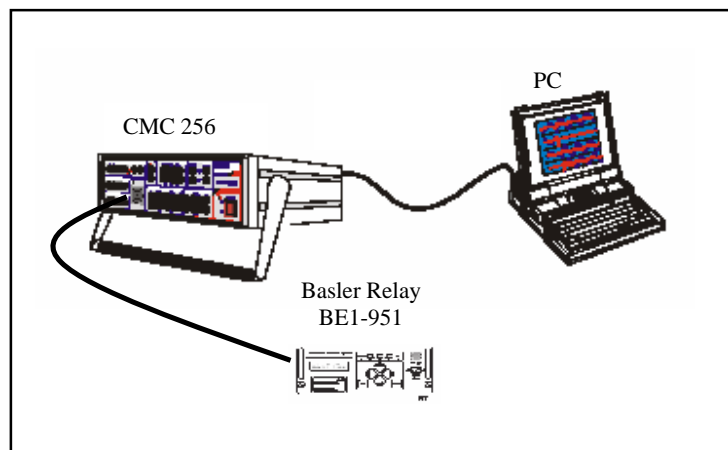
Figure 6.1 Test-Set Equipment

6.2 EMTP Cases Developed to Test the Digital Overcurrent Relays

The 50/5, C20 current transformer, described in chapter-3, will be utilized to create various study cases through the EMTP model to be used for injection in the OMICRON CMC 256, in common-trade format files. The following study cases were used to investigate the performance of the digital overcurrent relays:

- Secondary burden and accuracy class and its effects on Digital Overcurrent relays.

- Short circuit level and its impact on the CT's operation and performance of the relay.

- The effect of X/R ratio (DC offset) on CT's saturation and operations of the digital overcurrent relay.

- The effect of remanent flux in the core on CT's behavior and digital relay performance.

6.3 Effects of Symmetrical Current on Digital Overcurrent Relays

In this section, the evaluation of digital relays performance resulting from CT saturation on symmetrical AC current input will be conducted considering the following two factors:

- Current transformer burdens.

- Symmetrical fault current magnitude

As illustrated in Chapter 3, higher ohmic burdens in the CT secondary will result in a greater saturation of the core, and therefore, larger errors in the secondary current waveform. The reason for this is that a given secondary current requires more voltage from the CT for a higher burden, and the core flux density is proportional to the time-integral of this voltage. When the core becomes saturated, significant current is diverted through the CT magnetizing branch, and the desired secondary current is reduced and distorted [38]. Microprocessor-based overcurrent relays have very low impedances as seen by the CTs and can be neglected when considering CT saturation [39]. The impedance of CT's wires and the relay leads that interconnect CTs are the major causes for CT saturation. For example, CT's, located at transformers high-side, require long wires to be connected to relays, inside the substation building.

Table 6.1 summarize the cases, developed by EMTP for different CT secondary burdens that will be injected to the Basler overcurrent relay by the secondary test equipment OMICRON CMC 256. All these cases were converted to common-trade format files for the purpose of testing the digital relays by the secondary current injection Equipment. The burden is primarily due to CT windings and external leads to the relay. The relay burden itself is very small and can be neglected. In all three cases, it has been assumed that the full circuit run of #10 AWG (1.0 ? / 1000-ft) are 250 ft, 500 ft and 2000 ft respectively.

Table 6.1. Cases Applied to Examine the Burden Effect on Digital Relays

Primary Injected Current To EMTP 50/5 CT model	Burden		
	Case	Value (Ohm)	Multiple of standard burden
20 X CT Rating Current (1000 RMS Current)	Case 1	0.25	1.25
	Case 2	0.5	2.50
	Case 3	2.0	10.0

Figure 6.2 shows the EMTP simulated current-case-1 that was injected into the digital overcurrent relay. The relay response is shown in Figure 6.3. It is noticed that there is no CT saturation in the injected EMTP current. However, there is a decaying transient offset of the signal but otherwise the relay reproduces the input current accurate. Figure 6.4 compares between the EMTP simulated case and relay response. It shows that the magnitude of both signals were almost the same at the first cycle. Afterward, the relay response started to decay, and gave lower and fixed secondary current magnitude, compared to the EMTP simulated current. Around 16% reduction in the current magnitude is observed, compared to the injected EMTP current signal.

Figure 6.5 shows the simulated current that was injected into the digital overcurrent relay. The CT secondary burden is increased this time and initial saturation is detected. The relay response is shown in figure 6.6. Similar to case-1, decaying transient offset is experienced in the relay response and it then reproduces the same shape of the injected current waveform. Figure 6.7 compares between the simulated case and relay response. It shows that the magnitude of both signals were almost the same only at the first cycle. Around 16% reduction in the current magnitude was experienced, compared to the injected EMTP current signal.

Time (Second)

Figure 6.2 Burden Case-1, Injected COMTRADE signal to the Digital Relay

Time (Second)

Figure 6.3 Response of the Digital Relay to the Injected Current (Case-1)

Figure 6.4 Simulated EMTP Current versus Relay Current Response in Case-1 (Reflected at Primary of 50/5 CT)

Figure 6.5 Burden Case-2, Injected COMTRADE Signal to the Digital Relay

Figure 6.6 Response of the Digital Relay to the Injected Current (Case-2)

Figure 6.7 Simulated EMTP Current versus Relay Current Response in Case-2 (Reflected at Primary of 50/5 CT)

The third case uses 10 times the standard burden. As a result, severe saturation of secondary current is observed. The magnitude and shape of the current signal is severely affected as shown in the simulated EMTP current in Figure 6.8. The current magnitude is reduced to about 75% of the expected secondary current magnitude. The shape of the signal is severely distorted, although the primary current is pure sinusoidal. The response of the digital relay is shown in Figure 6.9. However, lower current magnitude is seen by the relay similar to the previous cases. Figure 6.10 compares the simulated current and actual relay response. Around 16% reduction in the current magnitude is again observed.

The RMS values of the current, seen by the digital relays, are shown on Figure 6.11. It shows that the ability of the relay to reproduce the injected current decreases as the burden is increased. Further evaluations of these current signals will be presented in sections 6.6 and 6.7.
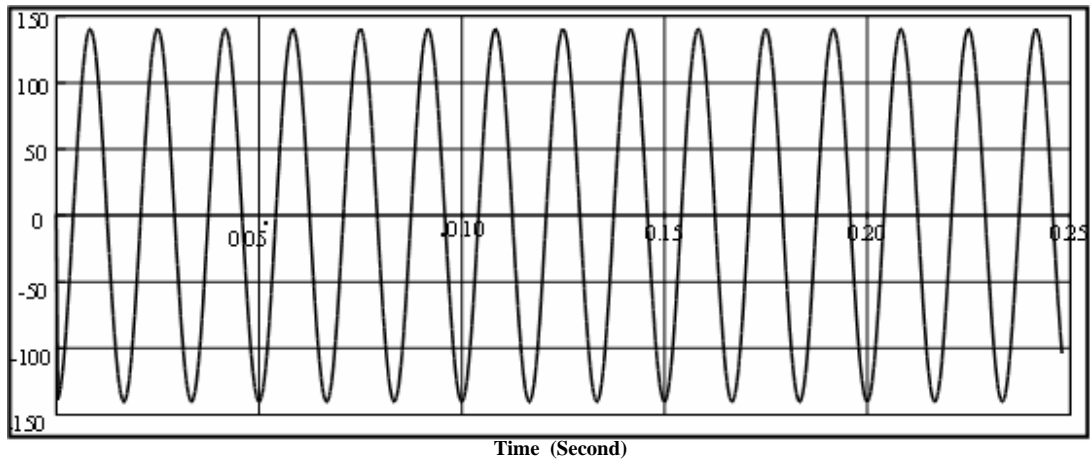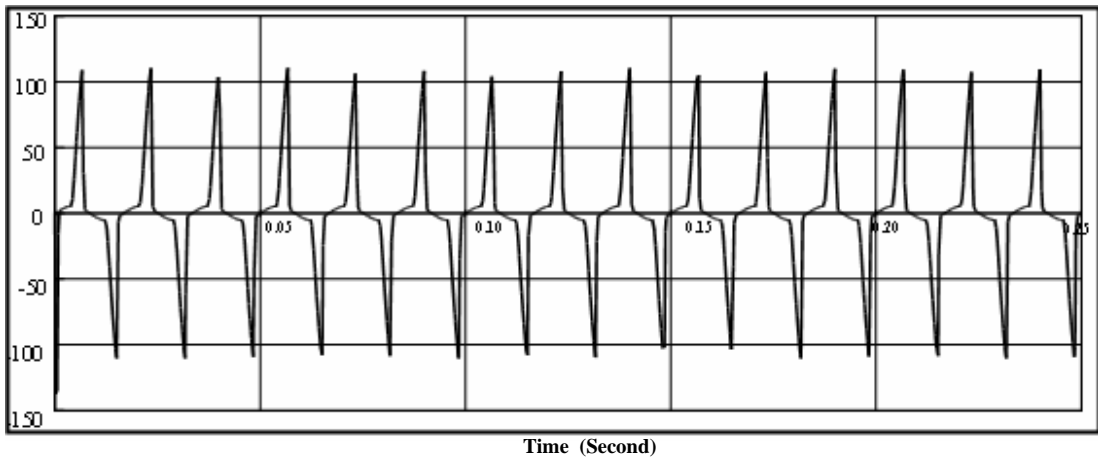
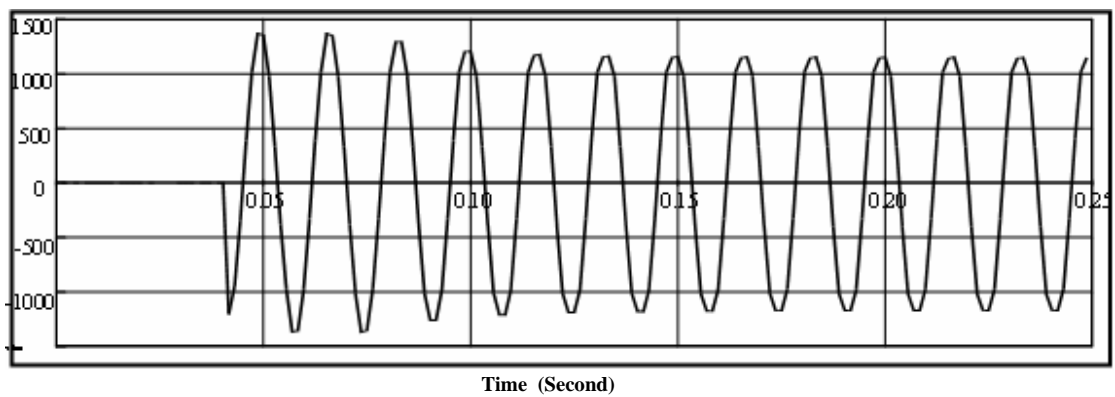**Figure 6.8** Burden Case-3, Injected COMTRADE Signal to the Digital Relay

Figure 6.9 Response of the Digital Relay to the Injected Current (Case-3)
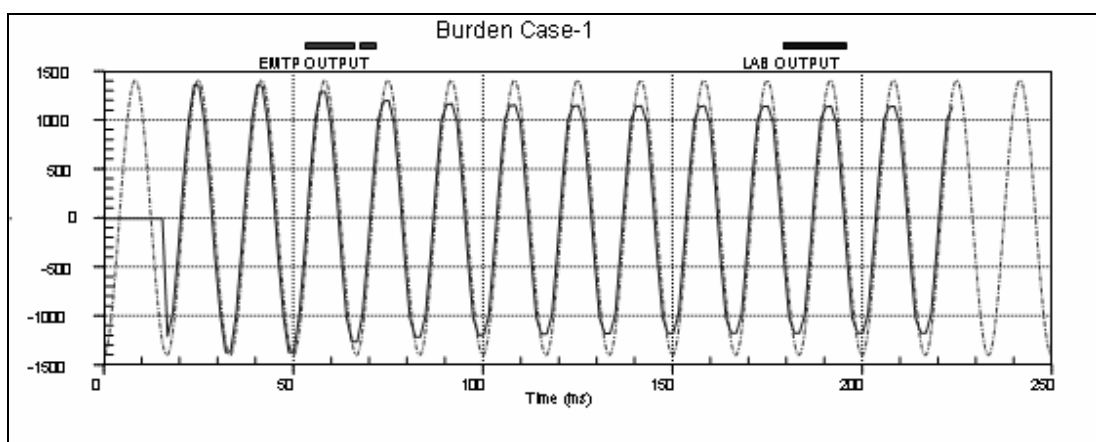
Figure 6.10 Simulated EMTP Current versus Relay Current Response in Case-3
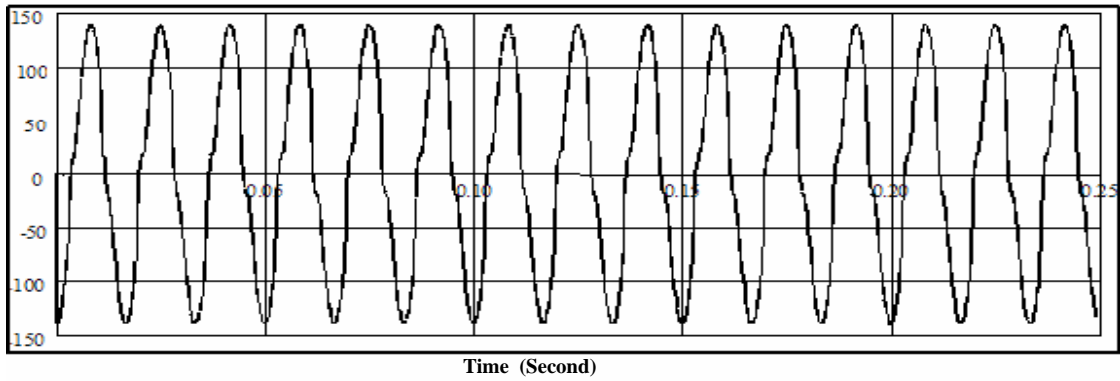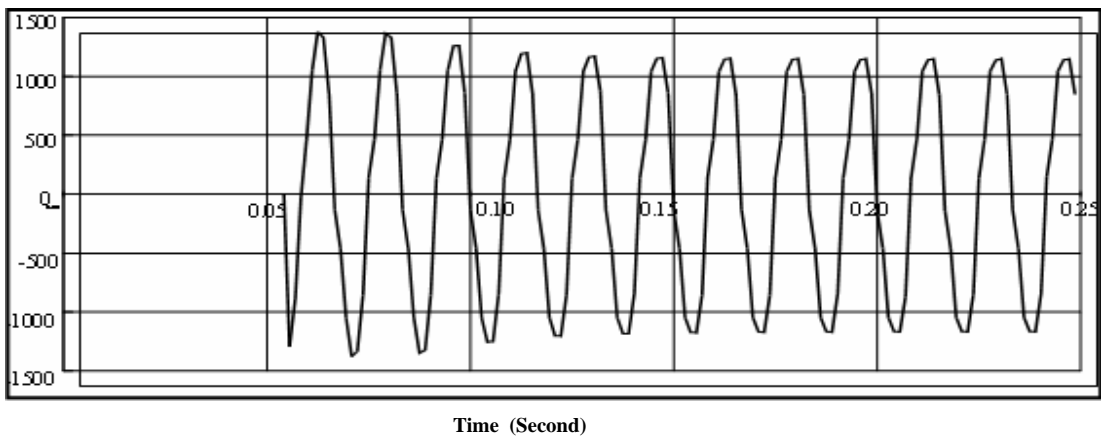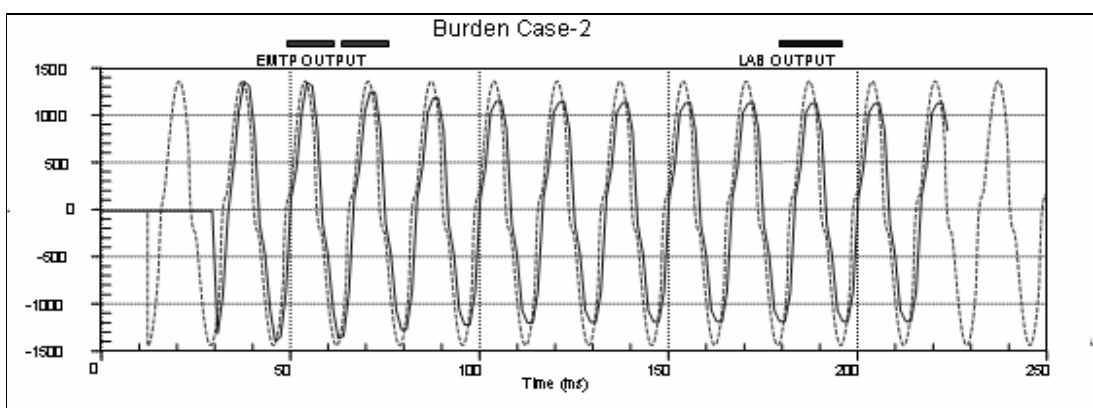(Reflected at Primary of 50/5 CT)
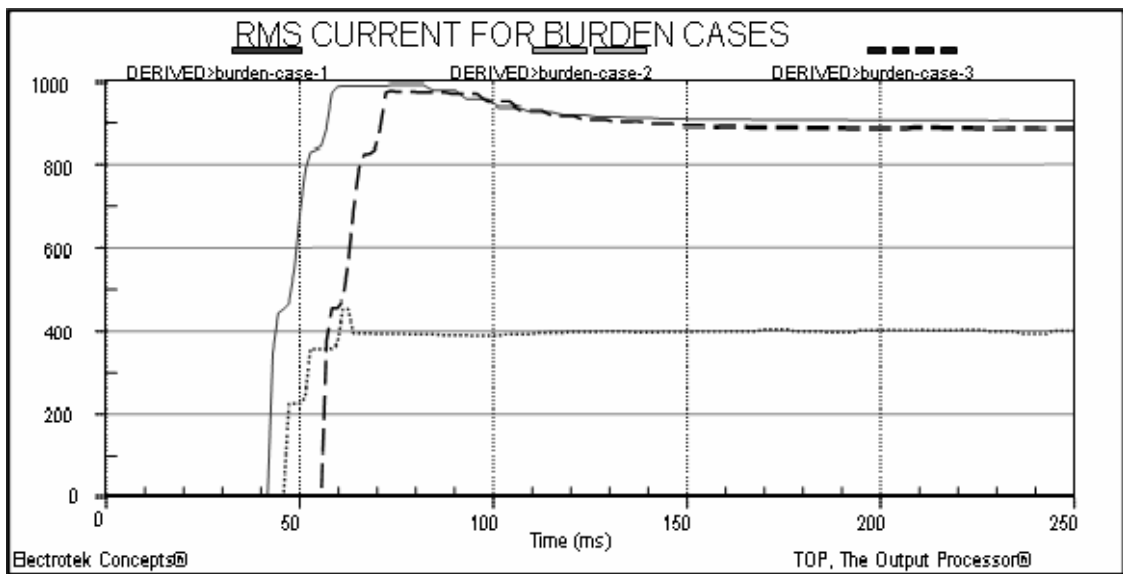
Figure 6.11 Relay Responses for the Three Burden Cases, based on its Current RMS
Measurements, Reflected at the Primary

Low ratio CT used in the circuits of high fault current will be examined, considering the a burden of 1 ? , assuming that the full circuit run of #10 AWG (1.0 ? / 1000-ft) is 1000 ft. The tests will be undertaken for various symmetrical short circuit levels as shown in Table 6.2.

Figure 6.12 shows the simulated current for case-1, where 10 times the CT rating is injected into the model with five times the standard secondary burdens. The signal shows initial saturation. The shape of the waveform is slightly distorted. The relay response is almost the same as the injected current as shown in Figure 6.13. The relay response and simulated secondary current can be compared by referring to Figure 6.14.

Figure 6.15 shows the simulated current for case-2, where 15 times the CT rating is injected in the CT model with five times the standard secondary burdens. The signal shows more severe symmetrical saturation. The shape of the waveform and magnitude of the secondary current are distorted and affected. The relay response is almost the same as the injected current as shown in Figure 6.16. The relay response and simulated secondary current can be compared by referring to Figure 6.17. The magnitude of the relay output is reduced by 5% compared to the injected current.

Table 6.2 Cases Applied to Examine the Primary Symm. Faults Effect on Digital Relays

Primary Injected Current To EMTP 50/5 CT model	**Burden (Ohm)**
Case 1 10 X CT Rating Current (500 RMS Current)	1.0 (5 X Standard Burden)
Case 2 15 X CT Rating Current (750 RMS Current)	
Case 3 30 X CT Rating Current (1500 RMS Current)	

Time (Second)

Figure 6.12 Symm. Short Circuit Case-1, Injected COMTRADE Signal to the Digital Relay

Time (Second)

Figure 6.13 Response of the Digital Relay to the Injected Current (Case-1)

Figure 6.14 Simulated EMTP Current versus Relay Current Response in Case-1 (Reflected at Primary of 50/5 CT)

Time (Second)
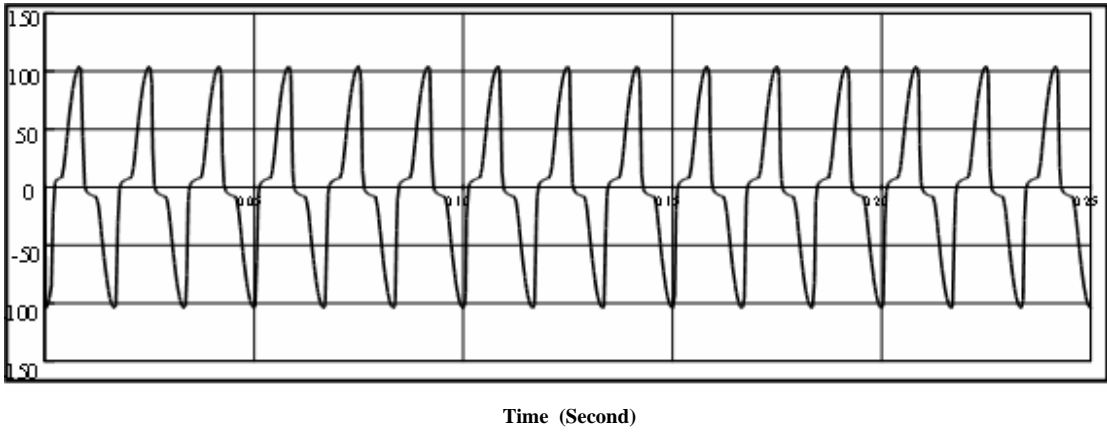
Figure 6.15 Symm Short Circuit Case-2, Injected COMTRADE Signal to the Digital Relay
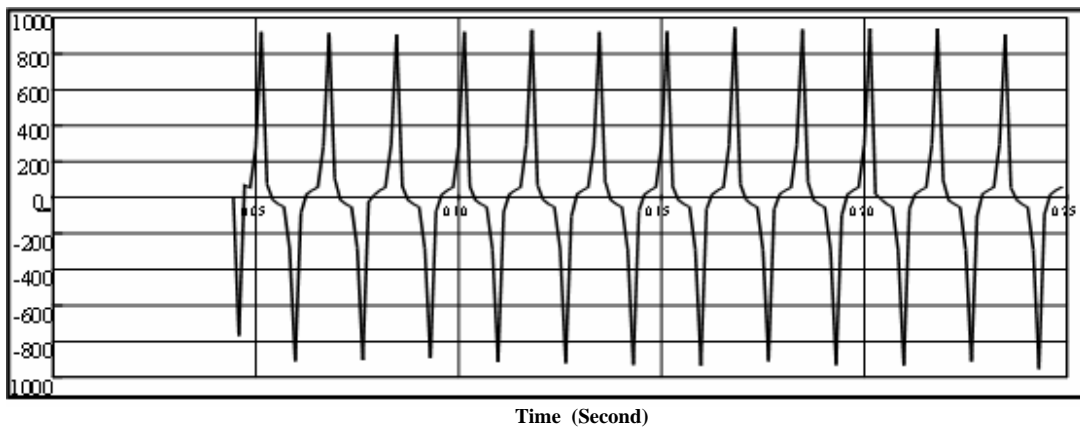

Time (Second)

Figure 6.16 Response of the Digital Relay to the Injected Current (Case-2)

Figure 6.17 Simulated EMTP Current Versus Relay Current Response in case-2 (Reflected at Primary of 50/5 CT)

A more severe short circuit case is considered, where 30 times the CT rating is injected with five times the standard secondary burdens. As shown in Figure 6.18, the signal exhibits very severe symmetrical saturation. The shape of the waveform and magnitude of the secondary current are very distorted and affected. The current magnitude is reduced to about 85% of the expected secondary current magnitude. The relay response was the same as the injected current in the first half cycle, then the relay current response started to decay as shown in Figure 6.19. The current seen by the relay is significantly reduced to around 69% of the injected current in the remaining cycles. Sharp edges of the injected waveforms could not be seen in the relay response. This is mainly due to the low sampling rate of the relay (12 samples/ cycle) where high frequency harmonic contents could not be captured by the relay. Although the CT's exhibited severe saturation, relatively high current could be delivered to the relay, which means that instantaneous relay could operate properly. Figure 6.20 compares the simulated signal with the relay current response.

The current values, seen by the digital relay, in the three cases are shown on figure 6.21. It shows that the ability of the relay to reproduce the injected current decreases as the symmetrical fault level increases. By considering the worst case, the relay could see a current of 490A, although severed CT saturation is experienced. Further evaluations of these current values will be presented in section 6.6 and 6.7.

Time (Second)
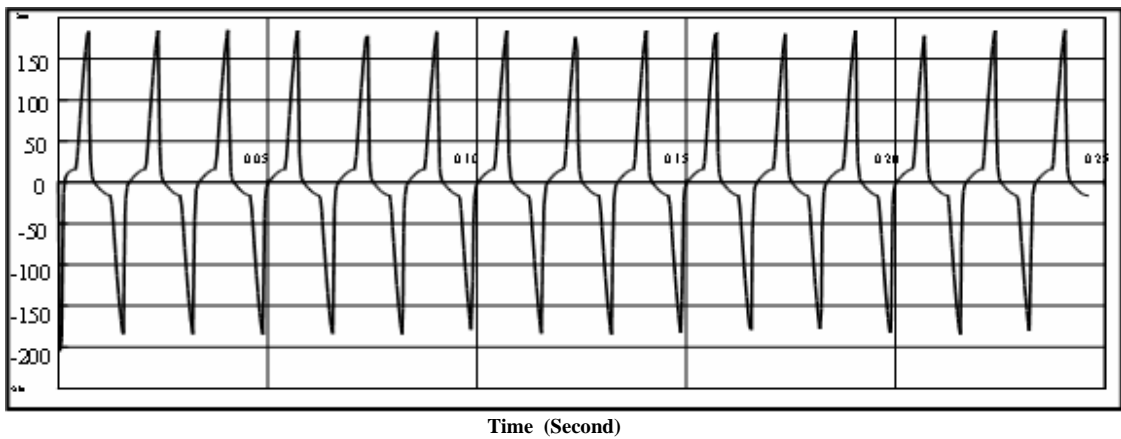
Figure 6.18 Symm. Short Circuit Case-3, Injected COMTRADE Signal to the Digital Relay

Time (Second)
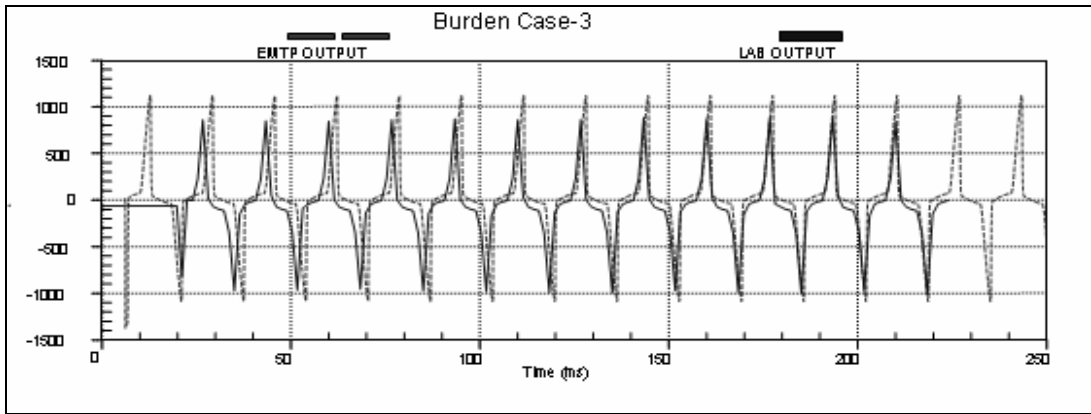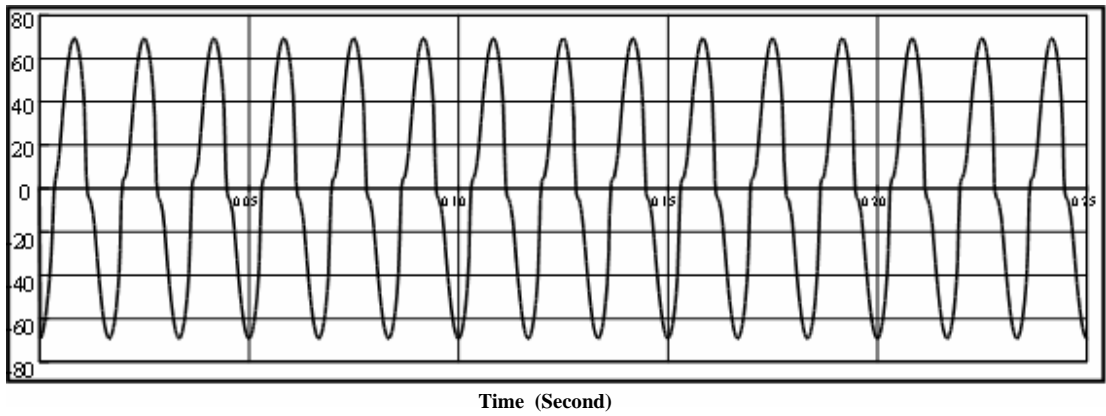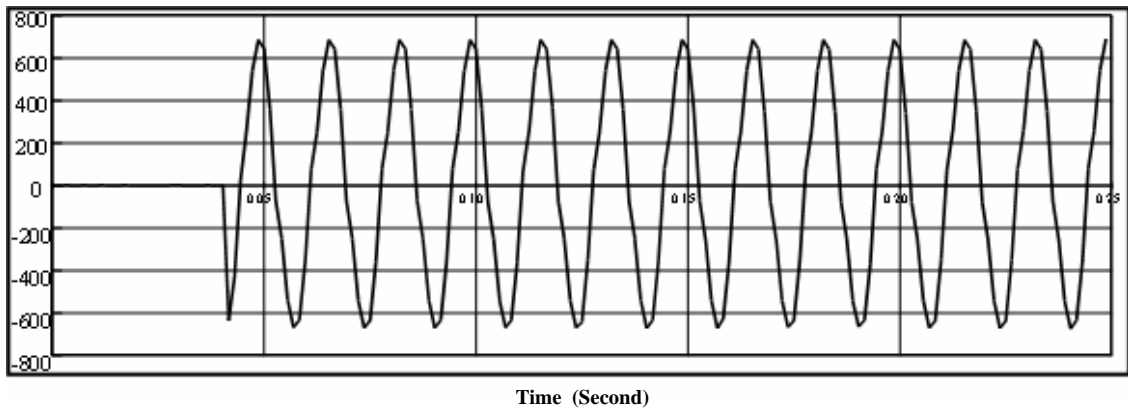**Figure 6.19** Response of the Digital Relay to the Injected Current (Case-3)
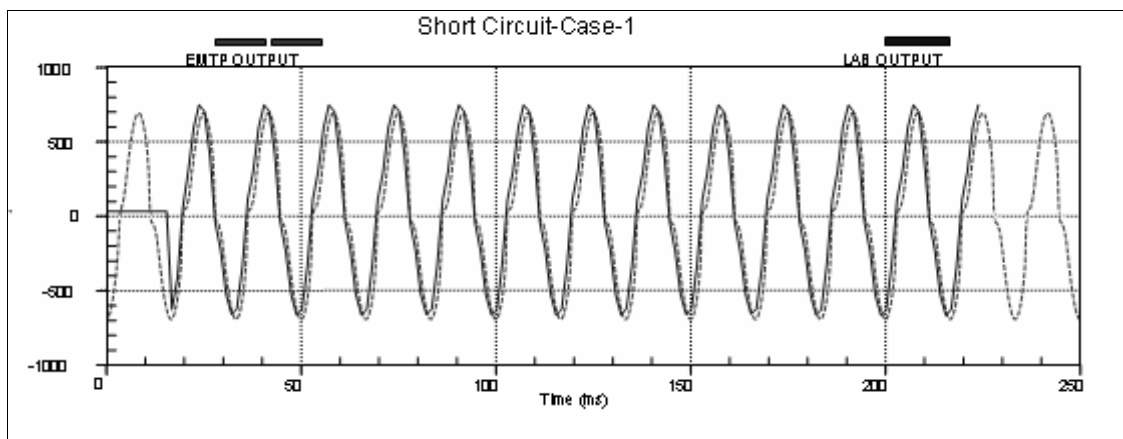
Figure 6.20 Simulated EMTP Current versus Relay Current Response in Case-3
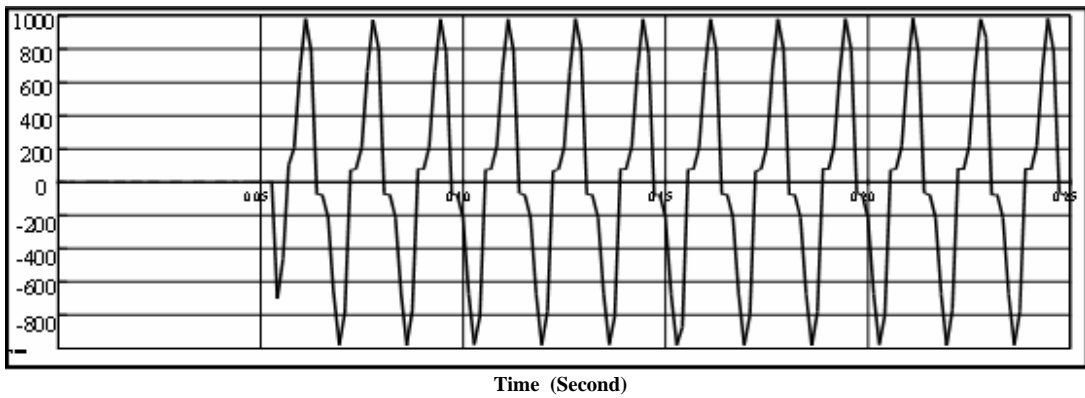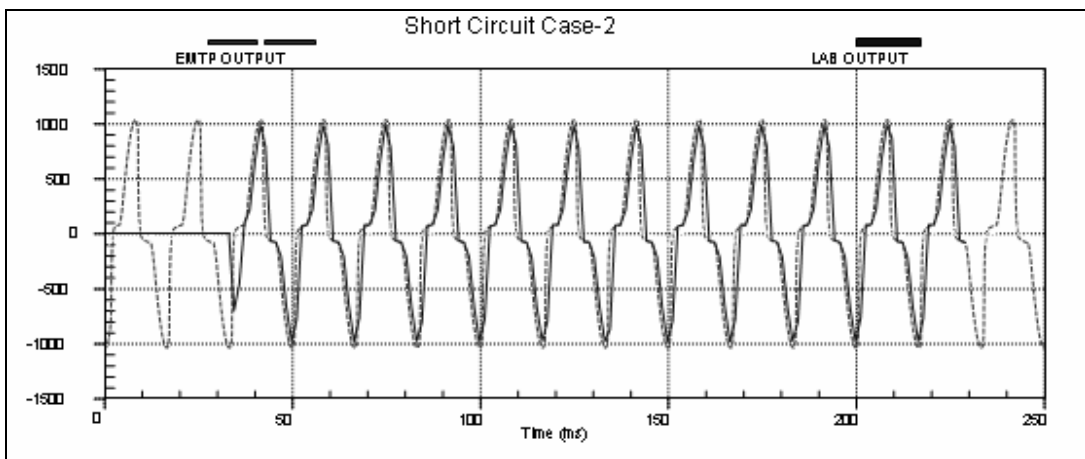(Reflected at Primary of 50/5 CT)
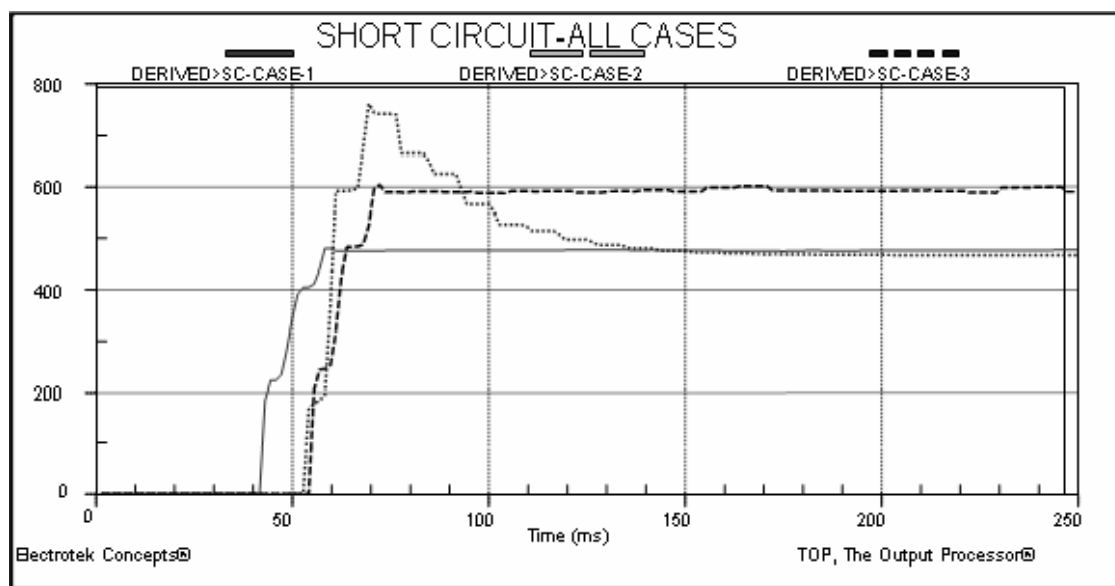
Figure 6.21 Relay Responses for the Three Symm Short Circuit Cases, based on its
Current RMS Measurements

6.4 Effects of Asymmetrical Currents on Digital Overcurrent Relays

The impact of asymmetrical faults on the CT and the associated effects on microprocessor-based overcurrent relays will be investigated in this section. Table 6.3 presents a summary of cases, developed and injected to the digital overcurrent relay through OMICRON CMC256. The objective is to examine the transient behavior of digital overcurrent relays and their response to the change in X/R ratio. All cases are developed based on 0.5 ? (2.5 times standard burden).

In case 1, a relatively low primary current, is injected with the dc offset has a time constant of 0.064 second or X/R ratio of 24. Figure 6.22 shows the simulated secondary current. The CT is driven into saturation within the second cycle and the current peak remains low and distorted for the three cycles. After that, the sinusoidal signals are recovered after the effect of the dc offset has disappeared. The relay response could closely predict the saturated peak of the secondary current as shown in figure 6.23. Figure 6.24 shows that the injected secondary current and relay current response were almost identical. The first three cycles shown in the relay response represents the pre-fault condition.

Table 6.3 Cases Applied to Examine the X/R Ratio Effect on Digital Relays

| Case	Primary Injected Current To EMTP 50/5 CT model Current	Time Constant	X/R Ratio	Saturation Voltage Using Equation Criteria (4.8) $20 \geq \left\| \dfrac{X}{R} + 1 \right\| \cdot i_f \cdot z_b$
1	3.25 x CT rated Current	0.064 s	24	203.1
2		0.042 s	16	138.1
3	20 x CT rated Current	0.064 s	24	1250
4		0.042 s	16	850

Figure 6.22 Assym. Fault with 24 X/R Case-1, Injected COMTRADE Signal to the Digital Relay

Figure 6.23 Response of the Digital Relay to the Injected Current (Case-1)

Figure 6.24 Simulated EMTP Current versus Relay Current Response in Case-1 (Reflected at Primary of 50/5 CT)

In case 2, the same injected current is used, but with lower X/R ratio (X/R = 16). Figure 6.25 shows the simulated secondary current. The CT is driven into saturation within the second cycle and the current peak remains low and distorted for less than two cycles. In this case, the sinusoidal signal recovered faster after the effect of dc offset had disappeared. Similar to case-1, the relay response could closely predict the saturated peak of the secondary current as shown in figure 6.26. Figure 6.27 Shows that the injected secondary current and relay current response are almost identical.

Figure 6.27 shows the RMS values of secondary currents for both cases. The effects of changing the system X/R ratios on the digital overcurrent relays are shown in figure 6.28. The RMS values shows that the higher the X/R ratio, the slower response of the digital relay. The magnitude of RMS current is reduced as the X/R ratio is increased.

Time (Second)
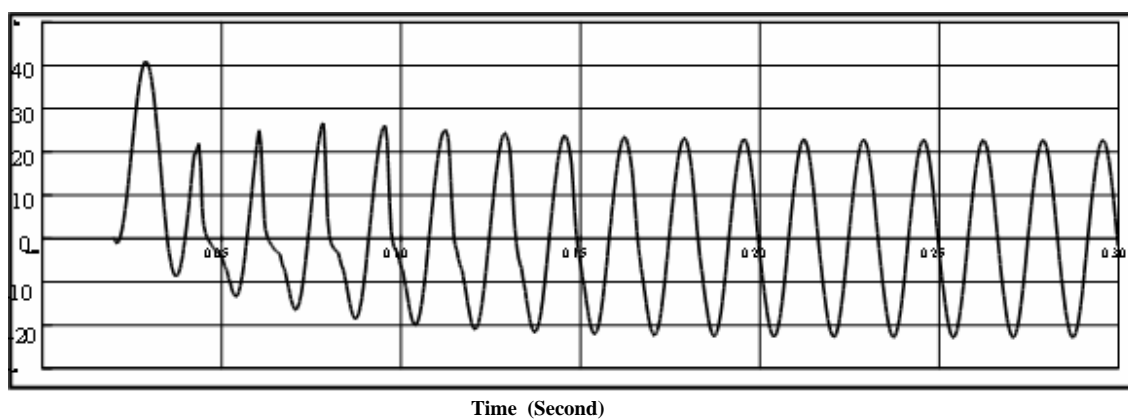
Figure 6.25 Assym. Fault with 16 X/R Case-2, Injected COMTRADE Signal to the
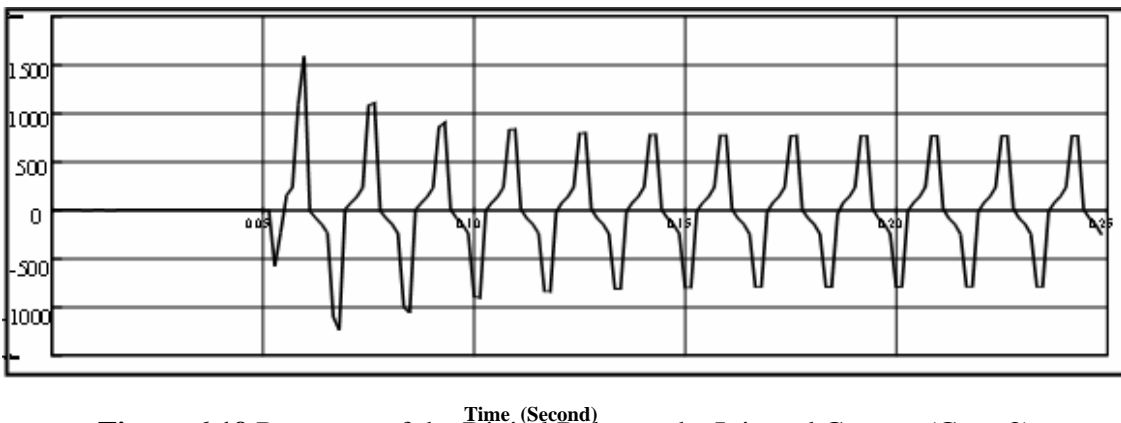Digital Relay

Time (Second)

Figure 6.26 Response of the Digital Relay to the Injected Current (Case-2**)**
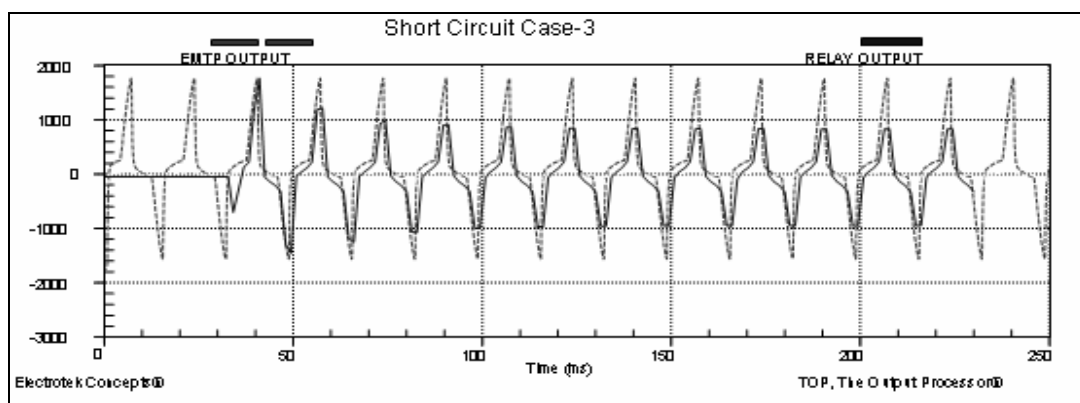
Figure 6.27 Simulated EMTP Current versus Relay Current Response in Case-2
(Reflected at Primary of 50/5 CT)
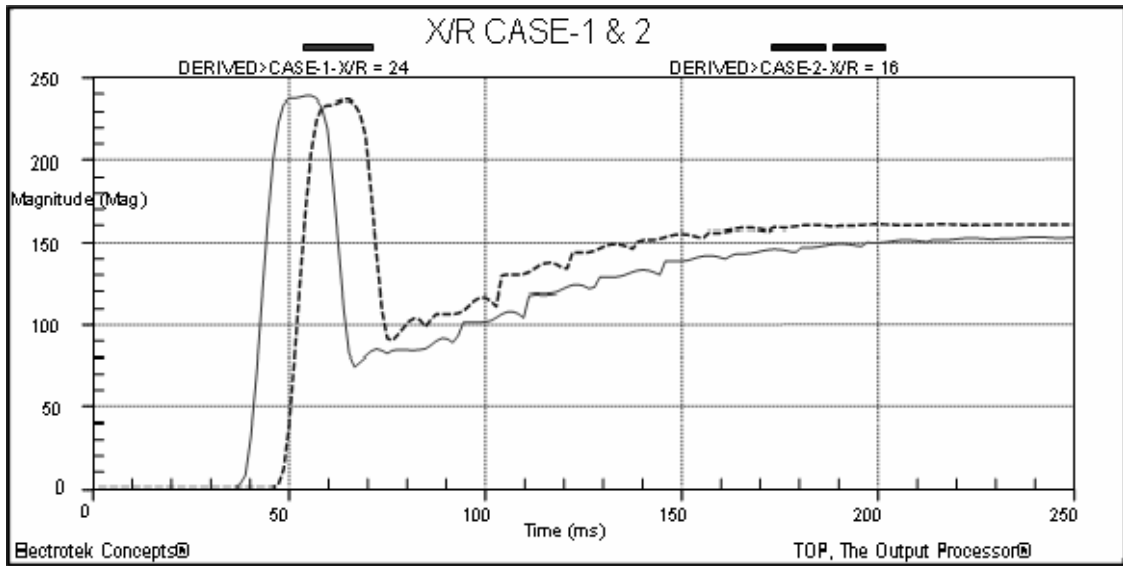
Figure 6.28 Relay Response for the Asymmt Fault with Different X/R Ratios, Case- 1&2,
based on its RMS Measurements

The simulated secondary current for case-3 is shown in figure 6.29. In this case, very high current is injected to the primary of the CT (20 X CT) with the same secondary burden and with X/R ratio of 24. The CT is driven into severe saturation within the second cycle and the secondary current remains low and distorted for the three cycles. The current wave is changed to symmetrical after the effects of dc offset disappeared. The response of the relay to the injected current was almost identical, in terms of shape as shows in figure 6.30. The magnitude of the relay current response had a reduction of about 5%, compared to the simulated current as shown in figure 6.31

In case-4, the same injected current is used, but with lower X/R ratio (X/R = 16). Figure 6.32 shows the simulated secondary current. The CT is driven into saturation within the second cycle and the current remains low and distorted for only less than two cycles. In this case, the sinusoidal signal recovered quicker after the effect of dc offset had disappeared. Similar to case-3, the relay response could closely predict the saturated peak of the current as shown in figure 6.33. Figure 6.34 shows that the injected secondary current and relay current response are almost identical.

Figure 6.35 shows RMS values of secondary currents for both cases. The RMS current values are reflected to the primary value using a ratio of 50/5. The effects of changing the system X/R ratios on the digital overcurrent relays are also shown. The RMS current values show that the higher the X/R ratio, the slower response of the digital relay. The RMS values of the current is reduced as the X/R ratio increased. In comparison to cases 1 and 2, the relay response took longer to reproduce the expected secondary current due to the high primary injected current (20 X CT).
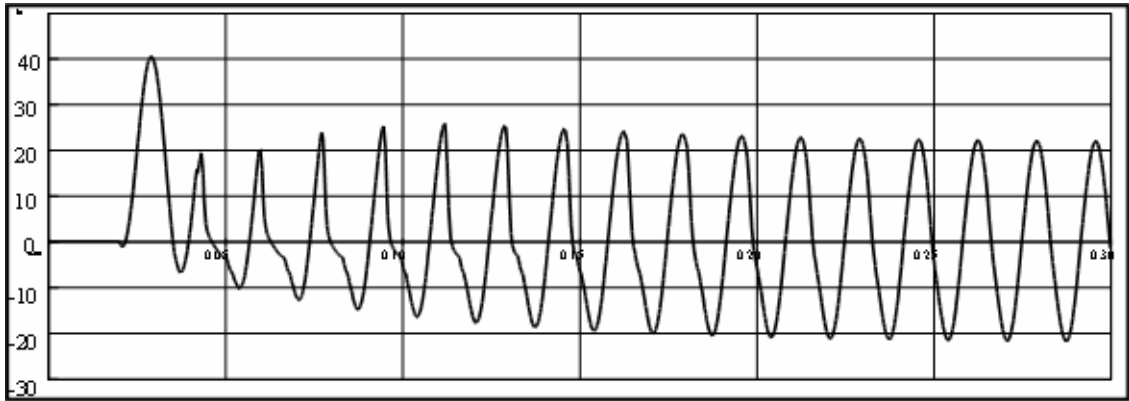
Time (Second)
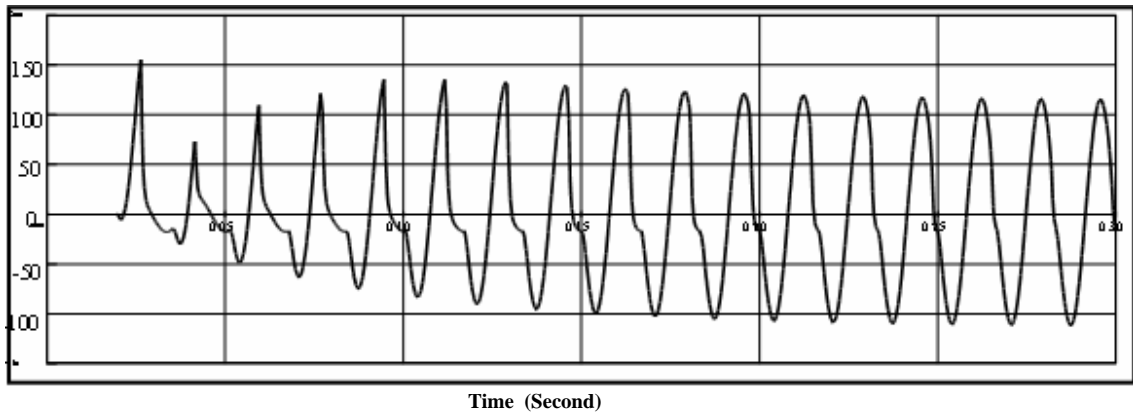
Figure 6.29 Assym. Fault with 24 X/R Case-3, Injected COMTRADE Signal to the Digital Relay
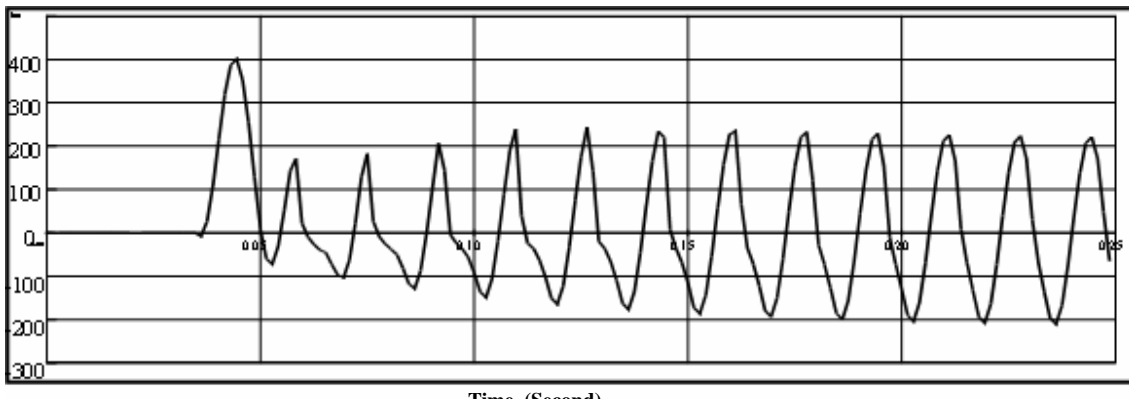

Time (Second)
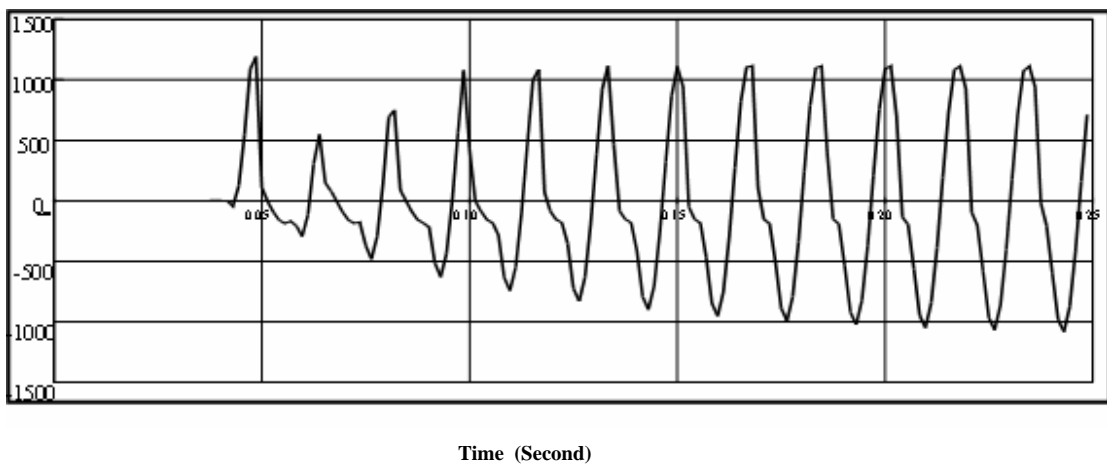
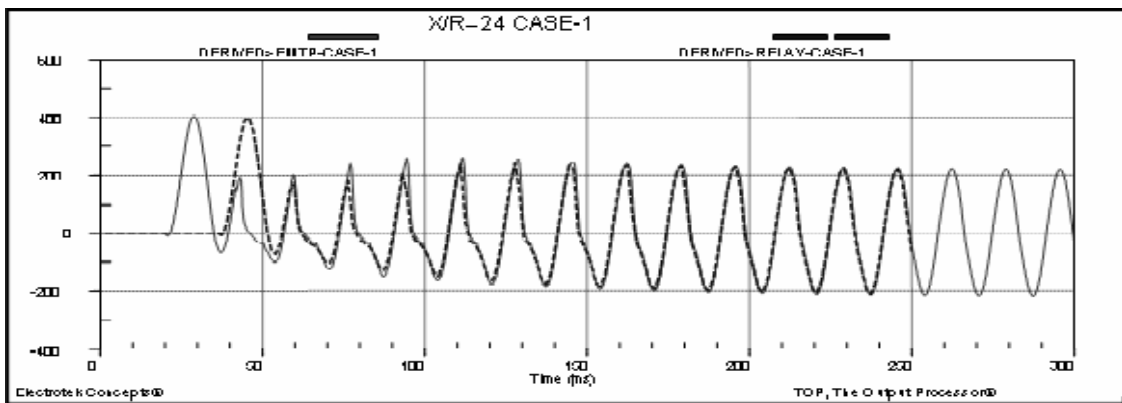**Figure 6.30** Response of the Digital Relay to the Injected Current (Case-3)
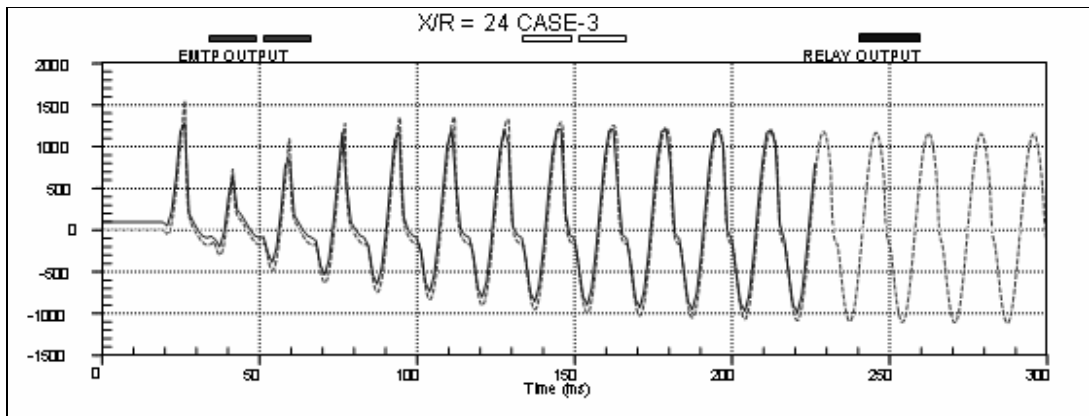
Figure 6.31 Simulated EMTP Current versus Relay Current Response in Case-3
(Reflected at Primary of 50/5 CT)

.
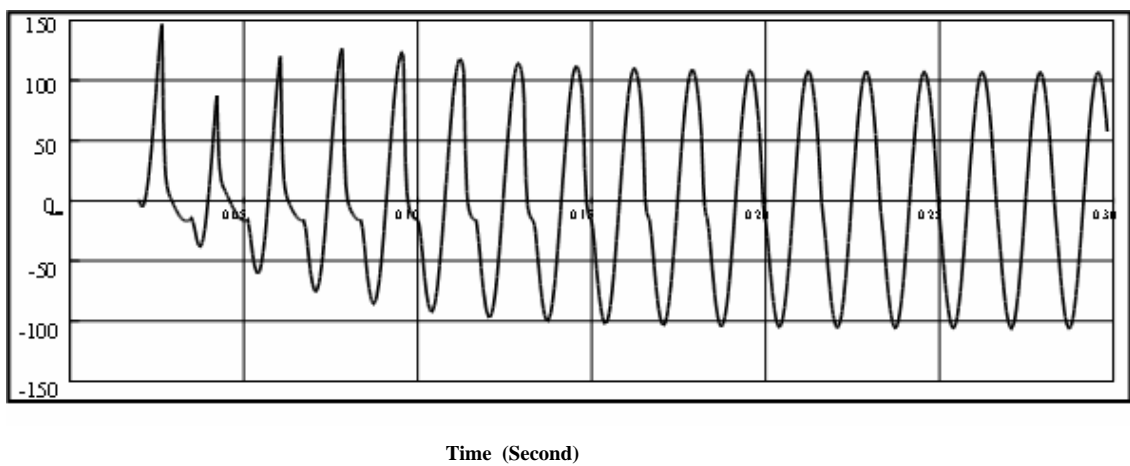
Time (Second)
Figure 6.32 Assym. Fault with 16 X/R Case-4, Injected COMTRADE Signal to the
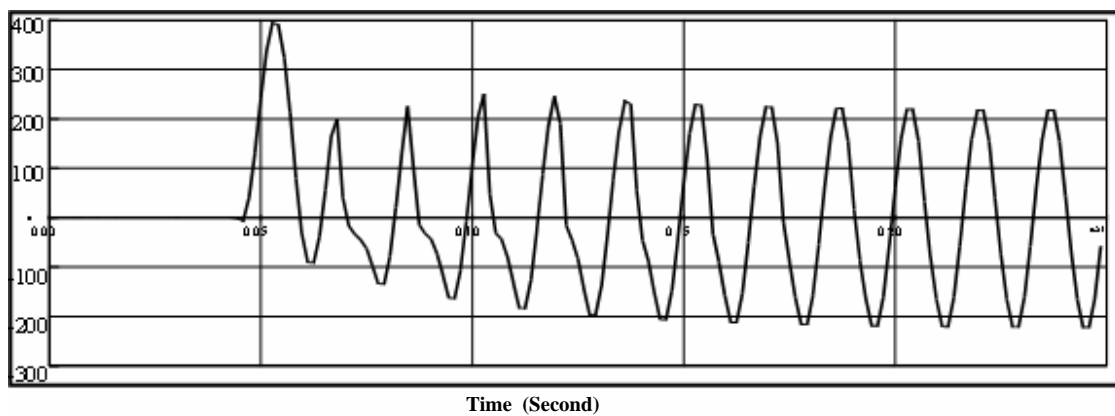Digital Relay

Time (Second)
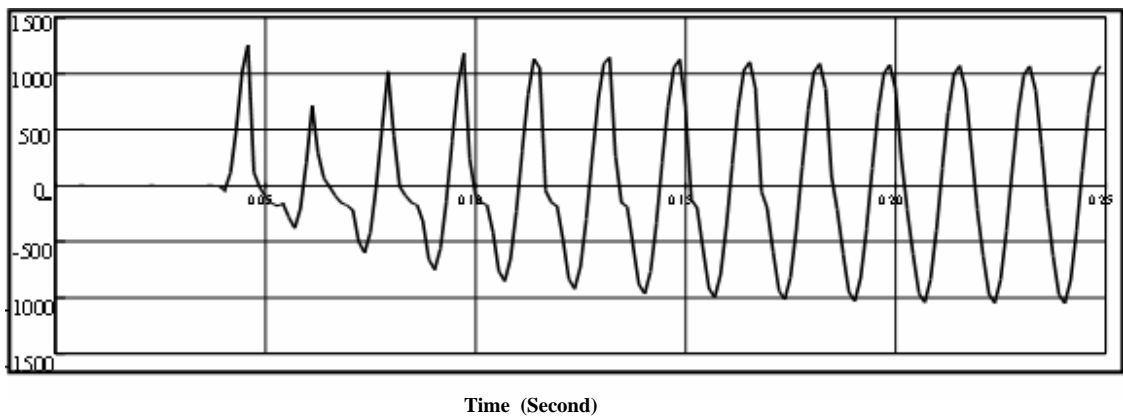
Figure 6.33 Response of the Digital Relay to the Injected Current (Case-4)
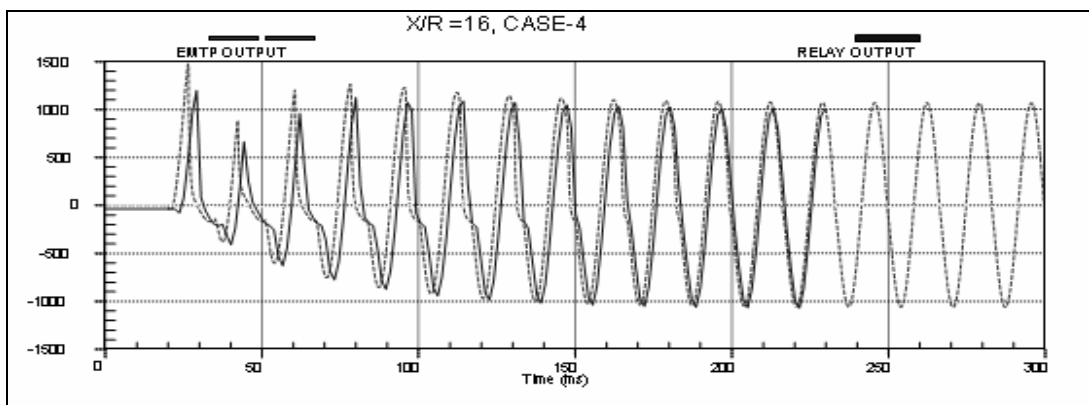
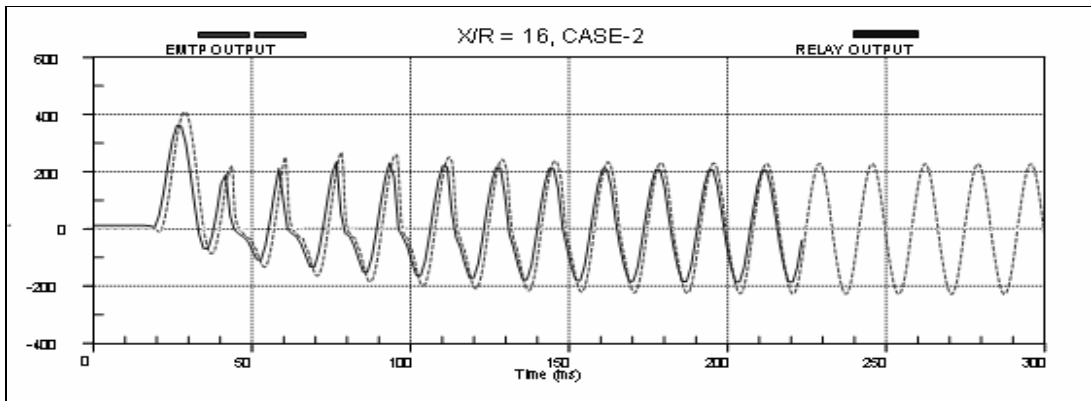**Figure 6.34** Simulated EMTP Current versus Relay Current Response in Case-4
(Reflected at Primary of 50/5 CT)
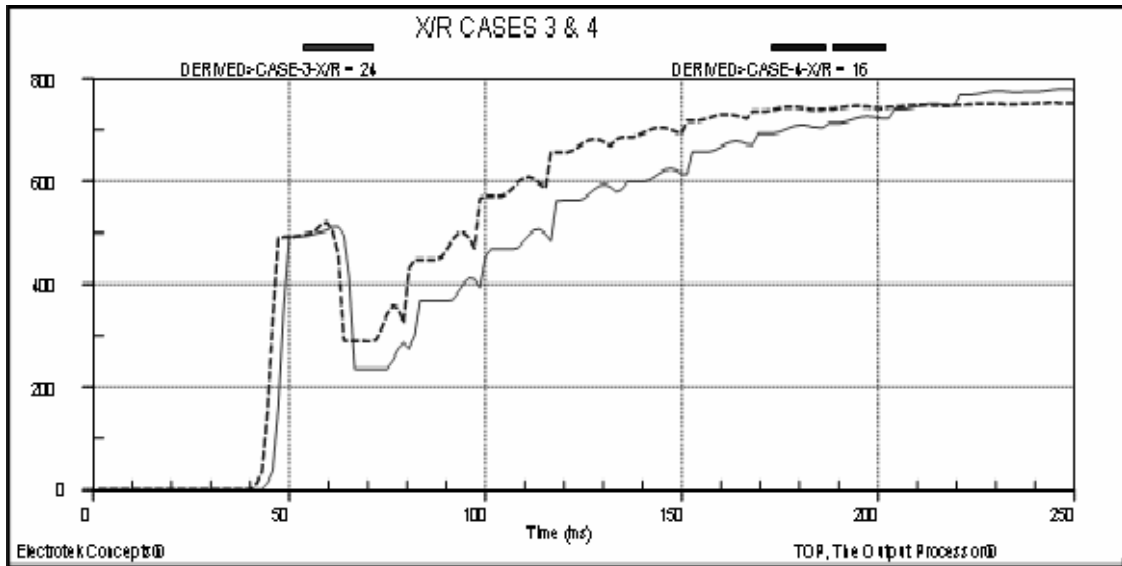
Figure 6.35 Relay Responses for the Asymmt Fault with Different X/R Ratios, Case-3 &4, based on its RMS Measurements

6.5 Effects of Remanent Flux on CT Saturation and Digital Relay Operation

Three current waveforms representing the output current of EMTP for a CT with remanence flux of 0%, 50%, and 100% are considered as shown in Figures 6.36, 6.38 and 6.40. These waveforms are related to the 50/5 C-20 CT considered in the previous analysis. The fault current in each case is 20XCT (1000A) and the dc offset has a time constant of 0.064 s (X/R = 24) and maximum amplitude. The total burden for all three cases is 0.5 ohm. The three waveforms show the CT behavior with remanence flux of 0%, 50%, and 100%. The response of the digital relay, with different remanence flux values, have been examined in the laboratory and shown in Figures 6.37, 6.39 and 6.41. In addition, a comparison between the three waveforms is shown in Figure 6.41.

Time (Second)
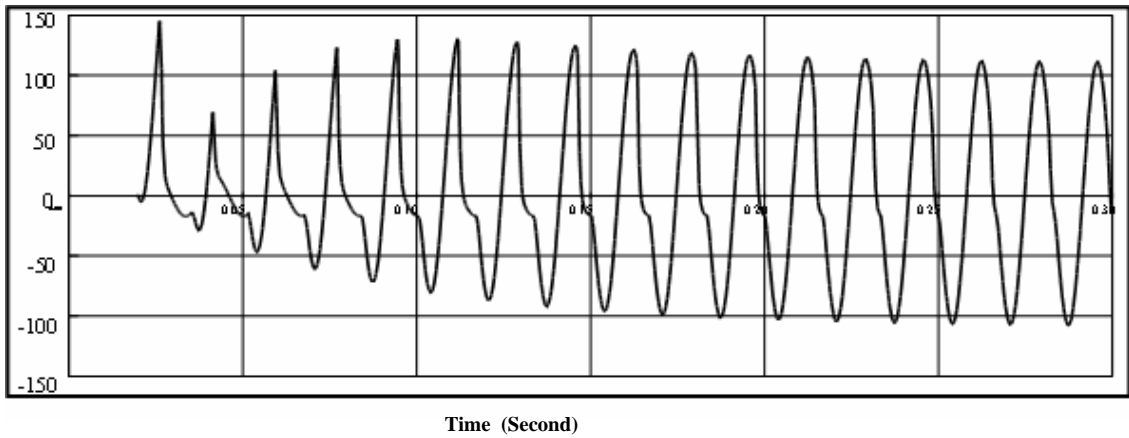
Figure 6.36 0% Remenance Flux Case-1, Injected COMTRADE Signal to the Digital Relay

Time (Second)
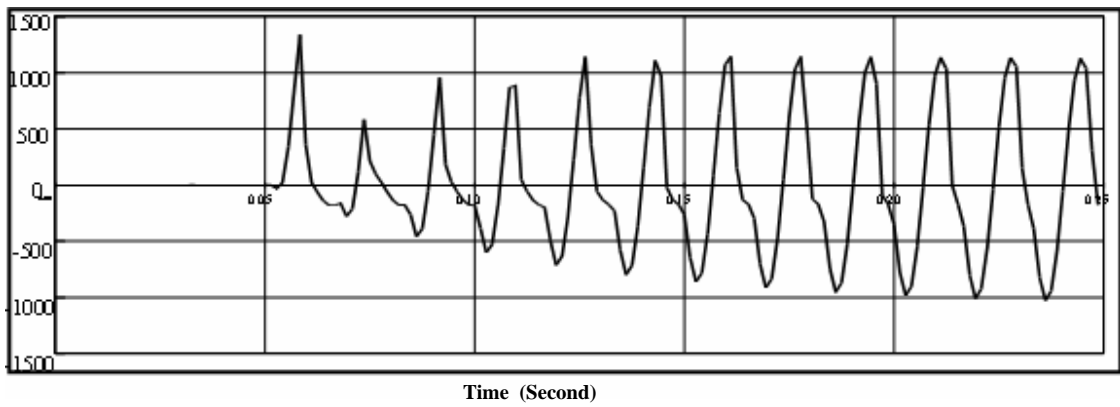
Figure 6.37 Response of the Digital Relay to the Injected Current (Case-1)

Time (Second)
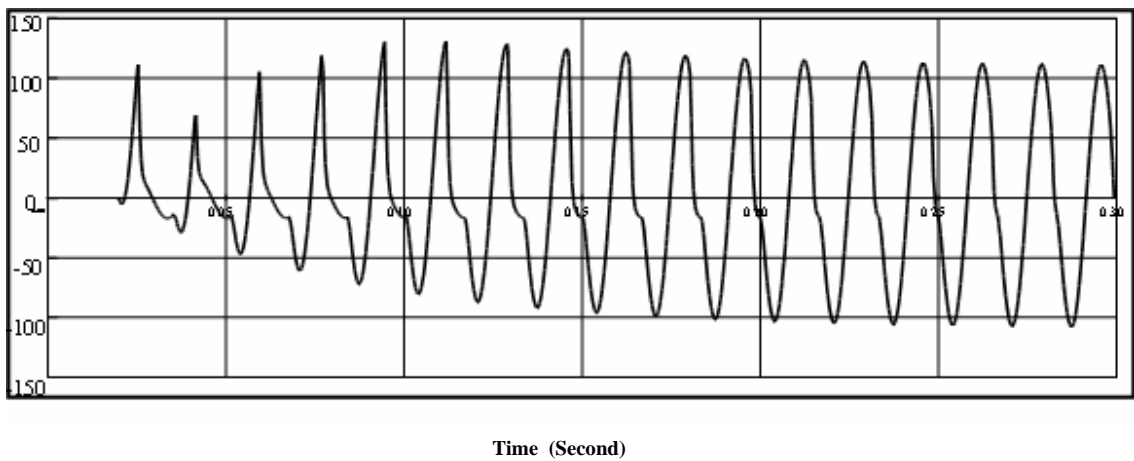
Figure 6.38 50% Remenance Flux Case-2, Injected COMTRADE Signal to the Digital Relay

Time (Second)
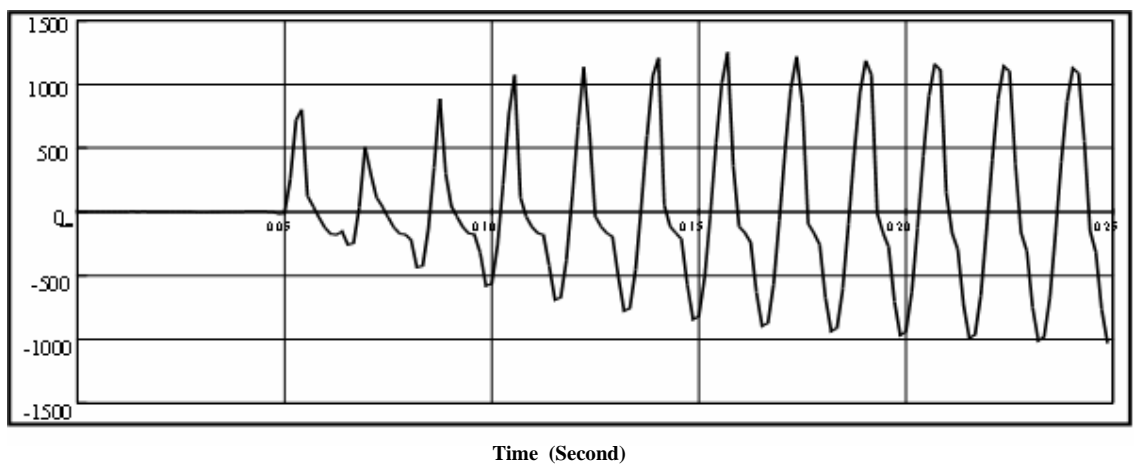
Figure 6.39 Response of the Digital Relay to the Injected Current (Case-2)

Time (Second)
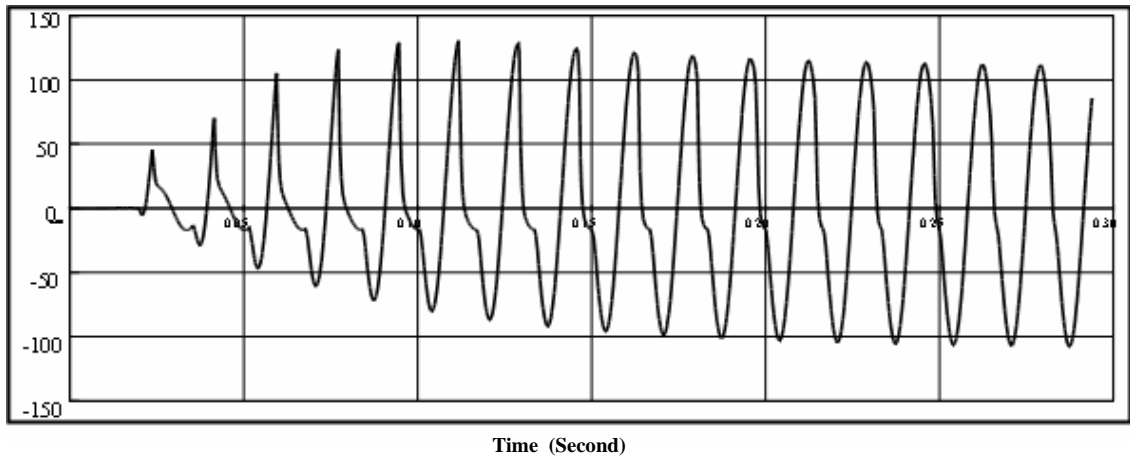
Figure 6.40 100% Remenance Flux Case-3, Injected COMTRADE Signal to the Digital Relay

Time (Second)
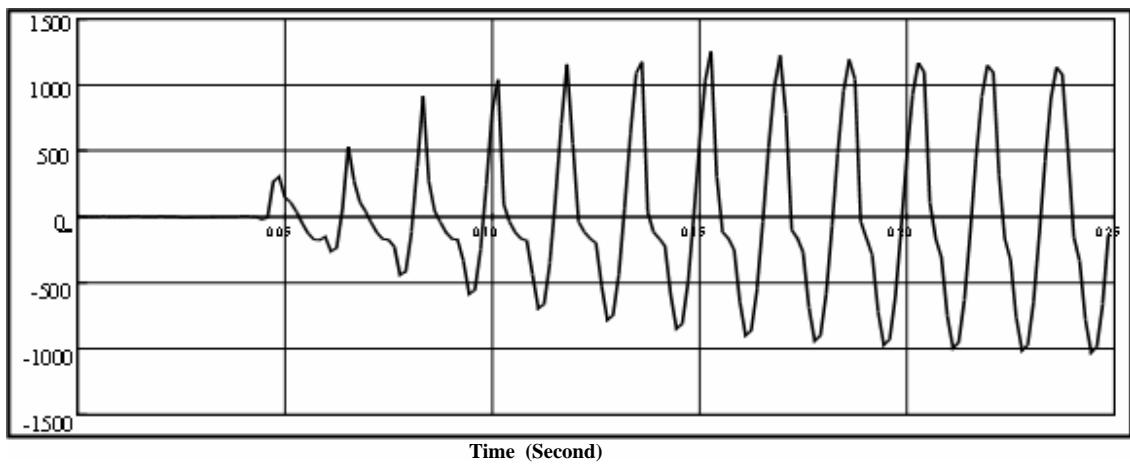
Figure 6.41 Response of the Digital Relay to the Injected Current (Case-3)
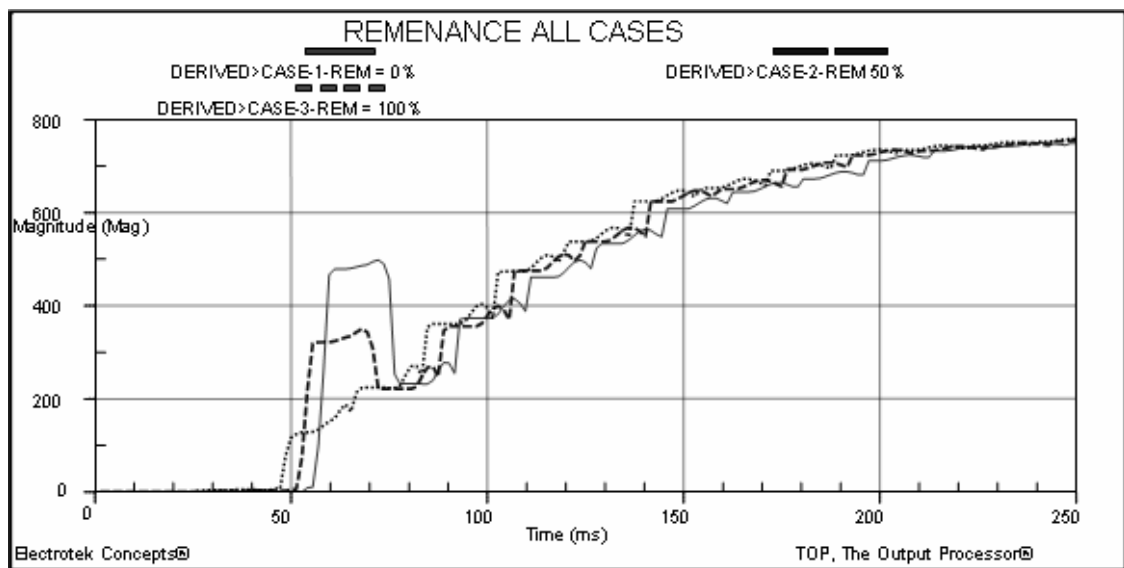
Figure 6.42 Relay Response for the Three Remenance Flux Cases, based on its RMS Measurements

6.6 General Observations on the Lab Test Results

The captured signals of the Basler digital overcurrent relay have been evaluated and the following observations were found:

- The Basler relay, as highlighted in its manual and as shown in figure 6.43, has the following features:

  1. The relay captures the signal and shows 3 cycles pre-trigger where no current is injected during the testing. This explained the time delay in signals captured by the relay, in comparison to the EMTP injected signal.

  2. The relay took only half a cycle to trigger. The time delay between the captured signal and EMTP injected signal is only 0.5 cycle.

  3. The trip action will be given when the trip current magnitude reaches the set-point and continues to flow for two cycles. This two-cycle delay allows the line transients to settle to provide data that are more accurate.

  4. The sampling rate (12 samples/cycle) of the recording feature in the relay used during the laboratory tests is quite to be low. In comparison, the EMTP model has high sampling rate that captures high frequency components of the secondary signals. This resulted in differences in the magnitude between the relay captured signals and EMTP injected signals.

- In the symmetrical analysis, a reduction of 15-30% in the secondary current magnitude has been experienced in the signals captured by the relay, compared to the injected EMTP secondary current signals. For instantaneous operations, relays

are set as low as possible, based on the load requirements and therefore this magnitude reduction shall not be of concern to the operations of relays. Detailed analysis and evaluations of this issue will be carried out throughout this Chapter.

- Transient dc offset in the current signals has been experienced. This is most likely due to the X/R effect of the secondary injection equipment.
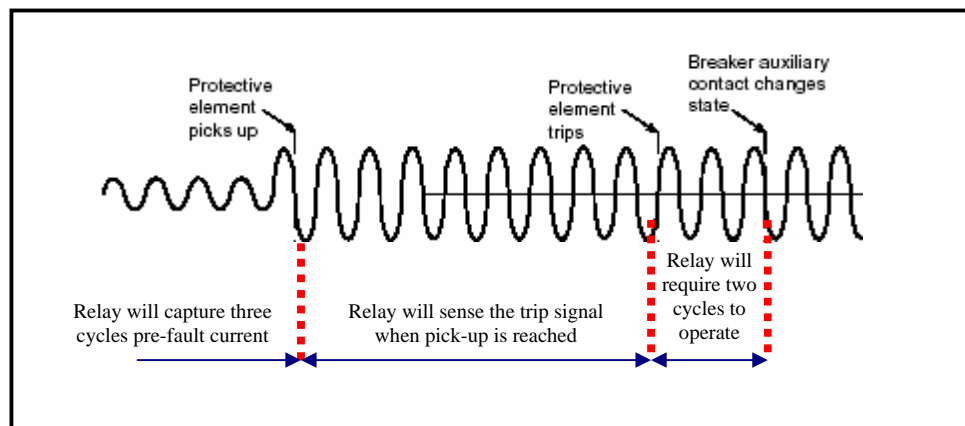
Figure 6.43 *Basler Overcurrent Relay Trip Response* [36]

6.7 Evaluations of Instantaneous Digital Relays Responses and Test Results

As explained in Chapter 4, the degree of saturation is defined by saturation voltage Vs. The saturation voltage of the 50/5 CT, used in the testing has been found to be 31V. The excitation curve for the CT has been obtained by testing, as explained in Chapter 3 and shown in Figure 6.44. The IEEE Standard C37-110-1996 offers selection rules of CTs to avoid both AC and DC saturation. In this section, these rules will be evaluated for both symmetrical and asymmetrical faults. First, AC saturation criteria will be evaluated. Then, IEEE Standard C37-110-1996 criteria to avoid saturation with DC component in the primary wave will be considered.

6.7.1 Evaluation of Instantaneous Digital Overcurrent Relay Response with Symmetrical AC Components

In order to avoid AC saturation, the following equation requirements shall be met:

$$V_S \geq i_f \cdot z_b \qquad (6.1)$$

Where: i_f is the maximum fault current in per unit of ct rating

z_b is the CT burden in per unit of standard burden

V_S is the CT saturation voltage in per unit and equal 20
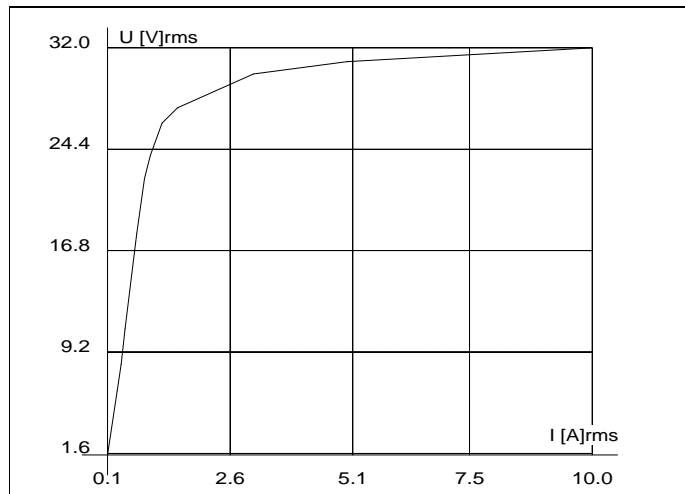
Figure 6.44 Laboratory Excitation Curve for 50/5 CT

The saturation voltage in equation (6.1) is limited to 20 times rated secondary current at standard burden without exceeding the relay accuracy class limit. Therefore, equation (6.1) can be rewritten as follows:

$$20 \geq i_f \cdot z_b \tag{6.2}$$

Using the 50A CT primary rating with 20 times CT rating (1000A fault current) will imply in the following:

$$i_f = \frac{I_{max}}{CT_{rating}} = \frac{1000}{50} = 20 \tag{6.3}$$

Using the C20 CT with the standard burden of 0.2 ? and the maximum CT burden, used in the burden analysis in section 6.3, which is 2 ?:

$$z_b = \frac{Z_{Burden}}{Z_{Stad}} = \frac{2.0}{0.2} = 10 \tag{6.4}$$

Therefore, the saturation voltage can be calculated using equation (6.1):

$$V_S \geq i_f \cdot z_b = 20 \cdot 10 = 200 \tag{6.5}$$

In figure 6.11, for burden of 2? , relay will respond instantaneously with maximum time delay of 3.25 cycles for a 400A primary fault. The time for the relay

operations is added to the maximum time delay (2 cycles). The operations of the relay within this time will be acceptable and will maintain relay coordination with upstream protective devices. Consequently, current transformers used with the microprocessor relay should meet the following criteria in order to ensure relay proper and acceptable operation:

$$200 \geq i_f \cdot z_b \tag{6.6}$$

To analyze the response of instantaneous digital relays, an example of microprocessor overcurrent relay with 400A instantaneous setting will be considered. Figure 6.11, shows that the digital relay will respond instantaneously with maximum time delay of 3.25 cycles for a burden of 10 times the standard burden. In this example, the relay will be used with a 50/5 CT, class C20, with a 0.1 total burden, as 100 feet full-circuit run of #10 AWG has been used. Accordingly, the maximum fault for secure operation can be calculated by using the following equation:

$$I_{MAX} = \frac{ANSIClass}{100 \cdot Z_b} \cdot V_{Burden} \cdot CT_{Rating} \tag{6.7}$$

The maximum fault current for the previous example can be calculated as follows:

$$I_{MAX} = \frac{20}{100 \cdot 0.1} \cdot 200 \cdot 50 = 20,000A \tag{6.8}$$

The instantaneous operations of 50/5 CT can be guaranteed with a saturation voltage of 400, within 3.25 cycles for the relay trip operations. This will resolve the problem of selecting CT's with 20 times rating based on available short circuit and will reduce the cost required for higher CT's with higher class.

6.7.2   Evaluation of Instantaneous Digital Overcurrent Relay Responses with Asymmetrical DC Components

Now, evaluation of the effects of asymmetrical faults, with DC offset, on operations of instantaneous digital relay will be considered. As per IEEE C37-110-1996, the following equation shall be satisfied in order to avoid DC saturation:

$$V_s \geq \left| \frac{X}{R} + 1 \right| \cdot i_f \cdot z_b \qquad \textbf{(6.9)}$$

Where:

i_f is the maximum fault current in per unit of ct rating

z_b is the CT burden in per unit of standard burden

V_S is the CT saturation voltage in per unit and equal 20

X/R   is the X/R ratio of the primary fault circuit

In the analysis, cases 3 & 4 for asymmetrical analysis with X/R ratio of 24 and 16 will be used. The two cases are considered to be the worst cases among the asymmetrical cases listed in Table 6.3. By referring to Figure 6.45, an instantaneous relay settings with 400 A is considered. Accordingly, the time delay of relay operation is calculated, taking into considerations the time required for the relay to operate (2 cycles), as shown in Table 6.4.

From Table 6.4, the trip time delay for a microprocessor-based overcurrent relay will be 4.7 and 4.1 cycles for asymmetrical faults with X/R ratios of 24 and 16 respectively. The operation of the relay is fairly acceptable as coordination with upstream protective devices will be achieved. The saturation voltage are calculated by using equation 6.9 and found to be 1250 and 850 for both cases. The operation of the instantaneous element is satisfactory, for these voltages. The saturation voltage for the 50/5 CT, C20 is only 31V (20 in per unit) and equation (6.9) is not satisfied.

Table 6.4 relay operation time for 400A instantaneous settings with 16 and 24 X/R Ratio

Instantaneous Current Setting (A)	Case	Trip time delay		Calculated Saturation Voltage Using Equation (6.9)
		Second	**Cycles**	
400A	Case 3 X/R = 24	0.078	4.7	1250
	Case 4 X/R = 16	0.068	4.1	850
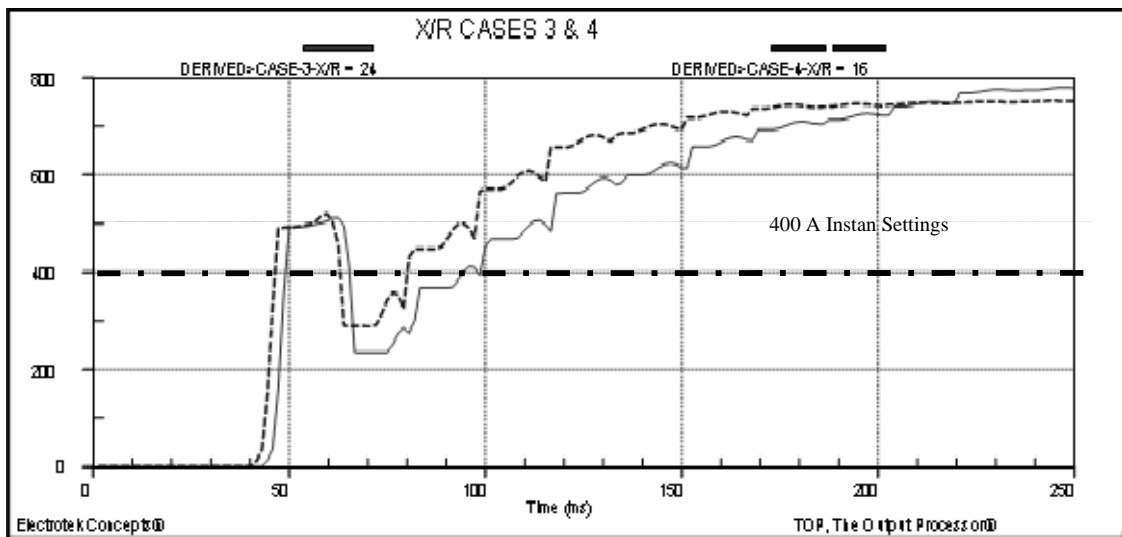
Figure 6.45 Response of Relay with 400 A Instantaneous Setting for Cases 3 and 4

Using the C20 with standard burden of 0.2 ? and CT burden of 0.5 ? , used in the X/R

cases:

$$Z_b = \frac{Z_{Burden}}{Z_{Stad}} = \frac{0.5}{0.2} = 2.5 \qquad\qquad (6.10)$$

Therefore, with X/R ratio of 24, the burden voltage can be calculated as follows:

$$V_s \geq \left|\frac{X}{R} + 1\right| \cdot i_f \cdot z_b = (24+1) \cdot 20 \cdot 2.5 = 1250 \qquad\qquad (6.11)$$

Consequently, current transformers used with the microprocessor relay should meet the

following criteria:

$$1250 \geq \left|\frac{X}{R} + 1\right| \cdot i_f \cdot z_b \qquad\qquad (6.12)$$

For evaluation purposes, a microprocessor overcurrent relay with 400A

instantaneous setting will be considered. The relay will be used with a 50/5 CT, class C20,

with a 0.1 total burden, as 100 feet full-circuit run of #10 AWG is used and X/R ratio of

20. Then, the maximum fault current be for secure operation can be calculated as follows:

$$I_{MAX} = \frac{ANSIClass}{100 \cdot Z_b} \cdot \frac{V_{Burden}}{(1+\frac{X}{R})} \cdot CT_{Rating} \qquad \textbf{(6.13)}$$

The acceptable calculated V_{Burden} is 1250V as in equation (6.12). Therefore, the maximum fault be for secure operation can be obtained from (6.13):

$$I_{MAX} = \frac{20}{100 \cdot 0.1} \cdot \frac{1250}{(1+20)} \cdot 50 = 5,952.4 \qquad \textbf{(6.14)}$$

This can be validated by using the EMTP model developed for the 50/5CT. Since the response of the relay was almost identical to the EMTP secondary current, secondary current output will be utilized to validate the operations of the relay with X/R of 20, secondary burden of 0.1 ohm and primary fault level of 5952.4A. Figure 6.46 shows that 400 A will be seen after one cycle. By considering the relay operating time (2 cycles), the total time delay will be around three cycles and proper operation of the relay will be achieved.
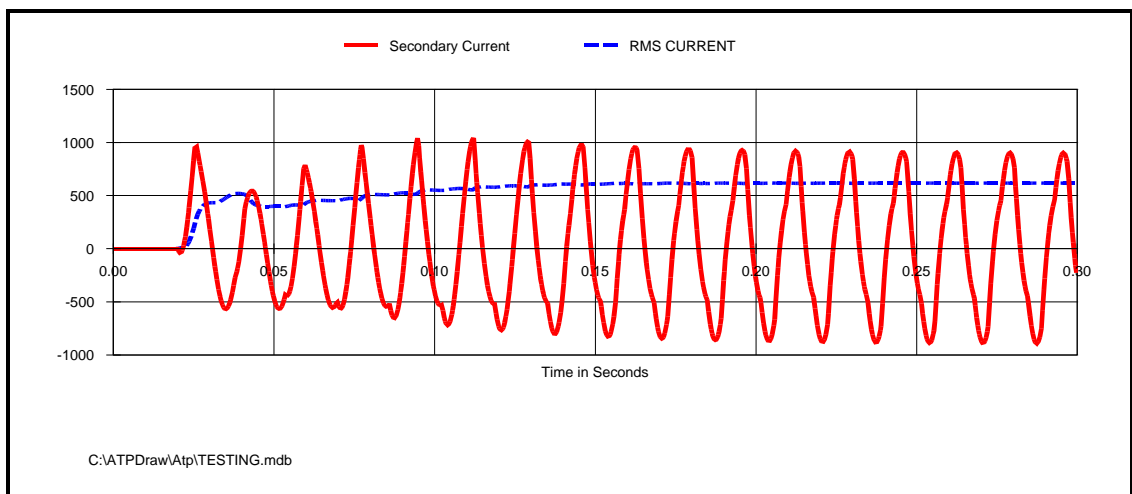
Figure 6.46 Case Study with X/R=20, Burden =0.1 and Primary Current of 5952.4 A

As illustrated in the previous example, the instantaneous operations of 50/5 CT can be guaranteed with saturation voltage of 119 with 20 X/R ratio, with time delay of around 4.7 cycles for the relay trip operations. This will eliminate the need for meeting the requirements of equation (6.9) for CT rating with DC offset. Table 6.5 lists the maximum fault current versus X/R ratio and secondary burden based on criteria of 6.13. Based on this analysis, CT rating can be selected based on short circuit level available, secondary burden connected, X/R ratio and required relay trip time delay. Consequently, the need for higher CT ratio with higher class could be eliminated.

6.7.3   Evaluation of Instantaneous Digital Overcurrent Relay Response with Remanence Flux

Figure 6.42 shows the response of the digital overcurrent relay to the different values of remanence flux with 24 X/R ratio. It shows considerable CT saturation in the first five cycles. The RMS value of the current is significantly reduced compared to the expected value, especially in the first cycles. Although, the more severe case will be experienced when the remanence flux reaches 100%, there is no significant difference or impact on the relay response to different fault levels. The relay will operate at almost the

same time with negligible time delay and with no practical effect on the instantaneous

operations of digital overcurrent relays.

Table 6.5 Maximum Current to Ensure Relay Operation

X/R Ratio	50/5, C20 Zb = 0.1	50/5, C20 Zb = 0.5
3.5	35, 714.3 A	7, 142.9 A
6.0	20, 833.3 A	4, 166.7 A
11	11, 363.6 A	2, 272.7 A
16	7, 352.9 A	1, 470.5 A
20	5, 952.4 A	1190.5 A

6.8 Evaluations of Time-delayed digital relays response and test results

CT saturation does not only impact the operation of instantaneous overcurrent digital relays. It also affects the time-delayed operation of digital overcurrent relays. The impact of the symmetrical and asymmetrical faults, resulting in CT saturations on digital overcurrent relays will be analyzed based on the laboratory tests results, shown in section 6.3 and 6.4 respectively. For the purpose of analysis, A Basler digital overcurrent relay-long inverse (L2) time-current characteristic is considered for evaluations purposes. A curve with 50A pickup is considered with 50/5 CT, C20, used for the conducted tests.

First, the impact of changing the CT secondary burden on time-delayed digital relays will be evaluated. Figure 6.47 presents the published curve of the digital overcurrent. With assumption that the fault level is 20 X CT (1000A), the operation time of digital relay will vary depending on the burden values. As illustrated in section 6.4, the magnitude and shape of secondary current will be more affected as the CT secondary burden is increased. Lower magnitude will be seen by the relay and thus will affect the operating time of the relay. Table 6.6, summarizes the operating time of the digital relay in comparison to the ideal case, where no saturation occurred.
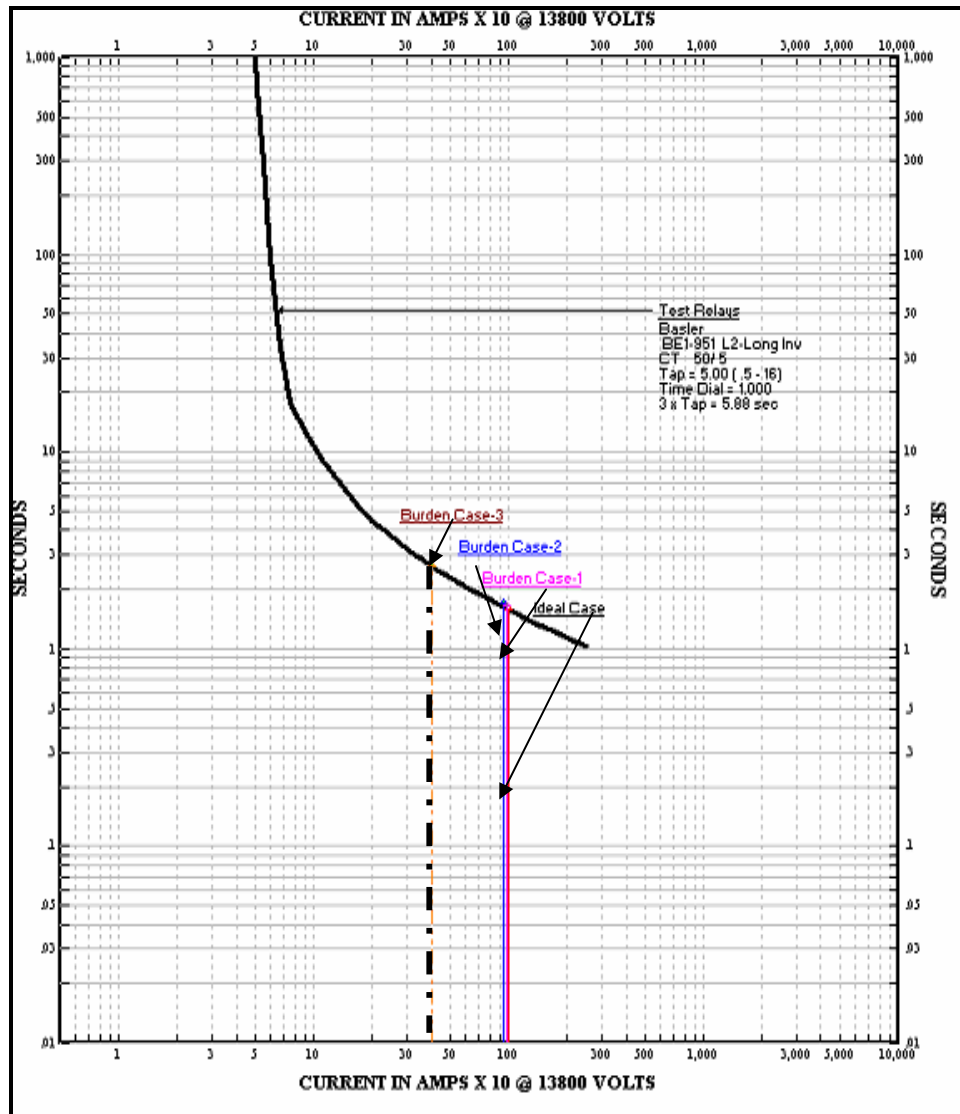
Figure 6.47 Impacts of Changing Burdens on Time-delayed Digital Relays

Table 6.6 Effects of Changing Burdens and CT Saturation on Digital Relay Time Operation

Case	Secondary current seen by the digital relay when 1000A primary fault occurred	Operation time (Seconds)	Time difference (Seconds)
Ideal Case	100A	1.7	
Case-1, with 0.25 ?	97A	1.72	0.02
Case-2, with 0.5 ?	94A	1.75	0.05
Case-3, with 5 ?	40A	2.6	1.1

Ideally, the relay is expected to see 100A, if full reproduction of the primary current is produced. However, this is not the case. In all burden cases, presented in section 6.3, a primary current of 1000 A was injected to the 50/5 CT in the laboratory test.

Figure 6.11 shows that currents of 97A, 94A and 40A were seen by the relay for secondary burdens of 0.25, 0.5 and 2.0 ohm respectively. The impact on the relay operating time will vary in the three cases. Figure 6.47 compares the operating time of the relay in the ideal case, compared to the three cases. It is clear from the time-current characteristics that a significant time delay will be experienced in the burden case-3 where the relay operations will be delayed by around 1.1 second. This will cause miscoordination with the upstream relays.

Now, effects of asymmetrical faults with dc offset on time-delayed digital relay operation will be examined. Study cases presented in Table 6.3 will be considered for evaluations. In cases 1 and 2, presented in Table 6.3, 170A primary current was injected to the 50/5 CT. However, lower current was seen by the relay for both cases, with considerable time delay as shown in figure 6.28. This has been calculated and added to the time delay of the ideal case. The calculated time delay values are presented in Table 6.7 for both cases. Figure 6.48 shows that a time delay of 0.24 and 0.13 seconds will be experienced for cases 1 and 2, in comparison to the ideal case.
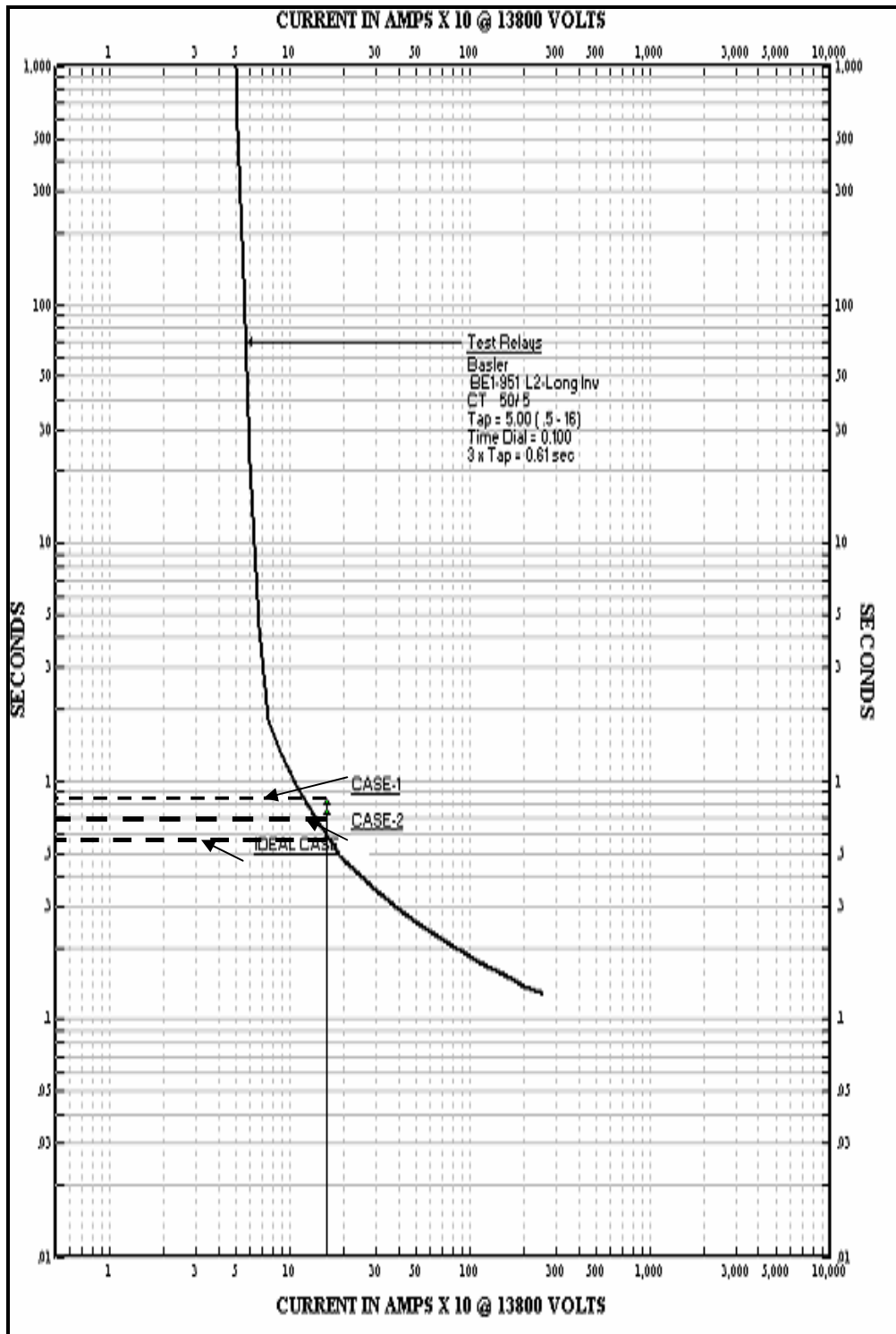
Figure 6.48 Impacts of Asymm Fault on Time-delayed Digital Relays (Case 1&2*)

Table 6.7 Effects of Asymmetrical Fault on Time-delayed Digital Relay (Case1&2)

Case	Secondary current seen by the digital relay when 170A primary fault occurred	Operation time (Seconds)	Time difference (Seconds)
Ideal Case	17A	0.58	
X/R = 24, case-1	15.5A	0.82	0.24
X/R = 16, case-2	16.0A	0.71	0.13

In cases 3 and 4, presented in Table 6.3, 1000A primary current was injected to the 50/5 CT. However, lower current was seen by the relay for both cases, with considerable time delay as shown in Figure 6.35. This has been calculated and added to the time delay of the ideal case. The calculated time delay values are presented in Table 6.8 for both cases. Figure 6.49 shows that a time delay of 0.27 and 0.12 seconds will be experienced for cases 3 and 4, in comparison to the ideal case.

Based on the test results, it has been concluded that the instantaneous digital overcurrent relays can operate with low CTs, under certain applications and conditions. On the other hand, time-delayed digital relays will be significantly affected by CT saturation, although the significance of the saturation varies, depending on the fault level, system X/R ratio, secondary burden and remanent flux in the core. Chapter 7 will present a case study, highlighting the area of applications for the testing findings.

Table 6.8 Effects of Asymmetrical Fault on Time-delayed Digital Relay (Case3&4*)*

Case	Secondary current seen by the digital relay when 1000A primary fault occurred	Operation time (Seconds)	Time difference (Seconds)
Ideal Case	100A	0.18	0
X/R = 24, case-3	75A	0.45	0.27
X/R = 16, case-4	77A	0.3	0.12
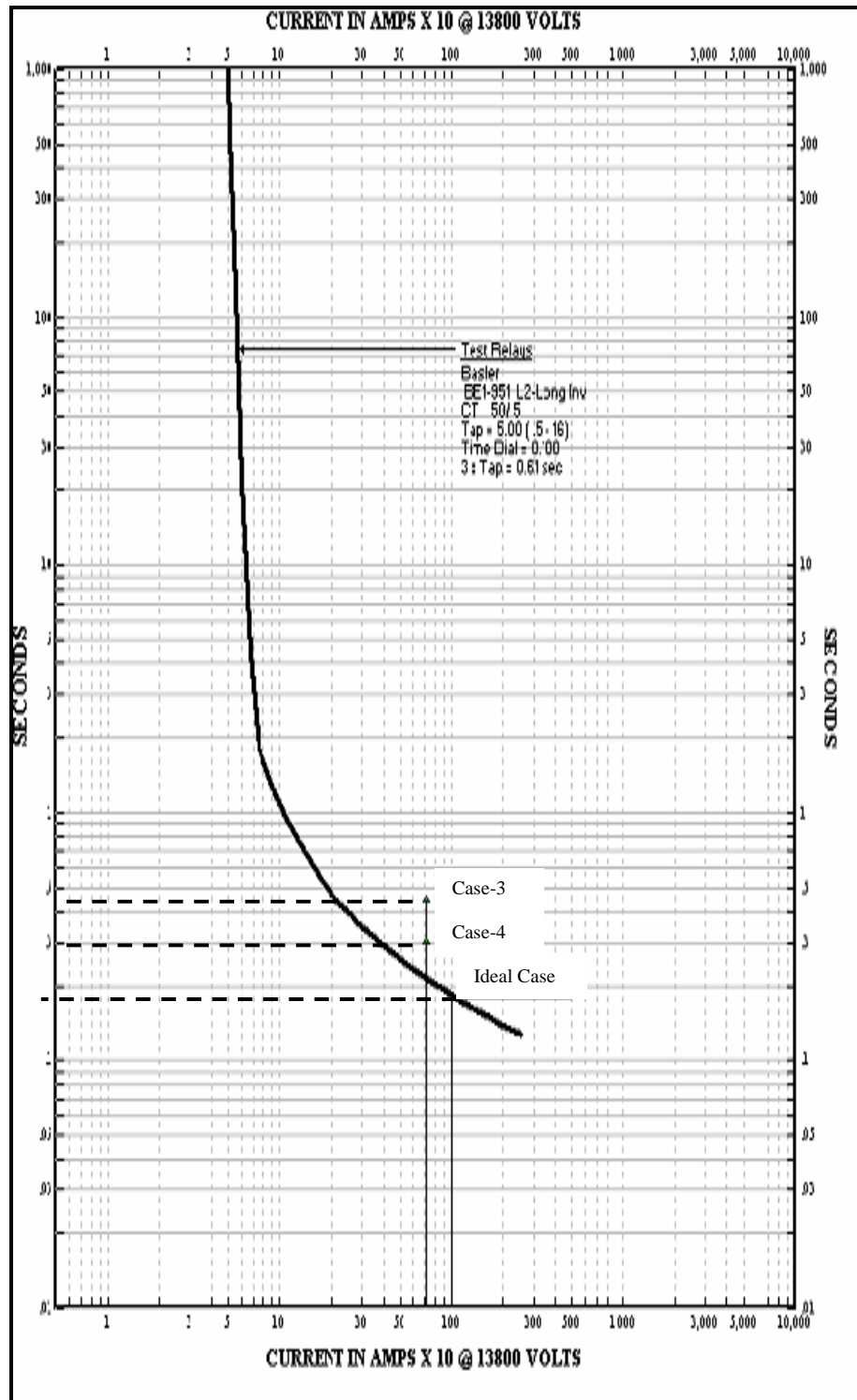
Figure 6.49 Impacts of Asymm Fault on Time-delayed Digital Relays (Case 3&4)

CHAPTER 7

AREA OF FINDINGS APPLICATIONS

7.1 Area of Applications

In distribution networks, relatively small loads, may be connected to a bus with inherently high short-circuit currents. This is mainly due to either economical constraints or space limitation problems, where large CT's practically cannot be installed. Since the maximum current for each load may be small, the CTs ratio tends to be low to provide thermal protection at moderate overloads. Low-ratio selection results in a low accuracy class, usually less than 100. This will provide satisfactory performance for moderate overloads but could be inadequate for short circuit current levels.

Figure 7.1 shows two examples of low CT's ratios connected to a bus with high-short circuit level. A transformer with full load current of 43.7 A, with 50/5 CT that adequately protect against overload. However, the short circuit rating is 300 times the CT rating. Similarly, a motor with an overload protection with 100/5 CT is shown. However, a concern is raised about the instantaneous relay response for short circuit level as the short circuit currents is 150 times the CT rating.

The results of digital overcurrent relays testing in chapter 6, showed that instantaneous digital relays could operate properly with low CT ratios and high short

circuit levels. The IEEE criteria for instantaneous relays are not mandatory. The CT rating can be selected based on short circuit level available, secondary burden connected, X/R ratio and required relay trip time delay. Consequently, the need for higher CT ratio with higher class could be eliminated. This will resolve the issue of space limitation problem, for high ratio CT's and will reduce the cost as this problem is common in distribution systems.
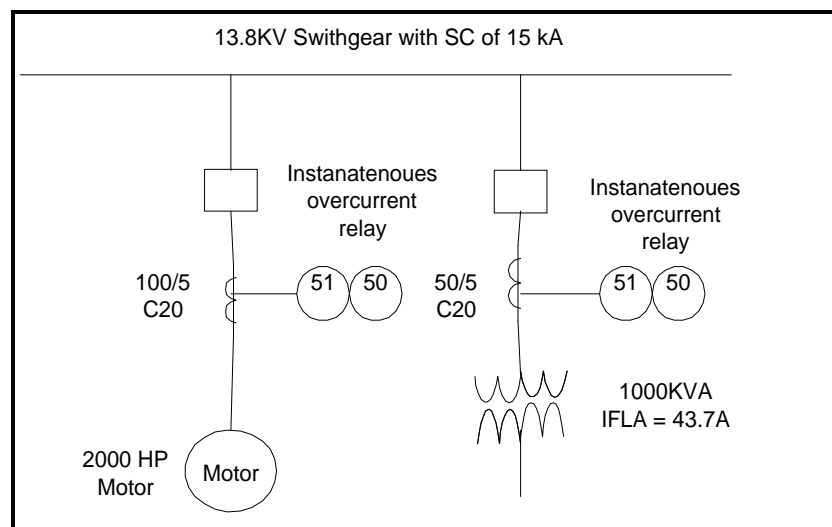
Figure 7.1 Typical Distribution System with Low CT Ratio and
High SC Level [1 and 20]

7.2 Case Study

A case study will be considered to show the area of applications of the thesis findings. A transformer with 1000KVA rating will be considered. The secondary burden is made of 0.1 ? or 100 ft of # 10 AWG control wires. The system X/R ratio is 6. A digital overcurrent relay is installed on the high-side of the transformer to protect against overload and short circuit. The CT is sized based on the full load current of the transformer which is 41.8 A. A 50/5 CT, with accuracy class of C20 is selected as shown in figure 7.2.

From section 6.7, it has been proven that the digital overcurrent relay will operate with 50/5 CT, C20 with instantaneous settings of 400A with no more than 4.7 cycles time delay, if the burden voltage of 1250 is met. This criteria will be utilized to check the adequacy of the selected CT with the available short circuit level:

$$1250 \geq \left| \frac{X}{R} + 1 \right| \cdot i_f \cdot z_b \tag{7.1}$$

The maximum fault current with 400 A instantaneous settings can be calculated using the following formula:

$$I_{MAX} = \frac{ANSIClass}{100 \cdot Z_b} \cdot \frac{V_{Burden}}{(1 + \frac{X}{R})} \cdot CT_{Rating} \tag{7.2}$$
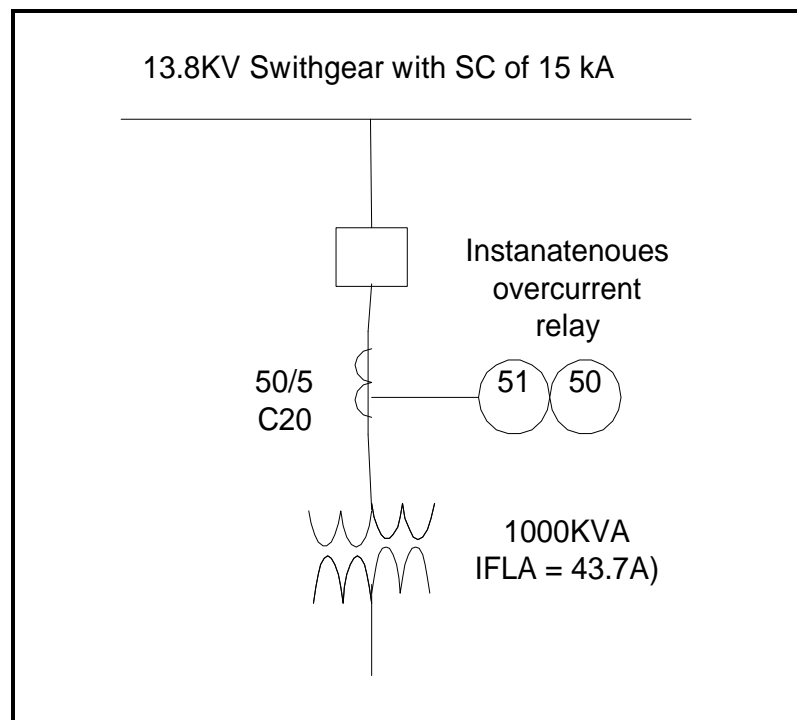
Figure 7.2 Case Study

The maximum fault that to ensure secure operation can be obtained from equation (7.2):

$$I_{MAX} = \frac{20}{100 \cdot 0.1} \cdot \frac{1250}{(1+6)} \cdot 50 = 17{,}857.1A \qquad (7.3)$$

The instantaneous operation of 50/5 CT can be guaranteed with 357 times CT rating with 6 X/R ratio. Figure 7.3 shows the response of the relay with 15,000 A short circuit for the case presented. It confirms that the instantaneous digital relay, with 400 A instantaneous settings, will respond to the fault in this case with no more than three cycles.

For comparison purposes, IEEE C37.110-1996 will be considered for sizing the CT's in the case study. The following equation shall be met:

$$20 \geq \left| \frac{X}{R} + 1 \right| \cdot i_f \cdot z_b \qquad (7.4)$$

To meet the requirements of equation (7.4), CT of ratio 600/5 and accuracy class of C100 is required. Substituting in equation 7.4:

$$20 \geq \left| 6 + 1 \right| \cdot 25 \cdot 0.1 = 17.5 \qquad (7.5)$$
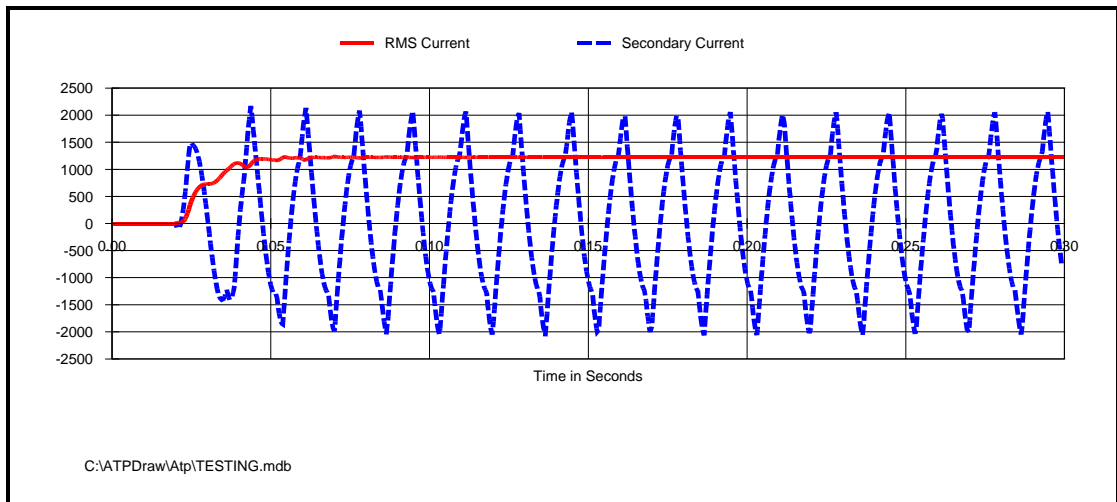
Figure 7.3 Case Study with X/R=6, Burden =0.1 and Primary Current of 15,000 A

7.3 Procedure for Selecting the CT's for Proper Instantaneous Operations with Digital Relays

1. Select the CT ratio based on the load requirements.

2. Calculate the required instantaneous relay settings.

3. Use equation (7.4) to calculate the V_S.

4. Run EMTP model for the CT to ensure proper operations of the relay at the instantaneous settings. Calculate the time required for the relay to operate and investigate if it is acceptable. Otherwise, change the CT ratio or accuracy class to higher ones.

5. For the same CT, define a criteria for CT selection by using the calculated V_S and calculate the maximum fault current based on the secondary burden and X/R ratio.

CHAPTER 8

CONCLUSION AND RECOMMENDATIONS

8.1 Conclusions

An acceptable and precise current transformers model was implemented, using the non-linear inductor model (Type-96) in EMTP. The model is a very convenient way to test the transient behavior of the CT's and digital overcurrent relays. The model was validated and tested in the laboratory to ensure appropriate and accurate suitability.

This CT model was then used to demonstrate and investigate the effects of secondary burden, accuracy class, symmetrical short circuit level, system X/R ratio (DC offset) and remanent flux in the CT core on the current transformers. Such analysis is very imperative to study the effects of CT's saturation on protective relays and consequently on the protection system. Full understanding of the behavior of CT's will allow the study and evaluation of the digital overcurrent relay response to transient events.

Effects of CT saturation on digital overcurrent relays were investigated throughout the thesis work by conducting laboratory tests. Various study cases were developed by using the EMTP CT model to investigate the effects of secondary burdens, symmetrical short circuit level, system X/R ratio (dc offset) and remanent flux on CT saturations. The operation of the instantaneous and time-delayed overcurrent digital relays were then

investigated. All these study cases were injected to the relay by using a secondary injection devise, after converting all cases to common-trade format files. The objective of all these analysis is to address the CT ratings used in distribution networks where fault currents exceed 200 time the CT primary rating and requirement of C37.110-1996 cannot be practically met, due to either size limitations or long secondary wires.

Based on the thesis results, the selection of CT could be done based on the operating time of the instantaneous relays. CT's subjected to 100 times fault current, for example, could work with no problem and without meeting the criteria of IEEE standard C37.110-1996. CT's driven to saturation, can still provide sufficient current to the instantaneous digital overcurrent relays. On the other hand, time-delayed digital relays will be significantly affected by the CT saturation, although the significance of the saturation varies, depending on the fault level, system X/R ratio, secondary burden and remenant flux in the core.

8.2 Recommendations

It is recommended that the developed CT model is used to investigate the operations and transients performance of other digital relays (i.e., transformer differential and ground differential). This will give applications guidelines for CT's selection.

Another area of improvement is to carryout further testing on digital overcurrent relays and different size of CT's with different accuracy classes in order to come up with a solid and practical criteria of CT's selection. Digital fault recorders with higher sampling rate will provide more accurate results. It has been shown that it is impractical and non-economical to apply the criteria of the IEEE C37.110-1996, as it will result in a relatively high CT ratio and accuracy class.

More ideas are to be examined by conducting further investigation on time-delayed digital overcurrent relays to come up with a criteria for calculating the time delay caused by saturation for consideration in the relay coordination. This will provide more flexibility to achieve coordination with under-sized CT's by taking into consideration the time delay, resulted from the CT's saturation.

References

[1] John R. Linders, C. W. Barnett, J. W. Chadwick, P. R. Drum, K. J. Khunkhun, Stanley E. Zocholl, W. C. Kotheimer, P. A. Kotos, D. W. Smaha, P. B. Winston and W. Walton, "Relay Performance Considerations with Low-Ratio CT's and High-Fault Currents," IEEE Transactions on Industry Applications, Vol 31, No.2, pp. 392-403, March/April, 1995.

[2] Lj. A. Kojovic, "Impact of Current Transformers Saturation on Overcurrent Protection Operation," Power Engineering Society Summer Meeting, 2002 IEEE, Volume: 3, pp. 1078-1083, July 2002.

[3] B. Bridger and Ted A. Burse, "Operation of Ground Sensor Relays Under Conditions of Partial CT Saturation," IEEE Transactions on Industry Applications, Vol 33, No.4, pp. 1111-1116, July/August, 1997.

[4] Jiuping Pan, Khoi Vu and Yi Hu, "An Efficient Compensation Algorithm for Current Transformer Saturation Effects," IEEE Transactions on Power Delivery, Vol 19, No.4, pp-1623-1628, October, 2004.

[5] Y. C. Kang, S. H. Ok, S. H. Kang and P. A. Crossley, "Design and Evaluation of an Algorithm for Detecting Current Transformer Saturation," IEEE Proc.-Gener. Transm. Distrib., Vol 151, No.1, pp-27-35, January, 2004.

[6] Yong Cheol Kang, Ui Jai Lim, Sang Hee Kang and Peter A. Crossley, "Compensation of the Distortion in the Secondary Current Caused by Saturation and Remanence in a CT," IEEE Transactions on Power Delivery, Vol 19, No.4, pp-1642-1649, October, 2004.

[7] Cheng Li-jun, "The Research of the Sampling Method for CT saturation for Numerical Busbar Protection," Development in Power System Protection, 2004, Eighth IEE International Confrence, Vol 1, pp-384-386, April, 2004.

[8] IEEE C37.110-1996 Guide for the Application of Current Transformers Used for Protective Relaying Purposes.

[9] M. W. Conroy, B. D. Nelson, B. Bozoki, J. W. Chadwick, P. R. Drum, L. L. Dovark, I. Hasenwinkle, J. Huddkeston, W. C. Kitheimer, J. R. Linders, M. J. McDonald, G. R. Moskos, G. C. Parr, R. Ryan, E. T. Sage, D. W. Smaha, K. A. Stephan, J. E. Stephens, J. T. Uchiyama and S. Zocholl, "C37.110 Guide for the Application of Current Transformers Used for Protective Purposes," IEEE Transactions on Power Delivery, Vol 14, No.1, pp. 94-97, January 1999.

[10] Stanley E. Zocholl and Joe Mooney, "Primary High-Current Testing of Relays with Low Ratio Current Transformers," Pulp and Paper Industry Technical Conference 2004, pp. 192-197, July 2004.

[11] D. A. Tziouvaras, P. MacLaren, G. Alexander, D. Dawson. J. Esztergalyos, C. Fromen, M. Glinkowski, I. Hasenwinkle, M. Kezunovic, L. Kojovic, B. Kotheimer, R. Kuffel, J. Nordstrom and S. Zocholl, "Mathematical Models for Current, Voltage, and Coupling Capacitor Voltage Transformers," IEEE Transactions on Power System, Vol 15, No.1, pp. 62-72, January 2000.

[12] M. Kezunovic, C. W. Fromen and F. Phillips, "Experimental Evaluation of EMTP-Based Current Transformer Models for Protective Relay Transient Study," IEEE Transactions on Industry Applications, Vol 9, No.1, pp. 405-413, Jan. 1994.

[13] Lj. A. Kojovic, "Comparison of Different Current Transformer Modeling Techniques for Protection System Studies," Power Engineering Society Summer Meeting, 2002 IEEE, Volume: 3, pp. 1084-1089, July 2002.

[14] Chuk-Hwan Kim, Myung-Hee Lee, Raj K. Aggarwal and Allan T. Johns, "Educational Use of EMTP MODELS for the study of a Distance Relaying Algorithm for Protecting Transmission Lines ," IEEE Transactions on Power Systems, Vol 15, No.1, pp. 9-15, February, 2000.

[15] A. Chaudhary, Kwa-Sur Tam and A. G. Phadke, "Protection System Representation in the Electromagnetic Transient Program," IEEE Transactions on Power Delivery, Vol 9, No.2, pp. 700-711, April 1994.

[16] Washington L. A. Neves and Hermann W. Dommel, "On Modeling Iron Core Nonlinearities," IEEE Transactions on Power System, Vol 8, No. 2, pp. 417-425, May 1993.

[17] Ralph Folkers "Determine Current Transformer Suitability Using EMTP Models " www.selinc.com.

[18] IEEE C57.13-1993 Standard Requirements for Instrument Transformers.

[19] N. T. Stringer, "The effect of DC Offset on Current-Operated Relays," IEEE Transactions on Industry Applications, Vol 34, No.1, pp. 30-34, January/February, 1998.

[20] G. Benmouyal and S. E. Zocholl, "The Impact of High Fault Current and CT Rating Limits on Overcurrent Protection, " www.selinc.com.

[21] Stanley E. Zocholl, Jeff Roberts, and Gabriel Benmouyal, "Selecting CTs to Optimize Relay Performance," Proceedings of the 23rd Annual Western Protective Relay Conference, Spokane, WA, October 15 – 17, 1996.

[22] Stanley E. Zocholl and Gabriel Benmouyal, "How Microprocessor Relays Respond to Harmonics, Saturation, and Other Wave Distortions," Proceedings of the 24th Annual Western Protective Relay Conference, Spokane, WA, October 21 – 23, 1997.

[23] Stanley E. Zocholl and D.W. Smaha, "Current Transformer Concepts," Proceedings of the 46th Annual Georgia Tech Protective Relay Conference, Atlanta, GA, April 29 – May 1, 1992.

[24] H. O. Pascual, J. L. Dampe and J. A. Rapallini, "Behavior of Current Transformers (CT's) Under Severe Saturation Conditions," IPST Conference, 2001. www.ipst.org.

[25] Lj. A. Kojovic, "Guidelines for Current Transformers Selection for Protection System," Power Engineering Society Summer Meeting, 2001 IEEE, Volume: 1, pp.593-598, July 2001.

[26] J. R. Marti, L. R. Linares and H. W. Dommel, "Current Tranfomers and Coupling-Capacitor Voltage Transfomers in Real-Time Simulations," IEEE Transactions on Power Delivery, Vol 12, No.1, pp. 164-168, January 1997.

[27] Blackburn, J. Lewis, *Protective Relaying, Principles and Applications*, New York: Marcel Eecker, Inc., Chapters 5 & 8, 1987. "

[28] D. W. Ackermann, "Current Transformer Measurements of Distorted Current Waveforms with Secondary Load Impedance," IEEE Transactions on Power System, Vol 8, No 2, May 1999.

[29] Walter A. Elmore, *Protective Relaying Theory and Applications*, New York: Marcel Eecker, Inc., Chapters 5, 1994. "

[30] S. Bittanti, F. Cuzzola, F. Lorito and G. Poncia, "Compensation of Nonlinearities in a Current Transformer for the Reconstruction of the Primary Current," IEEE Transactions on Control Systems Technology, Vol 9, No.4, pp.565-573, July 2001

[31] Silvano Casoria and Gilbert Sybille, "Hysteresis Modeling in the Matlab/Power System Blockset," www.transenergie-tech.com.

[32] Francisco de leon and Adam Semlyen, "A Simple Representation of Dynamic Hysteresus Losses in Power Transformers, " IEEE Transactions on Power Delivery, Vol 10, No.1, pp. 315-321, January 1995.

[33] Instruction Manual for alternative transients program (ATP).

[34] Reference Manual for OMICRON-CPC-100, Primary Test System for Substation Equipment

[35] IEEE C37.519-1992 IEEE Recommended Practices and Requirements for Harmonic Control in Electrical Power Systems.

[36] Instruction Manual for Overcurrent Protection System (Basler BE1-951)

[37] Operations Manual for OMICRON-CMC-256, PC controlled test device for protective relays and transducers.

[38] Stanley E. Zocholl, Cheryl Kramer and W. Elmore, "Effect of Waveform Distortion on Protective Relays," IEEE Transactions on Industry Applications, Vol 29, No.2, pp-404-411, March/April, 1993.

[39] Peter E. Sutherland, "Applying CTs with Digital Ground Relays, " IEEE Industry Applications Magazine, pp. 71-79, March/April 2001.

[40] Z. A. Yamayee and J. L. Bala, *Electromechanical Energy Devices and Power Systems*, New York: John Wiley & Sons, Inc., Chapters 4, 1994.